2015

# Optimal Location of Biomethane Gas Manufacturing Plants and Allocation of Feedstock and Liquified Carbon Product

Bingqing Wu
*Louisiana State University and Agricultural and Mechanical College*

# OPTIMAL LOCATION OF BIOMETHANE GAS MANUFACTURING PLANTS AND ALLOCATION OF FEEDSTOCK AND LIQUIFIED CARBON PRODUCT

A Dissertation

Submitted to the Graduate Faculty of the
Louisiana State University and
Agricultural and Mechanical College
in partial fulfillment of the
requirement for the degree of
Doctor of Philosophy

in

The Interdepartmental Program
in Engineering Science

by
Bingqing Wu
B.S., Nanjing University of Aeronautics and Astronautics, 2007
M.S.I.E., Louisiana State University, 2012
May 2015

# ACKOWLEDGEMENTS

I would like to express my sincere gratitude to my advisor, Dr. Bhaba R. Sarker, Elton G. Yates Distinguished Professor of Mechanical & Industrial Engineering (MIE) for his guidance and consistent support in pursuing this research. It was a pleasure working with him throughout the years I spent at Louisiana State University (LSU). Without his persistent help, this dissertation would not have been completed possibly.

I am also grateful to Dr. Guoli Ding of Mathematics Department, Dr. T. Warren Liao and Dr. Lawrence Mann, Jr. of MIE Department, and Dr. Krishna P. Paudel of Agricultural Economics and Agribusiness Department for serving on my committee and Dr. Vincent Wilson of Environmental Science Department as the Graduate School Representative. Their valuable inputs and insightful suggestions enlightened me on various aspects of this research. I am thankful to Dr. Hongchao Zhang for his valuable suggestions and Dr. Thomas Alan Gavin, Professor Emeritus of Cornell University, for his editing English of my dissertation.

I would like to thank my friends, and once colleagues and fellow researchers, Dr. Huizhi Yi (Northwestern State University, Natchitoches, LA), Dr. Qinglin Duan (Monsanto Company), and Dr. Cunrong Li (Wuhan University of Technology and Dr. Meng Yu (Wuhan University of Technology) for their contributions at the early stage of my research work. I would like to thank the LSU Graduate School for providing financial support through the Louisiana Economic Development Assistantship.

To the end, I would like to thank my husband, Dr. Xiaoyu Cai, for sharing his knowledge on this research and encouraging me to overcome all the difficulties I encountered during my research. Finally, I am thankful to my parents Min Wu and Shudong Wu for their love, and emotional and financial support.

# TABLE OF CONTENTS

# LIST OF TABLES

# LIST OF FIGURES

# ABSTRACT

Biomethane gas (BMG), known for its sustainability, low environmental impact, and high profitability, has received wide attention in recent years. To facilitate the process of making strategic plans for building a BMG production system, this dissertation leverages the mathematical modeling and optimization techniques to minimize the supply chain cost for such a system. Typical elements in a BMG production system consist of the local *farms* that produce the feedstock, the *hubs* that collect and store the feedstock produced by farms, the *reactors* that generate BMG from the feedstock transported from the hubs, the *condensers* that liquefy the BMG from the reactors, and the *delivery points* that act as end distributors and accept the liquefied BMG from condensers. The logistics of a BMG production system can be divided into four stages: farm-to-hub (F2H) stage, hub-to-reactor (H2R) stage, reactor-to-condenser (R2C) stage, and condenser-to-delivery point (C2DP) stage.

Depending on the variation on the elements and stages of a BMG production system, four supply chain configurations for BMG facility locations are proposed with increasing level of complexity: single-stage, single-reactor system (SS-SRS); single-stage, multi-reactor system (SS-MRS); three-stage, multi-facility system (TS-MFS); and four-stage, multi-facility system (FS-MFS). The objective for each configuration is to locate facilities optimally and to design the transportation/pipeline connecting network such that the supply chain cost, including the total of feedstock costs, labor costs, facilities building costs, and transportation/pipeline layout costs are minimized. A systematic approach, containing mathematical modeling and heuristic design, is proposed for each configuration. Numerical experiments are conducted for each designed heuristic to verify its performance.



**Key Words**: Biomethane industry, location-allocation problem, supply chain optimization.

# CHAPTER I
# INTRODUCTION

Non-renewable sources of energy, including fossil fuels, refers to the types of energy that have a consumption rate that far exceeds its natural renewal rate. Zittle and Schindler (2007) predict that the "peak coal" era (i.e., the moment when the global coal production rate becomes maximum, and then the rate will enter the terminal stage) will occur by 2025, and that natural gas reserves will be sustained for another 60 years, assuming that the production level remains at the 2011 level (US Energy Information Administration, 2013). It is now common knowledge that the depletion of non-renewable resources, particularly fossil fuels, is inevitable.

Another key concern about the use of fossil fuels are the harmful emissions generated by its combustion. Every unit of energy produced from fossil fuels results in a significant percentage of carbon dioxide emissions. It is estimated that coal releases 228.6 pounds of $CO_2$ and natural gas emits 117 pounds of $CO_2$ per million Btu of energy (USEIA, 2014). Because energy use contributes about 80.3% of total greenhouse gas (GHG) (IEA, 2013), excessive reliance on fossil fuel may result in significant environmental problems.

To prepare for the inevitable depletion and to reduce the environmental impact of fossil fuels, developing renewable energy becomes critical for human society. Numerous efforts are being devoted to the growth of renewable energy sources such as solar, wind, hydroelectric, and bio-energy. Renewable energy, which can replace conventional energy sources, is sustainable, has low greenhouse gas emissions, and high economic efficiency. Among these popular types of renewable energy, BMG is attracting increasing attention these days.

Methane gas, a key component of natural gas, is known for its high ratio of combustion heat to unit molecular mass. Therefore, it is widely used in power generation, household

heating, and vehicle fuels. It is estimated that 1/5 of the world's energy consumption is supplied by methane gas, which is distributed extensively on earth in the form of natural gas. Conventional ways of extracting natural gas from the ground are not only unsustainable, but they are also costly. BMG, as its name indicates, refers to the methane gas that is obtained through a series of bio-chemical reactions. The major feedstocks for generating BMG are usually obtained from bio-residues that consist of animal manure, plants and crops, and are widespread on local farms/ranches. The nearly inexhaustible feedstock for BMG determines its renewability and sustainability. BMG production is less expensive than other forms of renewable energy, because it utilizes biological waste. All these competitive benefits of BMG make it an ideal candidate as the alternative energy for the future.

## 1.1 DEVELOPMENT OF BIOMETHANE GAS INDUSTRY

Profitability in the BMG industry triggers its development all over the world. The BMG production in European countries such as Germany and England has increased dramatically. These countries started building large-scale BMG manufacturing facilities in 2000. Until 2008, Germany produced 4000 BMG reactors and UK produced around 60 non-sewage BMG plants. After ten years of development, BMG plants in Europe produced 30 billion kWh of power in 2010. By 2013, the European Biogas Association (EBA) attracted more than 60 members from 24 countries.

The number of BMG plants increased in Asia in recent years. In Japan, dairy cattle waste has been used as feedstock for BMG production since 1998 and 78 BMG plants has been built up to 2012. Small/family size biogas (consists of methane gas and carbon dioxide) plants are widely exist in developing countries. China started promoting biogas production in rural areas since 1950 and small size biogas plants began emerging since then. From 2003 to 2013, more than 40 million household size biogas digesters have been built in China.

In the US, BMG topped the list of renewable energy production and expanded rapidly since 2000s. In 2003, the BMG consumption in the U.S. was about 0.6% of the total U.S. natural gas consumption. By 2011, more than 180 BMG recovery systems operated in commercial livestock farms, which generate sufficient electricity for 47,000 homes. Furthermore, the EPA (Environmental Protection Agency)'s AgSTAR program (USDA, 2010) announced that about 8,000 farms supported BMG production systems, which reduced the emissions of global warming pollution equivalent to what is generated by 6.5 million cars. As a pioneer in implementing BMG for vehicles, California increases the BMG production from landfill waste and reduced vehicles' greenhouses gas emissions for more than 80% percent by using the BMG fueling vehicles. In Texas, animal manure are transferred into BMG which generates power that was equivalent to 1000 barrels of oil per day. Nowadays, about 2,000 sites are producing BMG in the U.S., and most of the plants are in the Southern and Great Lakes areas. In 2012, a consortium of federal agencies publicized a report titled "US Bioinitiative", which clarified the long-term goal of developing bio-energy. The report (US BioInitiative, 2012) predicted that based on the bio-energy production in the year 2000, production will increase 10 fold by 2020, and 20-30 fold by 2050.

### 1.2 BIOMETHANE GAS PRODUCTION PROCESS

The BMG is generated in a reactor by series of chemical reactions known as the "anaerobic digester process" that is conducted in absence of air. The feedstock for this process can be emanated from natural residues, such as crop, wood, or animal manure. The methane gas obtained from this process is called BMG to distinguish itself from the methane gas that is produced through other methods. The BMG production system is economically efficient due to the fact that the original feedstock comes from the agriculture waste.

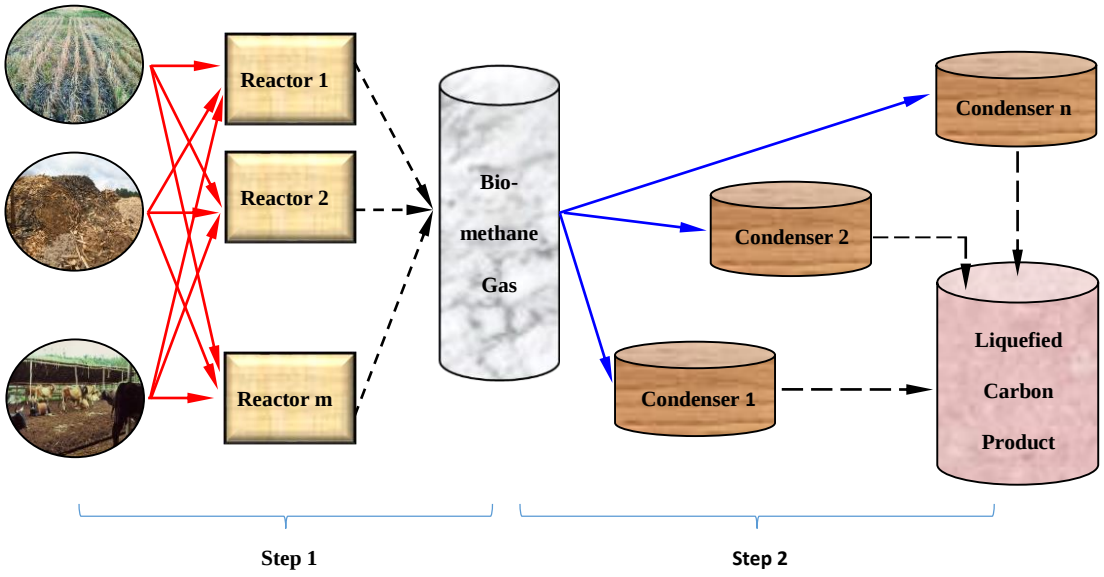


Figure 1.1: A typical BMG manufacturing system.

The production of the BMG comprises of two steps shown in Figure 1.1: BMG generation and liquefied carbon product (LCP) condensation. In the first step, bio-chemical reactions occur in the reactor using feedstock from farms. In the second step, BMG is liquefied in condensers to produce LCP as the final product. In practice, this two-step production process requires coordination of materials and product handling among different facilities from the local farms to the end users. A systematically designed supply chain ensures fluent coordination and yields a consistent output of product. This dissertation focuses on the supply chain optimization of the BMG production system, beginning with a thorough review of the literature in the next chapter.

# CHAPTER II
# LITERATURE REVIEW

With the rising of bio-energy manufacturing, many researchers have devoted into this area over the last decade. Being a significant form of bio-energy, BMG production takes up a large portion in the bio-energy industry. Other forms of bio-energy includes bioethanol, biodiesel, biobutanol etc. Although the forms of energy obtained from various bio-chemical process are distinctive, there is a resemblance in supply chain design for different forms of bio-energy production systems. Residue/biomass storage and collection, bio-energy reactors/refineries locations selection and end-product distribution plan are common topics that are studies in literature. Therefore, reviews on publications regarding bio-energy supply chain design is conducted instead of confining scope to BMG production systems. The literature review consists of two major aspects which are the system modeling and the heuristic development. Subjects on modeling supply chain of bio-energy production systems are reviewed in the first part. Heuristics on solving general location-allocation problems are reviewed from an operations research point of view.

## 2.1 SUPPLY CHAIN MODELS OF BIO-ENERGY PRODUCTION SYSTEMS

The prevailing models on supply chain of bio-energy production systems can be categorized into three aspects, which are linear or non-linear programming model, mixed integer linear programming model and mixed integer nonlinear programming model, depending on different programming types. In this section, the difference between the three models is addressed and their corresponding literature is reviewed.

### 2.1.1 Modeling with Linear or Non-Linear Programming

A Linear Programming (LP) or Non-Linear Programming (NLP) model comes with an objective function and constraints that are represented in a linear or nonlinear fashion. Both

models are utilized to describe continues scenario in supply chain design of bio-energy production systems.

Cundiff *et al*. (1997) constructed a LP model considered the uncertainty caused by weather in production levels. Tatsiopoulos and Tolis (2003) proposed a cotton biomass supply chain system. Dunnett *et al*. (2007) investigated a framework for an upstream biomass combustion plant, with storage strategy and task schedule. Gan *et al*. (2011) developed a generic framework for bioenergy production system by incorporating plant size, residue supply radius and production costs as optimization objectives. Theoretical results were extended to real world applications for strategic decisions. Recently, Illukpitiya *et al*. (2013) developed a LP model to maximize the biofuel production profit given the land availability in Hawaii is limited. Lim *et al*. (2014) provide a methodology to determine the capacity and distribution of biomass power plants in Sabah, Malaysia to minimized cost of electricity generation.

### 2.1.2 Modeling with Mixed Integer Linear Programming

A Mixed Integer Linear Programming (MILP) model contains a linear objective function and series of linear constraints with one or more of its variables set to be integers. MILP are usually used for linear discretized models in supply chain applications. Solving an MILP has been extensively studied in literature. Popular approaches includes Branch and Bound (B&B) method, dynamic programming are widely applied for solving MILP models.

Mele *et al*. (2009) proposed a MILP model for the bioethanol and sugar production system. By considering environmental issues, Zamboni *et al*. (2009) designed an optimization framework for the bioethanol production system based on a multi-echelon MILP. Under fluctuation in years of cost and selling price on biomass product, Dal-Mas *et al*. (2011) build a mathematical model of a bioethanol supply chain system for strategic decision. Cucek *et al*. (2010) deployed a four-layer supply chain model to optimize resource usage, product

distribution and transportation flows. Parker *et al*. (2010) studied biofuel supply in Western United State by providing a MILP. Existing refinery information was taken into account when new plants' locations and transportation networks were determined. Marvin *et al*. (2012) determined the optimal plants' locations and capacities for a biomass-to-ethanol production system. An economic optimization plan is proposed for the Midwestern United States to prevent financial fail of bio-refineries. Kim *et al*. (2011) used an MILP model to optimally select the plants' locations, capacities and residue distribution plans in a biofuel production system.

Case study involved scenarios in Southeastern region of the United States. Elia *et al*. (2012) suggested a quantitative way for optimized plan of a nationwide bio-energy supply chain design. Cucek *et al*. (2014) addresses a MILP approach for a bioenergy supply network with multi-period. Lin *et al*. (2014) presents a supply chain optimization model to minimize the production cost for a large-scale biogas plant. Liu *et al*. (2014) provides a life cycle assessment based a multi-objective biogas supply chain framework which can obtain balance among economy, energy and environment.

### 2.1.3 Modeling with Mixed Integer Non-Linear Programming

The objective function or constraints in a Mixed Integer Non-Linear Programming (MINLP) model contain nonlinear terms and integer variables. Real-world applications are usually accompanied by nonlinearity but introducing the nonlinear elements increases the computation complexity. When modeling the system with MINLP, compromise needs to be made between model accuracy and computational efficiency.

Corsano *et al*. (2011) addressed an optimization model for a sugar-ethanol supply chain system. Specific factors such as yeast production and residue recycles are considered for environmental purpose. Bai *et al*. (2012) applied game-theory in modeling biofuel supply

chain, which further influence the decision making between residue supplier and biofuel manufacturer. Walther *et al*. (2012) designed a mutli-period model for planning a second generation biofuel production system in Northern Germany. Shabani and Sowlati (2013) gives a dynamic model for forest biomass electricity generation system to improve its competitiveness and maximize the supply chain's overall value. Smith and Hobbs (2013) constitutes a supplying policy for a power generation system with biomass sources, and combines the output from existing agricultural optimization models. Chen and Önal (2014) addressed a MINLP model to simulate a price-endogenous biofuel feedstock supply chain system.

## 2.2 MODELS WITH FACILITY LOCATION-ALLOCATION

A facility location-allocation problem applied in the bio-energy industry concerns with determining an optimal location plan for reactors/bio-refineries and designing an optimal transportation network for collecting feedstock or distributing end-product. The models built in this research fall into the category as a facility location-allocation problem.

Huang *et al*. (2010) formulated a multi-stage model for residue to determine the location and size of new facilities. The study also gives the time scheduling for plant operation and expansion. Leduc *et al*. (2010) conducted a case study for the biogas production plant in Northern Sweden. The research tended to resolve the misalignment between the plants' location and biofuel consumer and obtain an optimized methanol production plant. Eksioglu *et al*. (2010) analyzed location decision for a biofuel supply chain by modeling with MINLP and using Mississippi State as test bench. Akgul *et al*. (2011) presented a mixed MINLP model to minimize the supply chain cost and optimize the location of the bioethanol production plant. Aksoy *et al*. (2011) investigated feasibility of using forest resource and mill waste in Alabama to produce biofuel based energy.

Facility location and residue allocation problems were to be determined in researches. Zhu *et al*. (2011) provided a model to optimize biomass storage and facilities locations by considering the effect of harvesting and non-harvesting seasons influencing operation time. Zhu and Yao (2011) determined the locations of warehouses for multi-feedstock system, and provided the size of harvesting team and the biomass storage. Jason *et al*. (2012) addressed a model for a feedstock biomass equipment location system. A depth research on Iran's biodiesel production system was conducted by Avami (2012).

Potential biodiesel locations were assessed based on techno-economic parameters. Mathematical tools are extensively used to describe current biodiesel production circumstance in Iran. Bowling *et al*. (2011) optimized facility locations for a bio-refinery supply chain. Various practical costs occurred in the supply chain planning are considered within a systematic configuration. Zhang and Hu (2013) designed an operational planning model for general biofuel plant to investigate the facility location and operational levels. Li and Hu (2013) optimized fast pyrolysis facility locations for a biofuel plant to maximize the net present value of total profit in next 10 years. Lin *et al*. (2014) presented an integrated strategic for biofuel production to minimize the annual cost and studies an actual case in Illinois.

## 2.3 HEURISTICS ON GENERALIZED FACILITY LOCATION-ALLOCATION PROBLEM

Generalized studies on the location-allocation problem have a long history since beginning of the 20th century. Since the model of location-allocation problems usually contain multiple local minima, seeking of a satisfactory optimum requires careful design of a heuristic. To achieve this goal, various methodologies were designed to efficiently solve the generalized location-allocation problems.

One of the most well-known studies on such problem is the Weber problem (WP) originated from Weber (1909). The original WP dealt with locating a single facility to serve all customers. It was then extended to the Multi-facility Weber Problem (MWP) which was shown as an NP-hard problem. Early works in solving MWP can be found in Weiszfeld (1937), Miehle (1958) and Cooper (1963). A considerable number of papers were published thereafter to solve the MWP. For example, exact solution of the MWP problem can be found in Rosing (1992) and du Merle *et al*. (1999). Brimberg and Mladenovic (1996) first applied the variable neighborhood search method into MWP and Hansen *et al*. (1998) proposed a heuristic to solve continues MWP based on discrete p-media problem. A further extension of MWP is Capacitated Multi-facility Weber Problem (CMWP) which takes account the various constraints such as facility or transportation capacity and customers' demands. Publications for solving the CMWP can be found in Cooper (1972), Zainuddin and Salhi (2007), Aras *et al*. (2007), Aras *et al*. (2008) and Luis *et al*. (2011). The Multi-commodity Capacitated Multi-facility Weber Problem (MCMWP) was first introduced by Akyuz *et al*. (2009) and several heuristics were developed in Akyuz *et al*. (2010) and Akyuz *et al*. (2012).

Recently, Hajipour *et al*. (2014) develops a new meta-heuristic algorithm to solving the facilities location problem with capacity and budget limitations. Vidyarthi and Jayaswal (2014) considered a location-allocation problem with stochastic demand and provided an efficient heuristic to solving the model.

## 2.4 SHORTCOMINGS OF PREVIOUS RESEARCH

Numerous publications (see section 2.1.1 to 2.1.3) presented constructive models on supply chain design in bio-energy industry, but a few have specifically shed light on BMG production systems. Although BMG production systems share some common configurations which are also used in general bio-energy production system, there are some specific structure

that only exists in the BMG production system. For example, the need of gas pipelines for gas distribution can be characterized as a unique setup for BMG production system. Therefore, modeling the supply chain of a BMG production system requires consideration of its distinctive characters.

The works reviewed in Section 2.2 addressed the location-allocation problem applied in the bio-energy industry. However, these studies merely focus on mathematical modeling of the supply chain in the bio-energy industry without proposing efficient heuristics. Generalized studies on the location allocation problems reviewed in Section 2.3 started from the beginning of 20th century, but lack of real-world background made these heuristics difficult to be applied directly to a practical BMG production system.

In this research, four MINLP models are proposed with increasing complexity to describe the supply chain of a BMG production system. An efficient heuristic is derived for each specific MINLP. Bridging of the real-world application and theoretical operations research is the foundation of this work.

# CHAPTER III
# PROBLEM AND METHODOLOGY

Various problems emerge with the development of the BMG industry and parts of them are reviewed in Chapter II. This chapter addresses the specific problems and their corresponding methodologies.

## 3.1 PROBLEM DESCRIPTION, RESEARCH GOALS, AND OBJECTIVES

This dissertation analyzes the supply chain optimization in constructing a BMG production system. The detailed research problems, goals, and objectives are described in this section.

### 3.1.1 Problem Description

This research focuses on a BMG manufacturing system. Assume, in a given area consisting of many farms, each farm produces one or more types of agriculture residue in a seasonal basis, such as crop residue, wood residue and animal manure. The entire area can be divided into small segment by zip codes (a five-digit number used mainly for postal zoning and sorting of mails in the U.S.A.) and assume that each zip code area contains several farms. In each zip code area, there is a hub that collects residues from every farm in that area. Furthermore, assume the farms can deliver all their available residues to the hubs, while the hubs can accept and storage all the residues. During the storage of the residue in the hubs, there exist deteriorations of these materials.

A BMG production plant is planned to be built in this area, one or more reactors are required to collect residues from the hubs as feedstock and produce BMG. Assume all hubs can supply the reactors with their entire residues inventory and the reactors can process all kinds of residues. For storage and transportation convenience, condensers are needed for BMG liquefaction. Pipeline will be laid between reactors and condensers to transport BMG. An ideal

condition is that the reactor processes all available residues in the hubs to maximize BMG production. However, in practice, available labor for transporting residue from hubs to the reactors is usually limited such that the reactors can only process limited amount of residues.

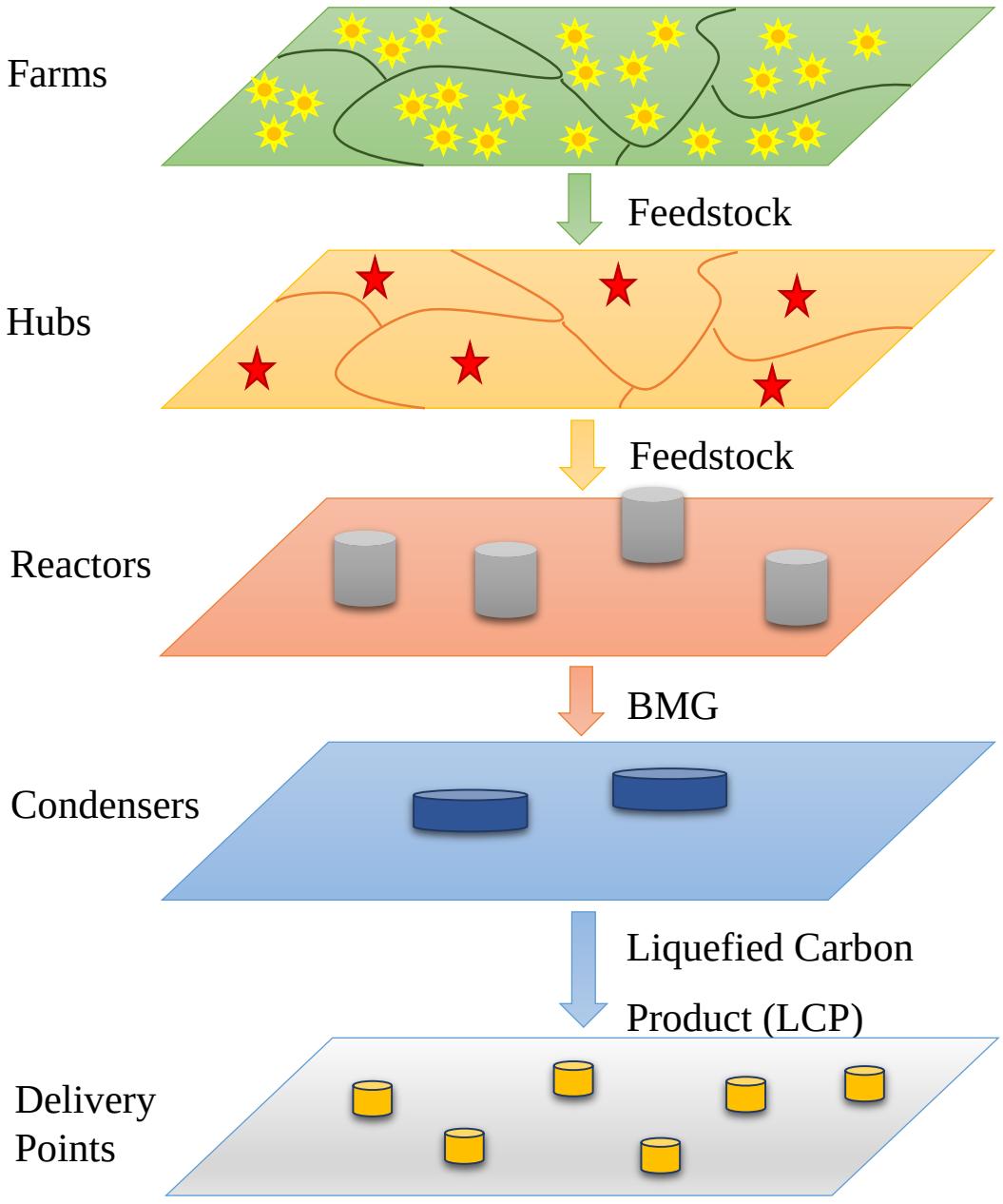


Figure 3.1: Schematic diagram of BMG manufacturing system.

To build this plant, feedstocks (residues) costs, building costs of facilities and pipelines, transportation costs of residues and BMG, and workforce costs should be taken into account. The building costs can be estimated by the construction market price, which is treated as a uniform price in the whole area. Trucks are used for transporting residues/liquefied Carbon Product and labor costs is considered for residues handling process which includes collecting, loading and unloading residues. The unit workforce cost is assumed to be homogeneous in the whole area. However, due to different roads' condition and transportation difficulties around each hub, the unit transportation cost between hubs and reactors may vary. For geographic reason, the unit pipeline laying cost varies between reactors and condensers.

A schematic diagram is provided in Figure 3.1 to illustrate the configuration of the system which can be divided into farm-to-hub (F2H) stage, hub-to-reactor (H2R) stage, reactor-to-condenser (R2C) stage and condenser-to-delivery point (C2DP) stage. Farms scattered in the same zip code area have one common hub, such that different types of residues from theses farms are transported and stored in that hub. The current research problem can be stated in the form of following goals and objectives.

### 3.1.2 Research Goals

The goal of this research is to minimize the total cost of building a BMG manufacturing system that involves fixed and variable building costs, transportation/pipeline layout costs, labor costs and residues procurement costs. Minimization of total cost is expected to be achieved by modeling the system and designing heuristics. The complete list of determine variables include the locations of hubs, reactors and condensers, the transportation network and the pipeline layout plan.

### 3.1.3 Research Objectives

This dissertation mainly focuses on the optimization of facility locations and the plan for the transportation network/pipeline layout. The determine variables depend on the type of facility and stages that a specific model contains. Therefore, the research objectives of this dissertation are described in detail for four system configurations:

1. Model I: Location-Allocation Problem of Single-stage, Single-reactor System

A single-stage, single-reactor system (SS-SRS) refers to the BMG production process going through the "hubs to reactors" layers as shown in Figure 3.1 and a single reactor being required to collect residue from the hubs. The objective of Model I is to determine an optimal location of the reactor and the amount of residue delivered to the reactor. The optimal plan is designed in the sense that the supply chain cost related to build the BMG manufacturing system is minimized.

The supply chain cost is modeled as a mixed-integer nonlinear programming (MINLP) which combines the fixed and variable building costs of reactors, transportation costs, feedstocks costs and labor costs. Various factors such as the workforce availability in a region, the demand of the reactor and the amount of residues available at each hub are considered as bounded constraints (a series of inequalities). An enumeration method is first investigated to solve for the optimal solution of the MINLP by enumerating all its feasible solutions. A heuristic is then developed to overcome the inefficiency of the enumeration method. The MINLP is decoupled into two sub-problems which consist of a convex nonlinear programming and a linear integer programming. Newton-Raphson method and B&B method are proposed to solve the two sub-problems, respectively. The heuristic is built upon alternatively solving the two sub-problems and obtaining the optimal/sub-optimal solution once convergence is achieved.

The first stage of a BMG manufacturing system is addressed and a single reactor is planned to build in Model I. The model and heuristic developed in this part serve as a foundation for the rest of subsequent models.

2. Model II: Location-Allocation Problem of Single-stage Multi-reactor System

Like an SS-SRS, a single-stage multi-reactor system (SS-MRS) covers the "hubs to reactors" layers in Figure 3.1, but it requires multiple reactors that collect residue from the hubs. It minimizes the total cost of building reactors, transporting residue, purchasing residues and hiring labor to optimally locate reactors and distribute residue to reactors. By considering multiple reactors to be built, model II allows one or more reactors collecting residue in one hub. A Heuristic is developed after modeling Model II with MINLP. A successive substitution algorithm is proposed to replace the Newton-Raphson method for efficiency purpose to solve the convex nonlinear programming which is one of the sub-problems decoupled from the original MINLP. Alternative search between two sub-problems using Successive Substitution and B&B method forms the heuristic to obtain an optimal/sub-optimal solution.

3. Model III: Three-stage Multi-Facility System Design

A three-stage multi-facilities system (TS-MFS) focuses on the configuration of BMG production system which includes "hubs to delivery points" layers as shown in Figure 3.1. In addition to determine the optimal distribution plan in H2R stage as in Model II, Model III considers the R2C and C2DP stages in which the location of the condensers , the pipeline layout plan and the transportation network for the C2DP stage are to be determined. The total supply chain cost for the three-stage model is composed of the fixed and variable building costs of the reactors and condensers, feedstocks costs, labor costs, transportation costs for collecting residues from hubs to reactors, pipeline layout costs and BMG delivery costs from

condensers to delivery points. Constraints including the demand of condensers and BMG availability are added into the new model.

Note the Model III is not simply an "add-up" of the costs from three separate stages. In fact, designing optimal plans for H2R, R2C and C2DP stages separately does not guarantee an overall optimal plan. All stages are intrinsically related. For example, the locations of the reactors influence the locations of condensers and delivery points' locations also influence condensers'. The transportation network built in the H2R stage affects the amount of residue collected by the reactors, which further has an impact on the BMG availability in each reactor. Therefore, all these correlated factors need to be reflected in building the system model. The heuristic derived in Model I and II will be extended to be compatible with Model III.

4. Model IV: Four-stage Multi-facility System Design

A four-stage multi-facilities system (FS-MFS) involves the layers from farms to delivery points in Figure 3.1. Model IV realized a more practical model by extending Model III into a complete system configuration. Instead of assuming the locations of hubs are known as in the previous models, Model IV considers a more pragmatic scenario such that each hub's location needs to be determined from the locations of local farms in each zip code area. In addition to the costs considered in Model III, the fixed and variable costs of hubs and transportation costs of residues from farms to hubs are included in Model IV. The hubs' storage capacity and workforce limitation on handling residue in a region are appended as constraints.

The supply chain design on one stage is highly dependent on the design of other stages. The convexity of the proposed MINLP no longer holds. The Genetic Algorithm is applied on solving the MINLP.

## 3.2 PROPOSED CURRENT RESEARCH METHODOLOGY

This research tends to overcome the shortcomings in literature mentioned in Section 2.4, to fill the gap between theoretical operations research and real-world practice, and to develop effective and efficient methodologies to address an emerging problem. Given the limited literature on modeling of biogas generation, it is the first time in literature that a mathematical model is developed for a complicated BMG production system location-allocation problem. Since practical cost such as transportation costs, labor costs, and reactors' building costs, is taken into consideration, the modeling process gives insightful guidance for building BMG reactors in a real world application. In the methodology aspect, novel heuristics are established specifically for the proposed models. Detailed methodologies that are used throughout the four models and contributions for each model are outlined in the following sections.

### 3.2.1 Single-Stage Single-Reactor System Model Solution Methodology

The purpose of research on an SS-SRS model is to obtain a fundamental understating of the supply chain modeling on a BMG production system and generalize an adaptive method to obtain heuristic for solving the MINLP model. This research begins with investigation on the supply chain cost and existing constraints, which are then included in the MINLP model as an objective function and inequality constraints. An enumeration algorithm is proposed to obtain the optimal solution by traversing all feasible solutions. The objective function of the MINLP is then decoupled into two sub-functions. One of the sub-functions is nonlinear and convex, which can be solved by the Newton-Raphson method. The other sub-function can be rewritten as a MILP whose optimal solution can be obtained by B&B method. The heuristic is developed based on alternatively searching between two sub-functions till convergence.

Matlab is used to realize the proposed heuristic and numerical examples are provided to verify the performance the heuristic.

### 3.2.2 Single-Stage Multi-Reactor System Model Solution Methodology

An SS-MRS model assumes multiple reactors to be built to collect residue from hubs. Follow the similar procedure as suggested in SS-SRS model to build an MINLP model. It can be seen that increasing number of reactors increases the computation complexity. Therefore, enumeration algorithm no longer be practical to solve the MINLP even for a relative small size problem. After the objective function is decoupled into two sub-functions, the more efficient Successive Substitution algorithm replaced the former Newton-Raphson method to solve one of the sub-functions. An alternative search based heuristic is proposed and its performance is evaluated by numerical examples conducted in Matlab.

### 3.2.3 Three-Stage Multi-facility System Model Solution Methodology

The TS-MFS model includes the H2R, R2C and C2DP stages. The transportation of BMG to condensers requires pipeline laying out between reactors and condensers. After modeling the TS-MFS, Nelder-Mead simplex algorithm (NMSA) along with the B&B method is applied alternatively to solve the MINLP built from the TS-MFS model.

### 3.2.4 Four-Stage Multi-Facility System Model Solution Methodology

The FS-MFS model contains all the stages shown in Figure 3.1. The locations of hubs are predefined in Model I, II and III while they are to be determined in this model. The modeling process considers seasonal inventory change of the residue in the farms. Assumptions are made such that the storage amount of some types of bio-residue including crop, wood or herb residue are changing with respect to the seasons in a year. Therefore, selection of a suitable function representing the seasonal change of inventory is needed. The Genetic Algorithm (GA) is exploit to solve the MINLP built from the FS-MFS model.

### 3.2.5 Comparison with a Classic Location-Allocation Problem

Noticeably, Francis *et al*. (1992) studied a well-platform location-allocation problem modeled by an MINLP. An ALA heuristic proposed by Cooper (1972) was used to solve their proposed MINLP. This research differ from Francis' work in several ways. First, they are modeled for different applications. One is for BMG production systems and the other is for a well-platform location-allocation scenario. Second, the models' complexity exceeds Francis' work. Even the most fundamental SS-SRS model considers more cost elements and constraints than those in the well-platform model. Third, the connection topology in Francis' work only had 0-1 logic, that is, the wells and platforms are either connected or disconnected. In this research, the amount of residue that is transported from hubs to reactors is confined as integers which has larger scope and increases the computation complexity. At last, the heuristic used for solving the models are distinct. ALA heuristic consistently locates the well to the nearest platform. This method is not applicable in this research. Take the SS-MRS model for example, since the transportation costs varies between hubs and reactors, even closer distance between a hub and reactor does not ensure a lower transportation costs. Therefore, one cannot simply located the reactors to the nearest hub. A B&B method is proposed to tackle this problem, which constitutes novelty of the heuristic in this research.

## 3.3 SCOPE

Four BMG production system models are considered in this dissertation. To achieve an optimized supply chain plan, an MINLP is proposed for each model. In this dissertation, each MINLP is specifically designed for the BMG production system and the solution for the MINLP can be adopted by decision-makers for planning new BMG production systems. However, it is reasonable to speculate that the systematic methodology for developing the MINLP model and heuristic has the potential to be extended to other systems. For example, in

the retail industry, optimizing the location of distribution centers and logistic network is critical for the control of supply chain cost. By analogy, one can expect an optimized supply chain plan for building biomethane distribution centers with reactors and end users with hubs when applying the methodology proposed in this dissertation. Another application is for the commercial airline companies building new hubs to reduce the overall traveling time. It is a straightforward procedure to replace the objective function of total cost with traveling time and to build the MINLP model with determine variables as locations of hubs and the flight network.

Not only can the modeling process proposed in this dissertation be adopted to other applications, but the designed heuristic can also be extended to other areas. For example, the alternative search-based heuristic proposed in the SS-SRS and SS-MSS models can be applied to an MINLP problem that can be decoupled into two sets of convex problems. The heuristic proposed in the TS-MFS model might be applied to MINLP problems that have no convexity observed. The GA used in the FS-MFS model has already been applied to a large set of practical problems.

That is, the methodologies proposed in this dissertation have the potential to be extended to other areas, and future research into those areas may partially rely on these results.

## 3.4 ORGANIZATION OF DISSERTATION

This dissertation is organized as follows. Chapter IV through VII investigates SS-SRS, SS-MRS, TS-MFS, and FS-MFS models, respectively. For each model, a heuristic is designed and a numerical experiment is conducted to verify the performance of the proposed heuristic. Chapter VIII further analyzes the numerical examples conducted in Chapters IV to VII. Chapter IX concludes the dissertation.

# CHAPTER IV
# MODEL I: A SINGLE-STAGE SINGLE-REACTOR SYSTEM PROBLEM

This chapter discusses the SS-SRS model which covers the hub to reactor layers in Figure 3.1. Assume hubs in different zip code areas have known position information from Geographic Information System (GIS) and all types of residue from local farms are stored in the hubs. Model I considers the supply chain design for the stage which contains the residue being transported from hubs to the reactor for producing BMG. The cost of reactor, transportation costs for the residue from hubs to the reactor, feedstocks costs and labor costs are given. Workforce limitation, reactor's demand of residue and deterioration of residue storage in hubs are considered as constraints in the model. The optimal reactor's location and the amount of residue that is transported from each hub to the reactor is to be determined.

This chapter is organized as follows. The detailed problem and notations are first described followed by assumptions made in this chapter. A MINLP model is then established for the supply chain of BMG production system. An enumeration method is proposed to find an optimal solution to such a problem. To overcome the inefficiency problem caused by the enumeration method, a heuristic is designed specifically for Model I. Several numerical examples are conducted to verify the performance of proposed heuristics. The conclusion stands at the end this chapter.

## 4.1 PROBLEM DESCRIPTION AND NOTATION

In this research, the BMG feedstock is assumed to be plant residues and livestock manure which is collected from local farms in a given area. The whole area may be divided into small pieces by zip codes and each zip code area contains several farms. There is one hub in each zip code, and the hub's location is determined by a GIS. After residues are generated,

every farm can send them to the hub in its zip code. In principle, farms can deliver all available residues to the hubs, while the hubs can accept and store all the residues.

Assume that a BMG production plant is built in a given area containing a single reactor, all hubs can supply this reactor with their residues inventory and the reactor can process all kinds of residues. An ideal condition is that the reactor processes all residues in the hubs to maximize BMG production. However, in practice, available labor for transporting residue from hubs to the reactor are usually limited such that the reactor could process limited amount of residues.

To build and operate a BMG manufacturing plant, feedstocks costs, building cost, transportation costs and labor costs should be taken into account. The building cost can be estimated from construction cost in the area. The transportation of residue is assumed to use trucks and laborers are hired for residues handling process which includes collecting, loading and unloading residues. According to the roads' condition and transportation difficulty of each hub, the unit transportation cost between hubs and the reactor may vary as well. A schematic diagram is provided in Figure 4.1 to illustrate the locations of farms, hubs, reactor and different transportation routes.

Thus, the objective of this research is to minimize the total cost of building the BMG manufacturing plant and delivering residues from the hubs to the reactor by determining the optimal location of the reactor and residues delivery quantity from each hub. Various factors such as the amount of residues available at each hub, feedstocks costs, building cost of the reactor, labor availability in the region, and transportation costs, are considered in this research.

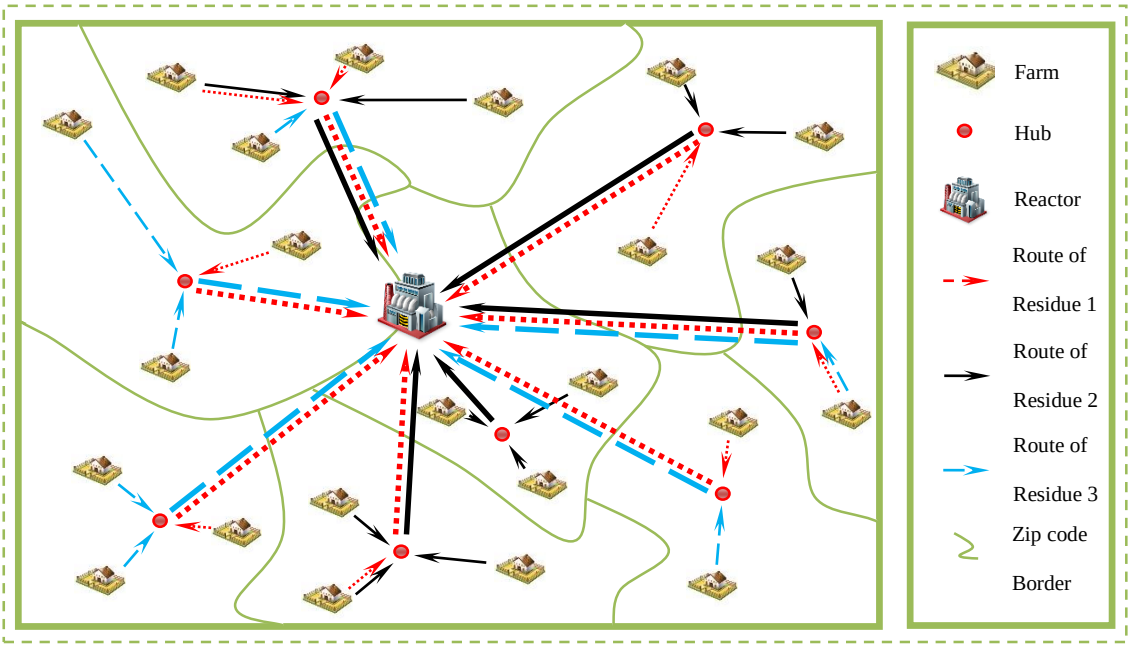


Figure 4.1: Illustration of location-allocation problem in SS-SRS BMG production system.

This dissertation follows the convention that vectors or matrices are denoted by boldface letters. Sometime an element of these vectors or matrices is also a vector or matrix depending on the interpretation of such an element. The following notations are used for modeling the problem:

**Parameters**

| | |
|---|---|
| $K$ | Total number of types of residues. |
| $Z$ | Total number of zip codes in the region. |
| $k$ | Index for residue types, $k = 1,\ldots, K$. |
| $z$ | Index of zip codes of a hub, $z = 1,\ldots, Z$. |
| $A_{zk}$ | Availability of the residue $k$ in the hub in zip code $z$ (truck-load). |
| $C^f$ | Fixed cost to build a reactor, share equally to unit time period (dollar). |
| $C^w$ | Unit cost for hiring a worker (dollar/person/truck load). |

$C_{zk}^{t}$ Unit transportation cost of moving the residue $k$ from the hub in zip code z to the reactor (dollar/truck-load/mile).

$C_{zk}^{r}$ Feedstock cost of the residue $k$ supplying from the hub in zip code $z$ to the reactor (dollar/truck-load).

$D_k$ Demand of residues $k$ at the reactor (truck-load).

$w_k$ Unit workforce required for collecting the residue $k$ (persons/truck-load).

$W$ Total workforce availability for the reactor (persons).

$\beta$ Percentage of deteriorated residue in hubs.

$\mathbf{h}_z$ $\mathbf{h}_z = (x_z^h, y_z^h)$ represents the coordinate of the hub in zip code $z$.

**Variables**

$\mathbf{r}$ $\mathbf{r} = (x, y)$ represents the coordinate of the reactor.

$\alpha_{zk}$ Number of truck-loads for moving the residue $k$ from the hub in zip code $z$ to the reactor.

$\boldsymbol{\alpha}$ A matrix $\boldsymbol{\alpha} = [\alpha_{zk}]$ representing truck-loads of residue $k$ ($k$ = 1,…, $K$) to be transported from zip code $z$ ($z$ = 1,…, $Z$) to the reactor.

**Measure of performance**

$TC(\mathbf{r}, \boldsymbol{\alpha})$ Total cost of the whole system (dollars) for locating a reactor at the coordinate point $\mathbf{r}$ and transporting $\boldsymbol{\alpha}$ truck-loads to the reactor from the residue collection hubs.

## 4.2 ASSUMPTIONS FOR MODEL I

The fundamental assumptions that are used for modeling the SS-SR system are listed as follows:

1. The locations of hubs can be collected by using a GIS.
2. The reactor has the capability to process all types of residue and has no capacity limit.
3. There is no loss of residue in transportation from the hubs to the reactor.
4. Deterioration occurs when residues are stored in hubs.
5. The constant rate of demand of residue in the reactor is given.

## 4.3 REACTOR LOCATION AND ALLOCATION MODEL

The total cost associated with construction of a BMG reactor consists of three aspects. The first aspect contains the fixed building cost that includes fixed investment for opening a reactor, such as business license fee and building design fee. The second aspect concerns with the transportation costs which is affected by the distance among hubs and reactor, the road condition, and the reactor truck capacity, and the third aspect corresponds to the expenses for hiring labor. The problem is to optimally determine the reactor's coordinate (variable), $\mathbf{r} = (x, y)$ that involves several cost factors for which the total composite cost in locating the reactor is to be minimized.

Now, define the Euclidean distance function

$$d(\mathbf{a}, \mathbf{b}) = \|\mathbf{a} - \mathbf{b}\|. \tag{4.1}$$

in which the planar location vectors $\mathbf{a} = (x_a, y_a)$, $\mathbf{b} = (x_b, y_b)$ and $\|\mathbf{a} - \mathbf{b}\| = \sqrt{(x_a - x_b)^2 + (y_a - y_b)^2}$. Let $d_z$ represent the distance from the hub in zip code $z$ to the reactor at $\mathbf{r} = (x, y)$; then

$$d_z = d(\mathbf{r}, \mathbf{h_z}) = \sqrt{(x - x_z^h)^2 + (y - y_z^h)^2} \tag{4.2}$$

Now, the reactor location problem for the BMG production system can be modeled as

**Problem BMG-R:**

$$\text{Min } TC(\mathbf{r}, \boldsymbol{\alpha}) = C^f + \sum_{z=1}^{Z} \sum_{k=1}^{K} C_{zk}^r \alpha_{zk}$$

$$+ \sum_{z=1}^{Z} \sum_{k=1}^{K} d_z C_{zk}^t \alpha_{zk} + C^w \sum_{z=1}^{Z} \sum_{k=1}^{K} w_k \alpha_{zk} \quad (4.3)$$

$$\text{Subject to:} \quad \sum_{z=1}^{Z} \sum_{k=1}^{K} w_k \alpha_{zk} \leq W, \quad (4.3a)$$

$$\sum_{z=1}^{Z} \alpha_{zk} \geq D_k, \text{ for } k = 1,\ldots, K \quad (4.3b)$$

$$\sum_{z=1}^{Z} \alpha_{zk} \leq (1-\beta) \sum_{z=1}^{Z} A_{zk}, \text{ for } k = 1,\ldots, K \quad (4.3c)$$

$$0 \leq \alpha_{zk} \leq (1-\beta)\, A_{zk} \text{ and } \alpha_{zk} \in \mathbb{Z}, \quad (4.3d)$$

where $\mathbb{Z}$ is the set of all integers. The last three terms in Equation (4.3) correspond to the building cost, feedstocks costs, transportation costs and labor costs, respectively. Constraint (4.3a) that represents the total workforce for transferring the residue $k$ from the hub of the respective zip code $z$ to the reactor is always bounded by the workforce availability in the reactor. Constraint (4.3b) indicates that the total truck-loads of residues delivered to the reactor should exceed the reactor's demand. Constraint (4.3c) that denotes the total delivered truck-loads of the residue $k$ is bounded by its availability. Constraint (4.3d) reflects that the number of truck-loads of transporting residue $k$ from the hub in zip code $z$ to the reactor is bounded by the availability of residue $k$ in the hub in zip code $z$ and is non-negative integer.

The objective function (4.3) is non-convex with respect to its two variables **r** and **α**. Therefore, it is a constrained nonlinear programming problem with possible multiple local minima. Solving such a nonlinear problem is a complex exercise to obtain the optimal solution to a mediocre size instance. Therefore, a clever techniques needs to be developed to obtain at a reasonable sub-optimal solution.

## 4.4 OPTIMAL SOLUTION

Since the biomethane gas reactor location problem, BMG-R in (4.3) is a MINLP, solving such a problem is a computational burden for a reasonable size problem. The complexity in solving these types of problems arises mainly from two perspectives: multiple stationary points due to the order and number of variables, and number of possible integer values of the variables. Therefore, a method is to be devised cleverly in a sound mathematical approach such that the sub-optimal solution is not far from the real optimum.

One such feasible and reasonable approach for a practical problem of this nature could be to fix a feasible set of $\boldsymbol{\alpha}$ values that represents the truck-loads of residues from hubs to the reactor. The problem also arises how to fix the set of $\boldsymbol{\alpha}$ values and what approaches needs to be followed to arrive at the optimal solution. Theorem 4.1 given below resolves part of these answers.

**Theorem 4.1**: Given $\boldsymbol{\alpha}$, the objective function (4.3) is always convex in $\mathbf{r}$.

**Proof:** see Appendix A.

Although the objective function (4.3) is non-convex in terms of both $\mathbf{r}$ and $\boldsymbol{\alpha}$, Theorem 4.1 states the convex property of (4.3) when $\boldsymbol{\alpha}$ is determined. Now, the present issue is to find the optimal or appropriate values of $\boldsymbol{\alpha}$. A procedure for solving the problem optimally is introduced as follows and will be discussed in details in the next section.

**Procedure 4.A:**

Step 4.A-1: List all feasible $\boldsymbol{\alpha}$ (given in next sub-section).

Step 4.A-2: For each instance of $\boldsymbol{\alpha}$, find the optimal location $\mathbf{r}$ of the reactor. A local optimal location exists when the first-order derivative of the objective function (which is a convex function in $\mathbf{r}$ for a given instance $\boldsymbol{\alpha}$) equals to zero, that is,

$$\begin{cases} \sum_{z=1}^{Z}\sum_{k=1}^{K}\dfrac{C_{zk}^{t}\alpha_{zk}(x-x_z^h)}{\sqrt{(x-x_z^h)^2+(y-y_z^h)^2}}=0 \\ \sum_{z=1}^{Z}\sum_{k=1}^{K}\dfrac{C_{zk}^{t}\alpha_{zk}(y-y_z^h)}{\sqrt{(x-x_z^h)^2+(y-y_z^h)^2}}=0 \end{cases}. \tag{4.4}$$

Step 4.A-3: Compute the total cost of locating the reactor at the local optima corresponding to the instance of **r** and **α**.

Step 4.A-4: Obtain global optimum by comparing the total cost of all instances all **r** and **α**. □

### 4.4.1 Determining the Best Set of α for Optimal Solution

An approach is proposed here to find the best feasible set of **α** values to minimize the total cost in (4.3). The allocation matrix, **α** = $[\alpha_{zk}]$, is an integer matrix since $\alpha_{zk}$ is an integer representing full truck-loads of residue for all $k$ ($k$ = 1,…, $K$) and zip code $z$ ($z$ = 1,…, $Z$). The constraints (4.3a) - (4.3d) indicates that there are limited number of feasible **α**, so an enumeration method is viable for ascertaining the best values of **α** for a small size system. Typically, there are few types residues, $K$ and zip code $Z$. For a realistic such reactor location-allocation problem, $K \leq 3$ (animal manure, wood residue and grass) and $Z \leq 15$.

Appendix B shows how to find the range of $\alpha_{zk}$ based on the constraints in Problem BMG-R. The upper and lower bounds of $\alpha_{zk}$ is thus given by (B.3)

$$\alpha_{zk} \in \left[0, min\left(\frac{W}{w_k}, (1-\beta)\sum_{j=1}^{Z}A_{jk}, A_{zk}\right)\right],\ z = 1,\ldots, Z,\ k = 1,\ldots, K,\ \alpha_{zk} \in \mathbb{R}.$$

Note that a random value of $\alpha_{zk} \in \mathbb{R}$ in (B.3) is not necessarily a feasible solution of the objective function in (4.3) because the set in (B.3) provides merely a relaxed limits of $\alpha_{zk}$. The purpose of estimating the bounds is to minimize the effort of finding all feasible **α** since the infeasible ones can always be removed by examining the constraints (4.3a) - (4.3d) with this **α** values. As a result, the feasible set becomes further reduced, contributing to the computational advantages.

As discussed above, the values of $\alpha_{zk}$ are between 0 and $min\left(W/w_k, (1-\beta)\sum_{j=1}^{Z} A_{jk}, A_{zk}\right)$. Then, the norm of the feasible set of *each* $\alpha_{zk}$ is

$$\theta_{zk} = \left\lceil min\left(\frac{W}{w_k}, (1-\beta)\sum_{j=1}^{Z} A_{jk}, A_{zk}\right)\right\rceil, z = 1,\ldots, Z, k = 1,\ldots, K. \quad (4.5)$$

Since $\boldsymbol{\alpha}$ has $Z \times K$ elements with norm $\theta_{zk}$, the number of possible instances of $\boldsymbol{\alpha}$, $\theta$, is given by

$$\theta = \prod_{z=1}^{Z}\prod_{k=1}^{K}\theta_{zk} = \prod_{z=1}^{Z}\prod_{k=1}^{K}\left\lceil min\left(\frac{W}{w_k}, (1-\beta)\sum_{j=1}^{Z} A_{jk}, A_{zk}\right)\right\rceil, \quad (4.6)$$

which reflects the worst computation complexity of enumeration for search of optimality. Since $\boldsymbol{\alpha}$ values are determinable in finite cases, the problem in (4.3) can yield the optimal solution as Problem BMG-R forms a convex function (Proof is presented in Appendix A). Thus, a gradient approach is adopted to arrive at the optimal solution.

### 4.4.2 Optimal Location with a Specified α

Theorem 4.1 provides the condition for the reactor's optimal location given in equation (4.4). Obviously, equations in (4.4) are simultaneous higher-order nonlinear equations which cannot be solved by direct method to obtain an explicit solution immediately. Thus, a Newton–Raphson method for solution of this problem is initially described and illustrated to approximate the solution to (4.4). Details of the transformation of (4.4) to adapt to Newton-Raphson method is given in Appendix C.

**Algorithm 4.A: Main Procedure**

Step 4.A-1: Initialize $TC^{min} = +\infty$.

Step 4.A-2: Substitute corresponding parameters into equation (B.3) and obtain the bounds of

$$\alpha_{zk} \in \left[0, min\left(\frac{W}{w_k}, (1-\beta)\sum_{j=1}^{Z} A_{jk}, A_{zk}\right)\right], z = 1,\ldots, Z, k = 1,\ldots, K.$$

Step 4.A-3: Generate a $\boldsymbol{\alpha}$ within the bound in Step 4.A-2.

Step 4.A-4: Check feasibility of the generated $\boldsymbol{\alpha}$ by the criterion (4.3a)-(4.3d). If $\boldsymbol{\alpha}$ fails to satisfy either one of the constraints, go to Step 4.A-3; else proceed to the next step.

Step 4.A-5: Find the location.

(a) Use Algorithm 4.B (given below) with the transportation allocation matrix $\boldsymbol{\alpha}$, and obtain the total cost *TC* and optimal reactor's location $\mathbf{r}$.

(b) If $TC < TC^{min}$, then $TC^{min} = TC$, $\boldsymbol{\alpha}^{opt} = \boldsymbol{\alpha}$, $\mathbf{r}^{opt} = \mathbf{r}$.

Step 4.A-6: If enumeration of $\boldsymbol{\alpha}$ is not completed, go to Step 4.A -3, else the optimal solutions are stored in $TC^{min}$, $\boldsymbol{\alpha}^{opt}$ and $\mathbf{r}^{opt}$.

Step 4.A-7: Stop. □

**Algorithm 4.B: Optimal location**

Step 4.B-1: Generate an initial random coordinate $(x_0, y_0)$ for the reactor. Set the minimum step size $\Delta_{min}$ and let $i = 0$.

Step 4.B-2: Update the next step of coordinate for the reactor with equation (C.4):

$$\begin{bmatrix} x^{next} \\ y^{next} \end{bmatrix} = \mathbf{r}^{curr} - H[TC(\mathbf{r}^{curr})]^{-1} \sum_{z=1}^{Z} \sum_{k=1}^{K} \frac{C_{zk}^{t} \alpha_{zk}}{\mathrm{d}(\mathbf{r}^{curr}, \mathbf{h}_z)} (\mathbf{r}^{curr} - \mathbf{h}_z).$$

Calculate the step size $\Delta$, update $x^{curr} = x^{next}$ and $y^{curr} = y^{next}$. Let $i = i + 1$.

Step 4.B-3: If $\Delta > \Delta_{min}$, go to Step 4.B-2.

Step 4.B-4: The optimal reactor's location is $\mathbf{r}^{opt} = \mathbf{r}^{curr} = (x^{curr}, y^{curr})$.

Step 4.B-5: Stop. □

The optimization algorithm considers all feasible $\boldsymbol{\alpha}$ and finds the optimal reactor's position as well as the minimum cost for each $\boldsymbol{\alpha}$. The whole solution algorithm for the problem is thus given by selecting the smallest total cost among all enumerating steps. The detailed algorithm is provided as follows.

**Example 4.1: A Three-hub Three-residue Problem**

A numerical example is provided here with 3 hubs ($Z$ = 3) and 3 types of residues (K = 3). Other system parameters are as follows: total workforce availability for the reactor, W = 60 persons, work-force requirement $(w_1, w_2, w_3)$ = (2, 3, 3) persons/truck-load, percent of deterioration residue $\beta$= 0.05, demand of residues ($D_1$, $D_2$, $D_3$) = (8, 5, 6) truck-loads, location of the hubs [$(x_1^h, y_1^h)$, $(x_2^h, y_2^h)$, $(x_3^h, y_3^h)$] = [(0,0), (60,10), (30,70)], fixed building cost $C^f$ = \$2,000,000, the unit work-force cost $C^w$ = \$10/person/truck-load. The unit transportation cost $\mathbf{C}^t = [c_{zk}^t] = \begin{bmatrix} 4.0 & 3.8 & 4.1 \\ 4.1 & 4.0 & 4.0 \\ 4.8 & 4.2 & 4.1 \end{bmatrix}$ dollar/truck-load/mile, feedstock cost $\mathbf{C}^r = [c_{zk}^r] = \begin{bmatrix} 150 & 200 & 200 \\ 160 & 190 & 130 \\ 138 & 185 & 120 \end{bmatrix}$ dollar/truck-load, and availability of the residue $\boldsymbol{A} = [A_{zk}] = \begin{bmatrix} 4 & 2 & 2 \\ 3 & 2 & 2 \\ 3 & 2 & 3 \end{bmatrix}$ truck-loads.

Given these system parameters for the reactor-in-farm location problem, the computational scheme for the main procedure is shown below to illustrate the algorithmic mechanics.

Step 4.A-1: Initialize $TC^{min} = +\infty$.

Step 4.A-2: Substituting the corresponding parameters into equation (B.3),

$$\alpha_{zk} \in \left[0, min\left(\frac{W}{w_k}, (1-\beta)\sum_{j=1}^{Z} A_{jk}, A_{zk}\right)\right],\ z = 1,\ldots, Z,\ k = 1,\ldots, K.$$

Then the upper and lower bound of each $\alpha_{zk}$ is

$\alpha_{11} \in \left[0, min\left(\frac{60}{2}, (1-0.05)(4+2+2), 4\right)\right]$=$[0, min(30, 7.6, 4)]$= [0,4] which means the feasible set of $\alpha_{11}$ = {0,1,2,3,4} where the lower bound (LB) and upper bound (UB) are 0 and 4, respectively.

$\alpha_{12} \in \left[0, min\left(\frac{60}{3}, (1-0.05)(4+2+2), 2\right)\right] = [0, min(20, 7.6, 2)] = [0,2]$

and the feasible set of $\alpha_{12}$ is {0,1,2} with lower bound 0 and upper bound 2.

Likewise, calculating the bounds of all $\alpha_{zk}$, the upper bounds of each element $\alpha_{zk}$ in $\boldsymbol{\alpha}$ is obtained as $UB_{\alpha} = \begin{bmatrix} 4 & 2 & 2 \\ 3 & 2 & 2 \\ 3 & 2 & 3 \end{bmatrix}$.

So considering *zero* as a value, the total number of feasible instances of $\boldsymbol{\alpha}$ equals to $5 \times 3 \times 3 \times 4 \times 3 \times 3 \times 4 \times 3 \times 4 = 77760$ in this case. Now the computation is performed using one instance of $\boldsymbol{\alpha}$, starting from the lowest to highest value of each $\alpha_{zk}$.

Iteration 4.A-1:

Step 4.A-3: The first instance, $\boldsymbol{\alpha} = \begin{bmatrix} 0 & 0 & 0 \\ 0 & 0 & 0 \\ 0 & 0 & 0 \end{bmatrix}$ is generated from within the UB in Step 4.A-2.

Step 4.A-4: The current $\boldsymbol{\alpha}$ in Step 4.A-3 does not satisfy all constraints (4.3a)-(4.3d), so pick up the next instance of $\boldsymbol{\alpha}$.

Iteration 4.A-2:

Step 4.A-3: Generating $\boldsymbol{\alpha} = \begin{bmatrix} 0 & 0 & 0 \\ 0 & 0 & 0 \\ 0 & 0 & 1 \end{bmatrix}$ within the bound in Step 4.A-2.

Step 4.A-4: Check feasibility of the generated $\boldsymbol{\alpha}$ by the criterion (4.3a)-(4.3d). $\boldsymbol{\alpha}$ does not satisfy all constraints, goes back to Step 4.A-3 [This computation repeats Step 4.A-3 and Step 4.A-4 until a feasible $\boldsymbol{\alpha}$ appears].

Step 4.A-3: Continuing, in this fashion, a new $\boldsymbol{\alpha} = \begin{bmatrix} 2 & 1 & 1 \\ 3 & 2 & 2 \\ 3 & 2 & 3 \end{bmatrix}$ within the bound in Step 4.A-2.

Step 4.A-4: The incumbent $\boldsymbol{\alpha}$ satisfies constraints (4.3a)-(4.3d).

Step 4.A-5: Algorithm 4.B prompts to find a location with the allocation matrix $\boldsymbol{\alpha}$.

Sub-iteration 4.B-1:

Step 4.B-1: Generating an initial coordinate $(x_0, y_0)$ = $(x^{next}, y^{next})$ = (30, 26.6667) for the reactor. Set the minimum step size $\Delta_{min}$ = 0.001 and let $i$ = 0.

Step 4.B-2: Update the next step of coordinate for the reactor with equation (C.4), obtain $x^{next}$ = 36.3301, $y^{next}$ = 31.9814. Calculate the step size $\Delta = \sqrt{(x^{next} - x^{curr})^2 + (y^{next} - y^{curr})^2}$ = $\sqrt{(36.3301 - 30)^2 + (31.9814 - 26.6667)^2}$ = 8.2654, update $x^{curr}$ = 36.3301 and $y^{curr}$ = 31.9814. Reset $i = i$+1 = 1.

Step 4.B-3: Since $\Delta$ = 8.2654 > $\Delta_{min}$ = 0.001, repeat Step 4.B-2.

Sub-iteration 4.B-2:

Step 4.B-2: Update the next step of coordinate for the reactor with equation (C.4), obtain $x^{next}$ = 37.7662, $y^{next}$ = 31.9814. Calculate the step size $\Delta = \sqrt{(x^{next} - x^{curr})^2 + (y^{next} - y^{curr})^2}$ = 2.7093, update $x^{curr}$ = 37.7662 and $y^{curr}$ = 31.9814. $i = i$+1 = 2.

Step 4.B-3: Since $\Delta$ = 2.7093 > $\Delta_{min}$ = 0.001, repeat Step 4.B-2.

After 48 iterations, the last iteration with current $\boldsymbol{\alpha}$ is:

Step 4.B-2: Update the next step of coordinate for the reactor with equation (C.4), obtain $x^{next}$ = 35.7578, $y^{next}$ = 41.3409. Calculate the step size $\Delta = \sqrt{(x^{next} - x^{curr})^2 + (y^{next} - y^{curr})^2}$ = 0.00093, update $x^{curr}$ = 35.7578 and $y^{curr}$ = 41.3409. $i = i$+1 = 48.

Step 4.B-3: Since $\Delta$ = 0.00093 < $\Delta_{min}$ = 0.001, proceed to the next step.

Step 4.B-4: The optimal reactor's location is $\mathbf{r}^{opt} = \mathbf{r}^{curr}$ = (35.7578, 41.3409).

The sub-iterations for finding an optimal location for the current $\boldsymbol{\alpha}$ = $\begin{bmatrix} 2 & 1 & 1 \\ 3 & 2 & 2 \\ 3 & 2 & 3 \end{bmatrix}$ stops and Algorithm 4.A is prompted to find the total cost.

Step 4.A-5: (b) For $\mathbf{r}^{opt} = \mathbf{r}^{curr}$ = (35.7578, 41.3409) and the current $\boldsymbol{\alpha}$ given above, the total cost using equation (3.3) is computed as TC = \$2,206,330 < $TC^{min} = +\infty$. Therefore, $TC^{min}$ = \$2,206,330 (updated) with the corresponding coordinate $\mathbf{r}^{opt}$ = (35.7578, 41.3409) and $\boldsymbol{\alpha}^{opt} = \begin{bmatrix} 2 & 1 & 1 \\ 3 & 2 & 2 \\ 3 & 2 & 3 \end{bmatrix}$.

Step 4.A-6: Enumeration is not completed. The procedure repeats between Steps 4.A-3 and 4.A-4 until the next feasible $\boldsymbol{\alpha}$ value is obtained.

Step 4.A-3: Generating $\boldsymbol{\alpha} = \begin{bmatrix} 2 & 1 & 2 \\ 3 & 2 & 1 \\ 3 & 2 & 3 \end{bmatrix}$ within the bound in Step 4.A-2.

Step 4.A-4: Check feasibility of the generated $\boldsymbol{\alpha}$ by the criterion (4.3a)-(4.3d). Because $\boldsymbol{\alpha}$ satisfy all constraints, proceed to the next step.

Step 4.A-5: (a) Call the Algorithm 4.B with the transportation allocation matrix $\boldsymbol{\alpha}$.

Iteration 4.B-1:

Step 4.B-1: Generating an initial coordinate $(x_0, y_0)$ = (30, 26.6667) for the reactor.

Set the minimum step size $\Delta_{min}$ = 0.001, $i$ = 0.

Step 4.B-2: Update the next step of coordinate for the reactor with equation (C.4), obtain $x^{next}$ = 33.1214, $y^{next}$ = 31.6319. Calculate the step size $\Delta = \sqrt{(x^{next} - x^{curr})^2 + (y^{next} - y^{curr})^2}$ = 5.8649, update $x^{curr}$ = 33.1214 and $y^{curr}$ = 31.6319. $i = i$+1 = 1.

Step 4.B-3: Since $\Delta$ = 5.8649 > $\Delta_{min}$ = 0.001, go to Step 4.B-2.

Iteration 4.B-2:

Step 4.B-2: Update the next step of coordinate for the reactor with equation (C.4), obtain $x^{next}$ = 33.9110, $y^{next}$ = 34.5235. Calculate the step size $\Delta = \sqrt{(x^{next} - x^{curr})^2 + (y^{next} - y^{curr})^2}$ = 2.9974, update $x^{curr}$ = 33.9110 and $y^{curr}$ = 34.5235. $i = i + 1 = 3$.

Step 4.B-3: Since $\Delta = 2.9974 > \Delta_{min} = 0.001$, go to Step 4.B-2.

After 47 iterations, the last iteration with current **α** is:

Step 4.B-2: Update the next step of coordinate for the reactor with equation (C.4), obtain $x^{next}$ = 32.5379, $y^{next}$ = 43.8558. Calculate the step size $\Delta = \sqrt{(x^{next} - x^{curr})^2 + (y^{next} - y^{curr})^2}$ = 0.00090, update $x^{curr}$ = 32.5379 and $y^{curr}$ = 43.8558. $i = i + 1 = 47$.

Step 4.B-3: Since $\Delta = 0.00090 < \Delta_{min} = 0.001$, proceed to the next step.

Step 4.B-4: The optimal reactor's location is $\mathbf{r}^{opt} = \mathbf{r}^{curr}$ = (32.5379, 43.8558).

Step 4.B-5: Stop.

Step 4.A-5: (b) Obtain $TC$ = \$2,206,378 > $TC^{min}$ = \$2,206,330. Therefore, no change on the optimal solutions.

Step 4.A-6: Enumeration is not completed, proceed to Step 4.A-3. □

The optimal solution is obtained after enumeration process is completed, which is listed below

| $\alpha^*$ | $r^*$ | $TC^*$ |
|---|---|---|
| $\begin{bmatrix} 4 & 2 & 2 \\ 3 & 2 & 2 \\ 1 & 1 & 2 \end{bmatrix}$ | (24.2831,14.5193) | \$2,206,224 |

The optimal method provided above can solve small size problems as well. However, as shown in (4.6), the computation complexity grows exponentially with $K$ and $Z$. Therefore, a heuristic will be given in the next section for solving large size systems, which usually contain hundreds of hubs and more types of residues.

## 4.5 HEURISTICS

The enumeration method is incapable of solving a large scale nonlinear mixed integer programming in a reasonable amount of time. Therefore, a heuristic is required to obtain a fast convergence to an optima/a sub-optimal solution. Before addressing the heuristic, a new problem is provided, which can be deduced by elementary algebraic computation from equation (4.3).

Let $T$: $\mathbb{R}^{Z\times K} \rightarrow \mathbb{R}^{ZK}$ be a function that transforms a $Z \times K$ matrix to a vector with length $ZK$ by rearranging all columns of the matrix into one column. Denote $\mathbf{1}_s$ a length $s$ vector of all ones and $\mathbf{I_s}$ an $s \times s$ identity matrix. Note the symbol $\otimes$ the Kronecker matrices product and the symbol $\circ$ the element-wise matrices product (Refer to Appendix D for definition details and examples of all notation in this section).

**Problem 4.1:**

If the location of the reactor **r** is known, the system model (4.3) can be written in the form of a linear integer programming (LIP):

$$\text{Min } TC(\mathbf{V}) = \boldsymbol{B}^T\mathbf{V} + \Theta \tag{4.7}$$

$$\text{Subject to: } \mathbf{PV} \leq \mathbf{Q} \tag{4.7a}$$

$$\mathbf{V} = (v_i) \in \mathbb{Z}^{ZK},\ v_i \geq 0 \text{ for } i = 1,\ldots, ZK \tag{4.7b}$$

where $\mathbf{V} = T(\boldsymbol{\alpha}) \in \mathbb{Z}^{ZK}$, $\mathbf{B} = T(\mathbf{C}^{\boldsymbol{r}}) + (\mathbf{1}_k \otimes \mathbf{d}) \circ T(\mathbf{C}^{t}) + T(\mathbf{C}^{\boldsymbol{r}}) + \mathbf{C}^{w}(\mathbf{w} \otimes \mathbf{1}_z)$, $\mathbf{C}^{\boldsymbol{r}} = (C_{zk}^{r}) \in \mathbb{R}^{ZK}$, $\mathbf{C}^{\boldsymbol{t}} = (C_{zk}^{t}) \in \mathbb{R}^{Z \times K}$, $\mathbf{w} = (w_k) \in \mathbb{R}^{K}$, $\mathbf{d} = (d_z) \in \mathbb{R}^{Z}$, $\Theta = C^{f} + \sum_{n=1}^{N} nC^{v}$, $\mathbf{P} = \begin{bmatrix} (\mathbf{w} \otimes \mathbf{1}_z)^T \\ -\mathbf{I}_k \otimes (\mathbf{1}_z^T) \\ \mathbf{I}_k \otimes (\mathbf{1}_z^T) \end{bmatrix}$, and $\mathbf{Q} = \begin{bmatrix} \boldsymbol{W} \\ -\mathbf{D} \\ (1-\beta)\mathbf{I}_k \otimes (\mathbf{1}_z^T) T(\mathbf{A}) \end{bmatrix}$.

Theorem 4.1 provides an optimal reactor's location **r** under a given **α**. On the other hand, Problem 4.1 states the existence of an optimal allocation **α** given the condition that the reactor's location **r** is known. As the convex program in Theorem 4.1 can be solved numerically by Algorithm 4.B, the LIP derived in Problem 4.1 can also be solved using the B&B method. The optimal solution of each node is obtained from a relaxed problem of (4.7). The relaxed problem has the same objective function and constraints with respect to its corresponding LIP except that it has no integer constraint.

**Algorithm 4.C: Depth-first Branch and Bound method**

Step 4.C-1: Let the best objective value (upper bound) of the linear integer problem (4.7) be $TC_{best}$ and set $TC_{best} = +\infty$.

Step 4.C-2: Solve the LP relaxed problem based on (4.7). If integer solution of **V** is obtained, stop the process. Otherwise, branch on the most-fractional number in **V** and form two new active nodes (sub-problems).

Step 4.C-3: Select an active node based on depth-first criterion and let it be inactive. Solve the current relaxed sub-problem. Obtain $\mathbf{V}^{*}$ and $TC^{*}$ as the optimal solution and objective value.

Step 4.C-4: If there is no feasible solution of the current node, fathom the current node and make it inactive.

Step 4.C-5: If $\mathbf{V}^*$ is an integer vector that is the first integer obtained, $TC_{best} = TC^*$, fathom the current node and make it inactive. Otherwise proceed to the next step.

Step 4.C-6: If $\mathbf{V}^*$is an integer vector but is not the first integer obtained, then if $TC^* < TC_{best}$, let $TC_{best} = TC^*$, fathom the current node and make it inactive. Otherwise fathom the current node and make it inactive.

Step 4.C-7: If $\mathbf{V}^*$ is not an integer vector, then if $TC^* \geq TC_{best}$, fathom the current node and make it inactive. Otherwise, branch on the most-fractional number in $\mathbf{V}^*$ and form two new active nodes.

Step 4.C-8: If there exists active node, then go to Step 4.C-3; otherwise, stop. □

The natural of the original model (4.3) can be considered as two sub-problems coupled. One of the sub-problem is convex so that global minimum can be obtained using Algorithm 4.A. The other sub-problem is a constrained linear integer programming whose optimal/sub-optimal solution can be obtained from B&B method in a reasonably finite time. The idea of heuristic comes from alternatively searching between both sub-problems. That is, use the result of one sub-problem as the input data to the other. Running both Algorithm 4.A and 4.C alternatively until the optimal result of both sub-problems becomes constant. The detailed heuristic is proposed as follows.

**Algorithm 4.D (Main Program): Alternating Local Minima Heuristic (ALMH)**

Step 4.D-1: Take $r_1 = \left(\frac{1}{Z}\sum_{z=1}^{Z} x_z^h, \frac{1}{Z}\sum_{z=1}^{Z} y_z^h\right)$. Set $TC_{opt} = +\infty$.

Step 4.D-2: Run the B&B procedure to find the optimal allocation $\boldsymbol{\alpha}_1$based on $\mathbf{r}_1$. Let the objective value be $TC_1$.

Step 4.D-3: Run Algorithm 4.B to find the optimal location $\mathbf{r}_2$ based on $\boldsymbol{\alpha}_1$. Let the objective value be $TC_2$.

Step 4.D-4: If $TC_2 < TC_{opt}$, then $TC_{opt} = TC_2$, $\boldsymbol{\alpha}_{opt} = \boldsymbol{\alpha}_1$, $\mathbf{r}_{opt} = \mathbf{r}_2$.

Step 4.D-5: If $|TC_1 - TC_2| >$ infinitesimal number, then $\mathbf{r}_1 = \mathbf{r}_2$ and go to Step 4.D-2. Else stop and the optimal solution are stored in $TC_{opt}$, $\boldsymbol{\alpha}_{opt}$ and $\mathbf{r}_{opt}$. □

**Example 4.2: A Three-Hub-Two-Residue problem**

Another numerical example is provided with 3 hubs ($Z$ = 3) and 2 types of residues ($K$ = 2). Other system parameters are as follows: total workforce availability for the reactor, $W$ = 40 persons, work-force requirement ($w_1$ , $w_2$) = (1, 1) persons/truck-load, percent of deterioration residue β = 0.05, demand of residues ($D_1$ , $D_2$ ) = (6.1, 7) truck-loads, location of the hubs [$(x_1^h, y_1^h)$ , $(x_2^h, y_2^h)$ , $(x_3^h, y_3^h)$] = [(0, 0), (60, 10), (30, 70)], for simplicity, the constants fixed building cost $C^f = 0$, and the unit work-force cost $C^w$ = \$10/person/truck-load. The unit transportation cost $\boldsymbol{C}^t = [C_{zk}^t] = \begin{bmatrix} 1 & 5 \\ 4 & 5 \\ 9 & 8 \end{bmatrix}$ dollar/truck-load/mile, feedstock cost $\boldsymbol{C}^r = [C_{zk}^r] = \begin{bmatrix} 4 & 5 \\ 4 & 1 \\ 7 & 8 \end{bmatrix}$ dollar/truck-load, and availability of the residue $\boldsymbol{A} = [A_{zk}] = \begin{bmatrix} 3 & 3 \\ 3 & 3 \\ 3 & 3 \end{bmatrix}$ truck-loads.

From Problem 4.1, the original model (4.3) can be transferred to a linear integer problem (4.7) given the reactor's location **r** is known. Therefore, with the data provided above,

$$\mathbf{V} = T(\boldsymbol{\alpha}) = [\alpha_{11}\ \alpha_{21}\ \alpha_{31}\ \alpha_{12}\ \alpha_{22}\ \alpha_{32}]^{\boldsymbol{T}}$$

$$B = T(\mathbf{C}^r) + (\mathbf{1}_k \otimes \mathbf{d}) \circ T(\mathbf{C}^t) + T(\mathbf{C}^r) + \mathbf{C}^w(\mathbf{w} \otimes \mathbf{1}_z)$$

$$= [4\ 4\ 7\ 5\ 1\ 8]^T + \left(\begin{bmatrix}1\\1\end{bmatrix} \otimes \begin{bmatrix}d_1\\d_2\\d_3\end{bmatrix}\right) \circ [1\ 4\ 9\ 5\ 5\ 8]^{\boldsymbol{T}} + 10\left(\begin{bmatrix}1\\1\end{bmatrix} \otimes \begin{bmatrix}1\\1\\1\end{bmatrix}\right)$$

$$= [4\ 4\ 7\ 5\ 1\ 8]^T + [d_1\ d_2\ d_3\ d_4\ d_5\ d_6] \circ [1\ 4\ 9\ 5\ 5\ 8]^{\boldsymbol{T}} + 10[1\ 1\ 1\ 1\ 1\ 1]^T$$

$$= [4 + d_1 + 10\ \ 4 + 4d_2 + 10\ \ 7 + 9d_3 + 10\ \ 5 + 5d_1 + 10\ \ 1 + 5d_2 + 10\ \ 8 + 8d_3 + 10]^T$$

$= [14 + d_1 \;\; 14 + 4d_2 \;\; 17 + 9d_3 \;\; 15 + 5d_1 \;\; 11 + 5d_2 \;\; 18 + 8d_3]^T$,

$\Theta = C^f + \sum_{n=1}^{N} nC^v = 0$

$$\mathbf{P} = \begin{bmatrix} (\mathbf{w} \otimes \mathbf{1}_z)^T \\ -\mathbf{I}_k \otimes (\mathbf{1}_z^T) \\ \mathbf{I}_k \otimes (\mathbf{1}_z^T) \end{bmatrix}$$

$$= \begin{bmatrix} 1 & 1 & 1 & 1 & 1 & 1 \\ -1 & -1 & -1 & 0 & 0 & 0 \\ 0 & 0 & 0 & -1 & -1 & -1 \\ 1 & 1 & 1 & 0 & 0 & 0 \\ 0 & 0 & 0 & 1 & 1 & 1 \end{bmatrix}$$

$$\mathbf{Q} = \begin{bmatrix} \boldsymbol{W} \\ -\mathbf{D} \\ (1-\beta)\mathbf{I}_k \otimes (\mathbf{1}_z^T) T(\mathbf{A}) \end{bmatrix}$$

$= [-27.0 \;\; -6.1 \;\; -7.0 \;\; 8.6 \;\; 8.6]^T$

Running the Algorithm 4.D (Main Program), yields:

Step 4.D-1: Taking $\mathbf{r}_1 = [30 \;\; 26.67]^T$, Set $TC_{opt} = +\infty$.

Iteration 4.D-1:

Step 4.D-2: Running the B&B method with $\mathbf{r}_1 = [30 \;\; 26.67]^T$. Since the location of the reactor is known, the distance vector $\mathbf{d}$ can be obtained $\mathbf{d} = [d_1 \;\; d_2 \;\; d_3]^T = [40.14 \;\; 34.32 \;\; 43.33]^T$. Therefore, the linear integer programming (4.7) can be solved by B&B method.

Step 4.C: The step of the B&B method is shown in Figure 4.2. Each rectangular box denotes a node in a tree. The depth-first convention renders the visiting order of the nodes as follows: sub-problem 1 → 2→4→6→7→8→9→5→10→11→3. The new constraints adding to the sub-problems are shown adjacent to the arrows. The optimal solution is found in sub-problem 6. Therefore, set $TC_1 = 2582.77$, $\boldsymbol{\alpha}_1 = T^{-1}(\mathbf{V}) = \begin{bmatrix} 3 & 3 \\ 3 & 3 \\ 1 & 1 \end{bmatrix}$.

Step 4.D-3: Based on $\boldsymbol{\alpha}_1$, run Algorithm 4.B and find the optimal location $\mathbf{r}_2 = [55.1 \;\; 12.3]^T$, $TC_2 = 2429.04$.

Step 4.D-4: $TC_2 < TC_{opt}$, then $TC_{opt} \coloneqq TC_2 = 2429.04$, $\boldsymbol{\alpha}_{opt} = \begin{bmatrix} 3 & 3 \\ 3 & 3 \\ 1 & 1 \end{bmatrix}$, $\mathbf{r}_{opt} = \mathbf{r}_2 = [55.1 \;\; 12.3]^T$.

Step 4.D-5: Setting the infinitesimal number to be 0.1. $|TC_1 - TC_2| >$ infinitesimal number, then $\mathbf{r}_1 = \mathbf{r}_2$ and go to Step 4.D-2.

Iteration 4.D-2:

Step 4.D-2: Running Algorithm 4.C with $\mathbf{r}_1 = [55.1 \;\; 12.3]^T$. Obtain $\boldsymbol{\alpha}_1 = \begin{bmatrix} 3 & 3 \\ 3 & 3 \\ 1 & 1 \end{bmatrix}$ and $TC_1 = 2429.04$.

Step 4.D-3: Running Algorithm 4.B and find the optimal location $\mathbf{r}_2 = [55.1 \;\; 12.3]^T$ based on $\boldsymbol{\alpha}_1$. $TC_2 = 2429.04$.

Step 4.D-4: $TC_2 < TC_{opt}$, then $TC_{opt} \coloneqq TC_2 = 2429.04$, $\boldsymbol{\alpha}_{opt} = \begin{bmatrix} 3 & 3 \\ 3 & 3 \\ 1 & 1 \end{bmatrix}$, $\mathbf{r}_{opt} = \mathbf{r}_2 = [55.1 \;\; 12.3]^T$.

Step 4.D-5: $TC_1 = TC_2$. Stop the procedure and the optimal solution is stored in $TC_{opt}$, $\boldsymbol{\alpha}_{opt}$ and $\mathbf{r}_{opt}$. □

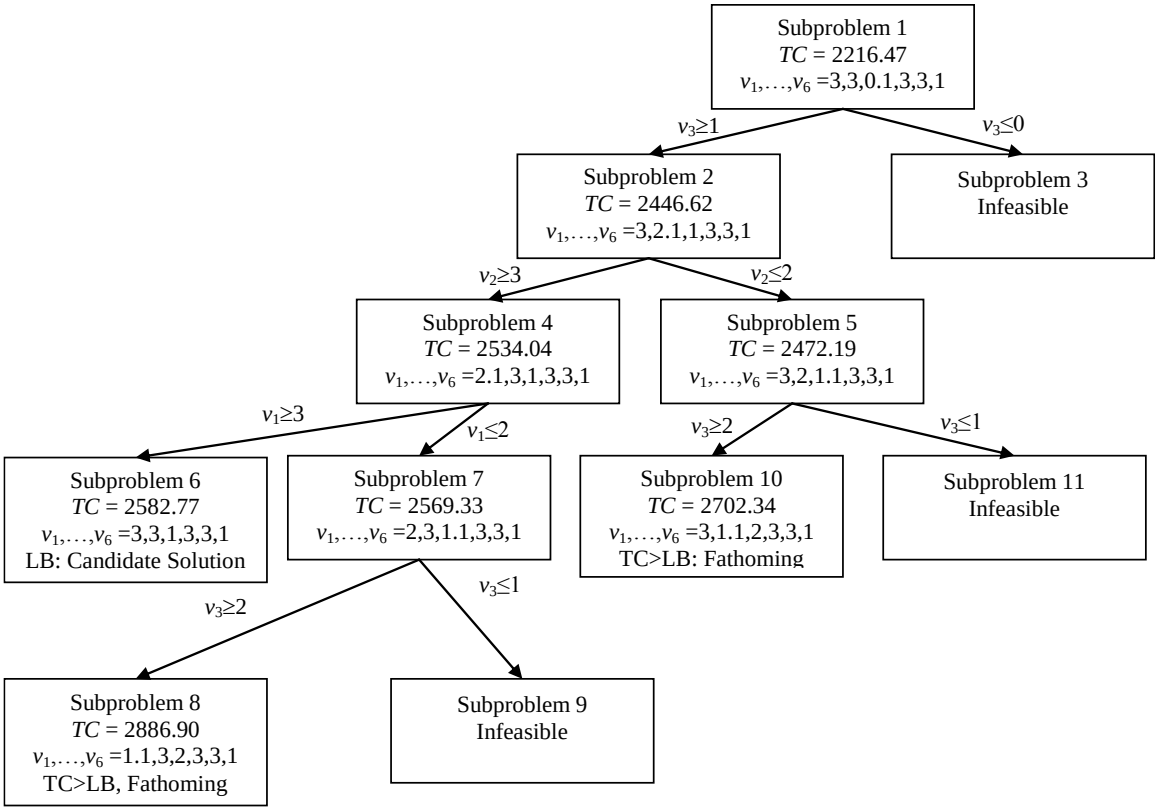


Figure 4.2: Branch and Bound method flow chart for Example 4.2.

By alternatively seeking optimal solutions for two decoupled minimization problems, a local optimal is expected to be derived for the BMG production system model (4.3). For both minimization problems, Newton-Raphson Method and B&B method are applied alternatively. Example 4.2 shows step by step the heuristic working for a relatively small-size problem and in the next section, more numerical examples are conducted to show its efficiency.

## 4.6 NUMERICAL EXAMPLES

To verify the performance of the heuristics ALMH proposed in the last chapter, numerical examples, whose parameters are selected according to the real-world applications, are conducted in this chapter. Common parameters for all the numerical examples are $C^f$ = 2,000,000, $C^v$ = 200,000, $C^w$ = 10, $\beta$ = 0.05. The rest parameters are randomly selected within

certain ranges conforming a uniform distribution. Assume that the area's bound is [100, 100], then the hubs locations $\mathbf{x}^h = [x_z^h] \in \mathbb{R}^{\boldsymbol{Z}}$ and $\mathbf{y}^h = [y_z^h] \in \mathbb{R}^Z$, the residue availability $\mathbf{A} = [A_{zk}] \in \mathbb{R}^{Z\times K}$ and the transportation cost $\mathbf{C}^t = [C_{zk}^t] \in \mathbb{R}^{Z\times K}$ are selected as

$$\mathbf{x}^h = 100\text{rand}(Z,1),\ \mathbf{y}^h = 100\text{rand}(Z,1), \tag{4.8a}$$

$$\mathbf{A} = 2 + 3\text{rand}(Z,K), \tag{4.8b}$$

$$\mathbf{C}^t = 3{+}2\text{rand}(Z,K), \tag{4.8c}$$

where $\text{rand}(m,n)$ creates an $m \times n$ matrix with each element ranging from 0 to 1 and is generated randomly according to uniform distribution. Therefore, the coordinates of hubs' locations are selected randomly in the range $[0{,}100] \times [0{,}100]$, the residue availability is chosen within 2 to 5 truck-loads for each hub and the transportation costs for each residue in a hub is between 3 and 5 dollar/truck-load/mile. The residue availability in the real world might be thousands truck-loads per hub. However, small parameters are chosen here for numerical calculation convenience.

The demand for the residues in the reactor $\mathbf{D} = [D_k] \in \mathbb{R}^K$, feedstock cost $\mathbf{C}^r = [C_{zk}^r] \in \mathbb{R}^{Z\times K}$ and unit workforce $\mathbf{w} = [w_k] \in \mathbb{R}^K$ are set to

$$\mathbf{D} = \text{randi}([1.5Z, 2Z], K, 1), \tag{4.9a}$$

$$\mathbf{C}^r = \text{randi}([100{,}150], Z, K), \tag{4.9b}$$

$$\mathbf{w} = \text{randi}([3{,}5], K, 1), \tag{4.9c}$$

where $\text{randi}([\text{lb}, \text{ub}], m, n)$ randomly creates an $m \times n$ matrix such that each element is an integer ranging from lb to ub and conforms the uniform distribution. Therefore, the demand of each residue at the reactor is a random integer between $1.5Z$ and $2Z$ truck-loads, the feedstock cost is an integer randomly chosen from 100 to 150 dollars/truck-load and the required unit workforce is bounded between 3 and 5 persons/truck-load.

The total available workforce $W$ is set empirically at $8ZK$. At total of 10 sets of numerical problems were tested based on the above random parameters and proposed heuristic. Note that the randomly generated set of parameters cannot always guarantee feasibility of the constrained programming. Therefore, parameters that leads to infeasible solutions are discarded during numerical experiments. The proposed heuristic is programmed in Matlab which runs on a computer with *Intel Core i7-4750HQ@ 2.00GHz*. The numerical instance also runs in Lingo for comparison in the first example. Table 4.1 shows 10 sets of numerical results (see Wu and Sarker 2014 for all data). The number of hubs are selected from 3 to 50 and the types of residues varies from 2 to 10. Four numerical results for each set of problems are listed in Table 4.1. The random parameters for problem set 1 to 10 are set by (4.8) and (4.9). The unit for CPU time is in seconds. Denote the number of iterations in Algorithm 4.D by $I$ and the number of nodes in the $i$th iteration ($i = 1,\ldots,I$) by $u_i$. The number of average nodes is computed as $(\sum_{i=1}^{I} u_i)/I$.

Table 4.1 shows that it requires 2 to 11 times the number of iterations for all sets of problems converging to optimal. Convergence in relatively small number of iterations shows the effectiveness of proposed ALMH heuristic. That is, by taking an initial guess suggested in Step 4.D-1, the heuristic works efficiently within less than or equal to 11 times for $TC_1$ becoming consistent with $TC_2$ as proposed in Step 4.D-5.

The average numbers of nodes being visited are close within each set of problem. This observation results from the fact that the parameters for sub-problems in a set are selected randomly in a certain small range. An increasing trend of the average number of nodes is displayed as the number of hubs and types of residues increase. The number of nodes being visited significantly relates to the CPU time. The increase of computation time is caused mainly

by the increase of number of nodes in a B&B method as well as the number of iterations. The data trend for the CPU time, number of iterations and average number of nodes are consistent with the expectation of the numerical results.

The nonlinear mixed integer programming (4.3) is not convex because it contains combination calculation in the third to fifth terms (for modeling allocation problem), therefore, a lower bound of the minimization problem cannot be readily obtained. To validate the numerical result, Lingo results with the same parameters are provided for comparison. It can be concluded from Table 4.1 that parts of the optimized total cost are equal either between Lingo and ALMH. Better optimal solutions are obtained by the ALMH for the remaining problems. The trade-off is a longer computation time of ALMH than Lingo. Although it takes up to 14 minutes to solve a $50 \times 10$ problem, it is expected for a shorter CPU time if optimization of code is conducted such as using parallel computation or using C code instead of Matlab. The comparison between Lingo and ALMH results verified that the proposed heuristic was validated and effective in finding an optimal solution for the BMG production problem.

Table 4.1: Comparison of numerical results between Lingo and ALMH.

| | *Prob. Size* | **Lingo** | | **ALMH** | | | | | |
|---|---|---|---|---|---|---|---|---|---|
| ***Prob.*** | ***Z×K*** | $TC^{min}$ | ***CPU Time (s)*** | $TC^{min}$ | ***CPU Time (s)*** | ***No. of Iter.*** | ***Avg. No. of Iter.*** | ***No. of Nodes per Iter. (Avg.)*** | ***Avg. No. of Nodes per Iter.*** |
| *SR1-1* | 3×2 | 2202082 | <1 | 2202082 | 0.23 | 3 | 2.5 | 7 | 7.2 |
| *SR1-2* | | 2203837 | <1 | 2203529 | 0.22 | 2 | | 7 | |
| *SR1-3* | | 2203557 | <1 | 2203557 | 0.36 | 3 | | 9.6 | |
| *SR1-4* | | 2202892 | <1 | 2202306 | 0.09 | 2 | | 5 | |
| *SR2-1* | 3×3 | 2203595 | <1 | 2203560 | 0.20 | 2 | 2.3 | 9 | 12.1 |
| *SR2-2* | | 2203479 | <1 | 2203479 | 0.26 | 2 | | 11 | |
| *SR2-3* | | 2204936 | <1 | 2204936 | 0.70 | 3 | | 18.3 | |
| *SR2-4* | | 2203118 | <1 | 2202944 | 0.22 | 2 | | 10 | |
| *SR3-1* | 5×3 | 2207903 | <1 | 2207903 | 3.62 | 3 | 3.5 | 97 | 88.1 |
| *SR3-2* | | 2207546 | <1 | 2207546 | 3.72 | 3 | | 95 | |
| *SR3-3* | | 2208312 | <1 | 2208312 | 5.00 | 5 | | 84.2 | |
| *SR3-4* | | 2209890 | <1 | 2209890 | 2.85 | 3 | | 76.3 | |
| *SR4-1* | 10×3 | 2218267 | <1 | 2217941 | 2.74 | 2 | 3 | 98 | 104.8 |
| *SR4-2* | | 2214427 | <1 | 2214427 | 4.04 | 3 | | 102 | |
| *SR4-3* | | 2213769 | <1 | 2213769 | 4.05 | 3 | | 112 | |
| *SR4-4* | | 2213326 | <1 | 2213198 | 10.89 | 4 | | 107 | |
| *SR5-1* | 10×5 | 2226874 | <1 | 2226864 | 5.08 | 3 | 4 | 110 | 109.0 |
| *SR5-2* | | 2236070 | <1 | 2236070 | 7.26 | 4 | | 124.2 | |
| *SR5-3* | | 2229903 | <1 | 2229903 | 7.80 | 5 | | 101.6 | |
| *SR5-4* | | 2224398 | <1 | 2224048 | 6.34 | 4 | | 100 | |
| *SR6-1* | 15×5 | 2239256 | 1 | 2238325 | 4.99 | 2 | 4 | 144 | 160.1 |
| *SR6-2* | | 2240143 | 1 | 2240143 | 15.03 | 5 | | 173 | |
| *SR6-3* | | 2239271 | 1 | 2239271 | 19.82 | 6 | | 180.2 | |
| *SR6-4* | | 2240655 | 1 | 2240655 | 7.07 | 3 | | 143 | |
| *SR7-1* | 20×5 | 2257640 | 1 | 2257640 | 40.22 | 6 | 4.5 | 326.2 | 313.1 |
| *SR7-2* | | 2253014 | 1 | 2253014 | 32.29 | 5 | | 327.8 | |
| *SR7-3* | | 2257705 | 1 | 2257674 | 23.01 | 4 | | 294.2 | |
| *SR7-4* | | 2264099 | 1 | 2264075 | 19.97 | 3 | | 304 | |
| *SR8-1* | 20×10 | 2308714 | 1 | 2308714 | 87.41 | 5 | 4.5 | 592.6 | 548.7 |
| *SR8-2* | | 2310992 | 1 | 2310975 | 79.32 | 5 | | 518.3 | |
| *SR8-3* | | 2309054 | 1 | 2308609 | 34.57 | 2 | | 591.5 | |
| *SR8-4* | | 2298581 | 1 | 2298559 | 91.43 | 6 | | 492.5 | |
| *SR9-1* | 30×10 | 2348002 | 1 | 2348002 | 316.09 | 11 | 5.5 | 783.4 | 803.2 |
| *SR9-2* | | 2374388 | 1 | 2373483 | 60.88 | 2 | | 839 | |
| *SR9-3* | | 2357722 | 1 | 2357722 | 123.95 | 4 | | 822.75 | |
| *SR9-4* | | 2354570 | 1 | 2354564 | 143.57 | 5 | | 767.8 | |
| *SR10-1* | 50×10 | 2492260 | 2 | 2492134 | 395.89 | 3 | 3.3 | 2373.6 | 2404.0 |
| *SR10-2* | | 2490104 | 2 | 2490054 | 477.36 | 4 | | 2158.3 | |
| *SR10-3* | | 2506995 | 2 | 2506995 | 468.81 | 3 | | 2797.3 | |
| *SR10-4* | | 2510088 | 2 | 2510088 | 365.20 | 3 | | 2287 | |

* Computer: *Intel Core i7-4750HQ@ 2.00GHz*

Table 4.2: CPU time of numerical results of ALMH.

| *Problem Sets* | *Problem Size* | *MAX CPU Time(s)* | *MIN CPU Time(s)* | *Avg CPU Time(s)* |
|---|---|---|---|---|
| *SR1* | 3×2 | 0.91 | 0.06 | 0.22 |
| *SR2* | 3×3 | 1.23 | 0.38 | 0.35 |
| *SR3* | 5×3 | 6.28 | 1.75 | 4.27 |
| *SR4* | 10×3 | 13.23 | 2.03 | 5.82 |
| *SR5* | 10×5 | 9.82 | 5.23 | 7.34 |
| *SR6* | 15×5 | 20.98 | 4.99 | 13.76 |
| *SR7* | 20×5 | 67.92 | 15.34 | 31.45 |
| *SR8* | 20×10 | 120.38 | 27.45 | 68.57 |
| *SR9* | 30×10 | 423.56 | 47.14 | 230.10 |
| *SR10* | 50×10 | 570.65 | 247.32 | 371.95 |

* Problem size, $Z \times K$. Computer: *Intel Core i7-4750HQ@ 2.00GHz*

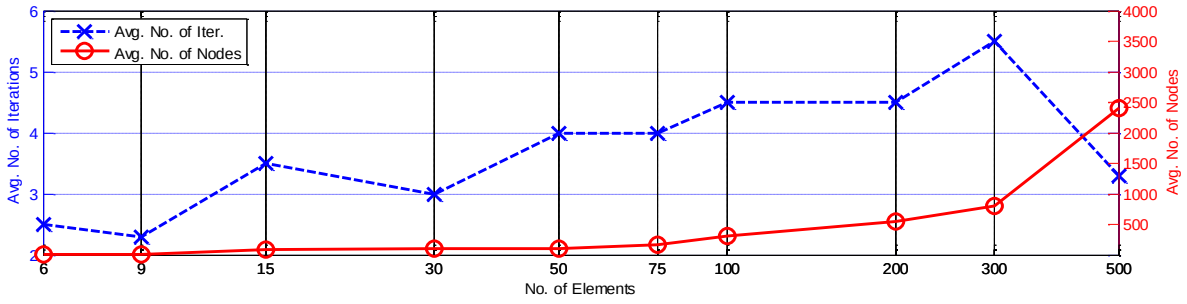


Figure 4.3: Average evaluate iterations and nodes versus problem size.

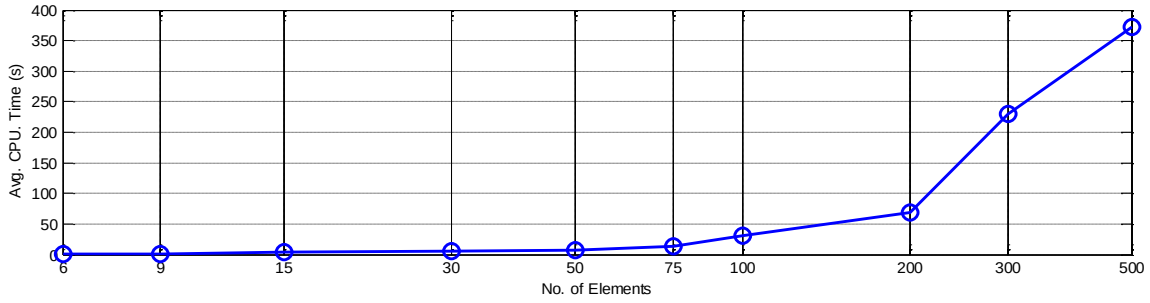


Figure 4.4: Average CPU times versus problem size.

To further evaluate the efficiency of the algorithm, a second experiment is conducted by running 30 random problems for each size in Table 4.1. Table 4.2 provides the maximum, the minimum and the average CPU time for solving these problems. As suggested in Table 4.2, a reasonable amount of computation time (average around 12 minutes) is expected for the $50 \times 10$ problem which is a relatively large size problem in a real world application.

Figure 4.3 shows the tendency of the average number of iterations and nodes with respect to the number of elements, which is computed as the number of hubs multiplied by the number of residue types. When the problem size increases, the number of nodes in the B&B method increases dramatically. Therefore, it can be seen from Figure 4.3 that the average number of nodes increase from 7.2 to 2404 as the number of elements goes from 6 to 500. The average number of iterations is related to the initial guess of the reactor's location. Therefore, a closer initial guess leads to a faster convergence of the heuristic, which further causes a smaller number of iterations. Figure 4.3 shows an irregular pattern (neither increase nor decrease) of the number of iterations, which is due to variance in the quality of initial guesses.

Figure 4.4 shows the average CPU time under different number of elements. As the number of nodes increases while the problem size increases, the average CPU time is expected to increase as shown in Figure 4.4.

## 4.7 CONCLUDING REMARKS

The logistic of the BMG production systems, which plays an important role in cost control, is the major concern in this chapter. A mathematical model, which can be generalized as a nonlinear mixed integer programming, is developed here to minimize the cost that occurs in building the BMG reactor. Both enumeration algorithm and heuristic are proposed to solve the programming. Numerical examples are provided validate performance of the proposed heuristic.

It’s the first time in the reviewed literature that a mathematical model is developed for a complicated multi-feedstock BMG production system location-allocation problem. The major contributions lie in two aspects: first, the modeling process gives insightful guidance for building a BMG reactor in a real world application. And, second, the novel B&B based heuristic proposed in this model is proved to be both efficient and effective.

# CHAPTER V
# MODEL II: A SINGLE-STAGE MULTI-REACTOR SYSTEM PROBLEM

The previous chapter builds an SS-SRS model. To increase the BMG production capability and profitability, multiple reactors are needed for processing more residue. This chapter extends the SS-SRS model to the SS-MRS model which has a larger BMG productivity than the SS-SRS. In this model, multiple reactors collect residue from hubs in different zip code areas. By assuming the hubs locations are given, the objective is to obtain a strategic supply chain plan which includes optimal locations of reactors and optimal amount of residue that is transferred from each hub to the reactors.

In the subsequent section, the SS-MRS problem is described in detail and notations used in this chapter are listed. An MINLP model is developed for the SS-MRS in the second section. The third section illustrates the heuristic designed specifically for the proposed problem and gives a small-size numerical result to test the heurist step by step. More numerical analyses is presents in the fourth section, followed by the conclusions in last section.

## 5.1 PROBLEM DESCRIPTION AND NOTATION

Assume that the local farms are located in a geographical area delineated by U.S. Zip Code. All farms can generate one or more types of residue, such as crop residue, wood residue and livestock manure. In each zip code area, there is a hub that collects the residues from the local farms. The location of the hubs in different zip code areas are determined by a GIS. The farms and hubs have the configuration such that the farms deliver all their available residues to the hubs, and the hubs receive in and store all the residues.

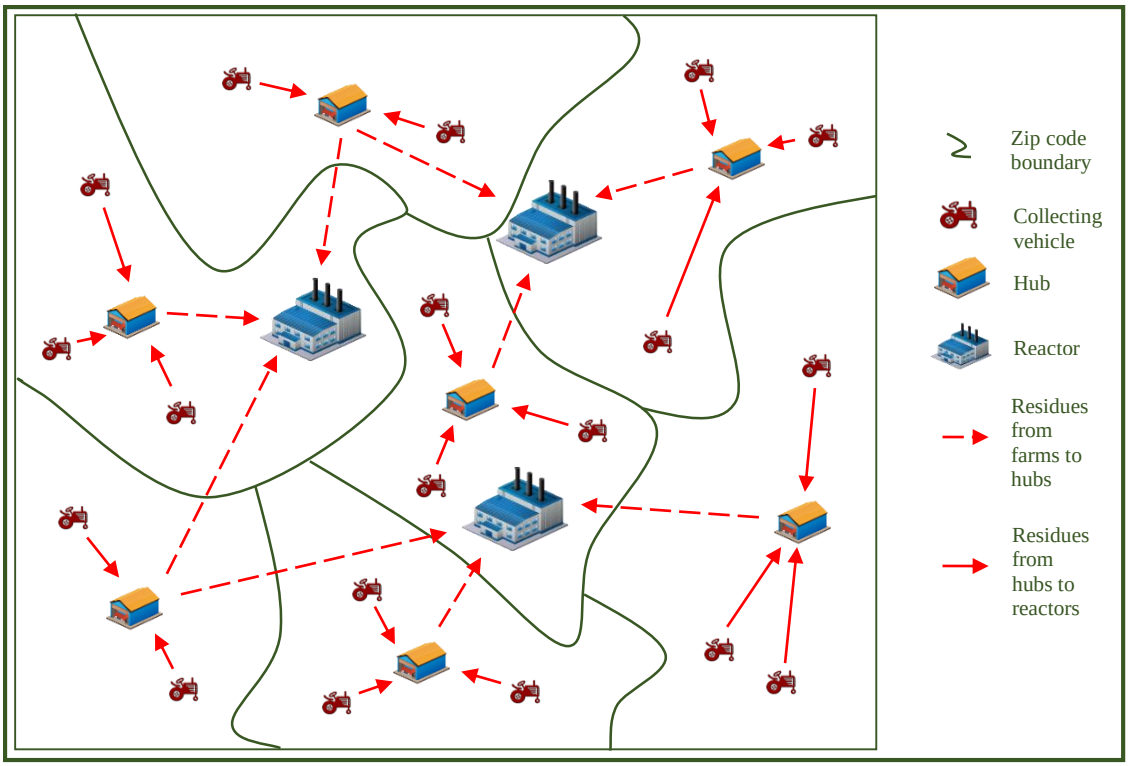


Figure 5.1: Illustration of location-allocation problem in SS-MRS BMG production system.

When a BMG production system is planned in a certain area, reactors are needed to produce BMG by collecting and processing residues from the hubs. Assume all the hubs can supply to all the reactors with their entire residue inventory and all the reactors can process all the types of residues. The best scenario for the BMG production system construction plan is that all the available residues in the hubs are transported to and processed by the reactors to maximize the BMG output. However, due to the limitation on the practical constraints, such as labor availability, the ideal condition is usually not achievable. All these constraints requires careful considerations while planning the BMG production systems.

Since the total cost of the supply chain is the major concern of construction and operating the BMG production system, building costs, feedstocks costs, transportation costs and workforce costs will be taken into account for they all consists of a notable portion in the

total cost. The building costs includes both fixed and variables costs, which can be obtained from the construction contract. The residues are transported by trucks and unit transportation cost can be determined based on fuel, insurance, maintenance and license cost (Trucks Report, 2013). However, due to the different condition of the road in different zip code areas, the unit transportation cost may vary between reactors and hubs. Labors are hired to collect and unload the residues. The unit labor cost and building cost are assumed to be consistent in the whole area.

The notations are defined under several classifications:

**Parameters**

| | |
|---|---|
| $K$ | Total number of types of residues. |
| $Z$ | Total number of zip codes in the region. |
| $N$ | Total number of reactors to be built. |
| $k$ | Index for residue types, $k = 1, \dots, K$. |
| $z$ | Index of zip codes of a hub, $z = 1, \dots, Z$. |
| $n$ | Index for reactors, $n = 1, \dots, N$. |
| $A_{zk}$ | Availability of the residue $k$ in the hub in zip code $z$ (truck-load). |
| $C^f$ | Fixed cost to build $N$ reactors, share equally to unit time period (dollar). |
| $C_n^v$ | Variable cost to build the $n$th reactor, share equally to unit time period (dollar). |
| $C^w$ | Unit cost for hiring a worker (dollar /person/truck load). |
| $C_{zk}^t$ | Unit transportation cost of moving the residue $k$ from the hub in zip code $z$ to a reactor (dollar/truck-load/mile). |
| $C_{zk}^r$ | Feedstock cost of the residue $k$ supplying from the hub in zip code $z$ to a reactor (dollar/truck-load). |

$D_{kn}$ Demand of residues $k$ at the *n*th reactor (truck-load).

$w_k$ Unit workforce required for collecting the residue $k$ (persons/truck-load).

$W_n$ Total workforce availability of the $n$th reactor (persons).

$\beta$ Percentage of deteriorated residue in hubs.

$\mathbf{h}_z$ $\mathbf{h}_z = (x_z^h, y_z^k)$ represents the coordinate of the hub in zip code $z$.

**Variables**

$\mathbf{r}_n$ $\mathbf{r}_n = (x_n, y_n)$ represents the coordinate of the reactors.

$\mathbf{r}$ $\mathbf{r} = (r_n) \in \mathbb{R}^{2N}$ is a vector containing all the coordinates of the reactors.

$\alpha_{zk}^n$ Number of truck-loads for moving the residue $k$ from the hub in zip code $z$ to the $n$th reactor.

$\boldsymbol{\alpha}^n$ A series of matrices $\boldsymbol{\alpha}^n = [\alpha_{zk}^n]$, $n = 1,\ldots,N$, representing all truck-loads of residue $k$ ($k = 1, \ldots, k$) to be transported from zip code $z$ ($z = 1, \ldots, Z$) to the *n*th reactor.

**Measure of performance**

$TC(\mathbf{r}, \boldsymbol{\alpha}^1, \ldots, \boldsymbol{\alpha}^n)$ Total cost of the whole system (dollars): For $n = 1, \ldots, n$ it's the summation of locating *n*th reactor at coordinate point $\mathbf{r}_n$ and transporting$\boldsymbol{\alpha}^n$ truck-loads to the *n*th reactor from the residue collection hubs.

## 5.2 ASSUMPTIONS FOR MODEL II

All assumptions for Model II are given below:

1. The hubs locations are given by GIS.
2. The reactors has the capacity to process all residue collecting from the hubs.
3. There is no loss of residue during the transportation process.
4. Residue deterioration occurs in hubs.

5. The demand of each reactor for each residue is known.

6. The number of reactors to be built is given.

## 5.3 REACTOR LOCATION AND ALLOCATION MODEL

The goal of a system modeling process is to mathematically interpret the total cost of constructing a BMG production system by considering the different types of cost and constraints. The components of the various cost is given below:

1. The fixed building costs that may include the fixed investment, such as business license fee and building design fee, for building a reactor.
2. The variable building costs that depends on the demand of the reactor.
3. The feedstocks costs of BMG production.
4. The transportation costs that relates to the distance among the hubs and reactors, the road condition and the capacity of the residue delivering truck.
5. The labor costs concerning hiring labors for handling the residues.

Practical constraints are considered, including the availability of labors, the demands of reactors, and the deterioration of residues.

Now, for planar location vectors $\mathbf{a} = (x_a, y_a)$ and $\mathbf{b} = (x_b, y_b)$, the Euclidean distance function can be written as $\|\mathbf{a} - \mathbf{b}\| = \sqrt{(x_a - x_b)^2 + (y_a - y_b)^2}$. If $d_{nz}$ represents the distance from the hub in zip code $z$ to the $n$th reactor at $\mathbf{r}_n = (x_n, y_n)$, then $d_{zn} = d(\mathbf{r}_n, \mathbf{h}_z) = \sqrt{(x_n - x_z^h)^2 + (y_n - y_z^h)^2}$. Considering all the above factors, the system model for BMG multi-reactor location problem can be built as

**Problem BMG-MR:**

$$\text{Min } TC(\mathbf{r}, \boldsymbol{\alpha}^1, \dots, \boldsymbol{\alpha}^N) = C^f + \sum_{n=1}^{N} C_n^v + \sum_{z=1}^{Z} \sum_{k=1}^{K} \sum_{n=1}^{N} C_{zk}^r \alpha_{zk}^n$$

$$+\sum_{z=1}^{Z}\sum_{k=1}^{K}\sum_{n=1}^{N} d_{zn} C_{zk}^{t} \alpha_{zk}^{n}$$

$$+C^{w}\sum_{z=1}^{Z}\sum_{k=1}^{K}\sum_{n=1}^{N} w_k \alpha_{zk}^{n} \quad (5.1)$$

Subject to: $\sum_{z=1}^{Z}\sum_{k=1}^{K} w_k \alpha_{zk}^{n} \leq W_n$, $n = 1, \ldots, N$ (5.1a)

$\sum_{z=1}^{Z} \alpha_{zk}^{n} \geq D_{kn}$, for $k = 1,\ldots, K$, $n = 1, \ldots, N$ (5.1b)

$\sum_{z=1}^{Z} \alpha_{zk}^{n} \leq (1-\beta)\sum_{z=1}^{Z} A_{zk}$, for $k = 1,\ldots, K$, $n = 1, \ldots, N$ (5.1c)

$0 \leq \alpha_{zk}^{n} \leq (1-\beta)A_{zk}$ and $\alpha_{zk}^{n} \in \mathbb{Z}$, for $n = 1, \ldots, N$ (5.1d)

The proposed model is obtained according to the assumptions made in previous section. From the assumptions 1 to 4, the objective function (5.1) is obtained. It consists of five terms which, from the first to the last, represent the fixed building costs, variable building costs, feedstocks costs, transportation costs, and labor costs, respectively. Four constraints are considered in the system model. Constraint (5.1a) provides an upper limit of the total workforce for transferring the residue $k$ from the hub of the zip code $z$ to the nth reactor. Constraint (5.1b) gives a lower bound, which is the reactor's demand, for the total truck-loads of residues delivered to the $n$th reactor. Constraint (5.1c) considers the deterioration of the stocked residue in the hubs and denotes that the total amount of the residue $k$ is bounded by its availability. Constraint (5.1d) states that the amount of residue $k$ from the $z$th hub to the $n$th reactor is bounded by the availability of residue $k$ in the $z$th hub and is a non-negative integer.

It can be shown that the production system model BMR in (5.1) is a mixed-integer non-convex constrained programming problem with respect to its variables $\mathbf{r}$ and $\boldsymbol{\alpha}$. Since $d_{zn}$ is a nonlinear function of coordinates, BMR is basically an MINLP problem for which finding an optimal solution for a large instance is computationally prohibitive. Therefore, it's impractical to enumerate all feasible solutions in order to obtain the optimal one. A compromised methodology is to develop a heuristic such that an optimal/sub-optimal solution can be

obtained within a reasonable amount of time. Such a heuristic is thus provided in the next section for solving BMR.

## 5.4 SOLUTION PROCEDURE

With the expression of Euler distance in Equation (5.1) and the integer constraint (5.1d), the BMR location-allocation problem can be considered as a mixed-integer nonlinear programming problem (MINLP). Solving such a problem is a computational burden if the algorithm is not properly developed. The complexity in solving this type of problems results from two aspects: conventional gradient based method gets trapped at local minima and discontinuity of the variables occurs due the integer constraint. Therefore, a heuristic needs to be devised with a sound mathematical approach such that the sub-optimal solution is not far from the real optimum.

An alternative search to convergence heuristic (ASTCH) is proposed in this research to obtain such a result. The ASTCH is designed based on decoupling of two sets of coupled functions in the objective function (5.1). The motivation behind this heuristic is that function (5.1) is coupled in a way that two sets of variables $\mathbf{r}$ and $\boldsymbol{\alpha}$ influence one to another, which renders the function to be non-convex. Decoupling of the function (5.1) in terms of $\mathbf{r}$ and $\boldsymbol{\alpha}$ forms two separate sets of problems that are both convex. An alternative search is then applied to each set of functions until the results for both problems are consistent and converge to the optimal/sub-optimal problem.

### 5.4.1 Decoupling the Mixed Integer Non-Linear Programming in Terms of r

Before devising the heuristic, the convexity of the two sub-problems from the MINLP (5.1) is analyzed first. First, a theorem is proposed below to prove the convexity properties on one of the sub-problems.

**Theorem 5.1**: Given $\boldsymbol{\alpha}$, the objective function (5.1) is always convex in $\mathbf{r}$.

**Proof**: see Appendix E.

Theorem 5.1 provides one set of decoupled convex function. Although the objective function (5.1) is non-convex in terms of both **r** and **α**, it is convex in **r** when **α** is determined. Therefore, this set of decoupled objective function can be rewritten as in (E.1). The difference of the objective function (5.1) and (E.1) is that on the left side of the equation, (5.1) has both variables **r** and $\boldsymbol{\alpha}^n$ while (E.1) has only variable **r**. The discrepancy between (5.1) and (E.1) indicates that allocation $\boldsymbol{\alpha}^n$ are known and constant in (E.1). From Theorem 5.1, since (E.1) is a convex function, the optimal occurs at the point where the first-order derivative of (E.1) with respect to **r** is zero; that is, (E.2) equals to zero implies

$$\mathbf{r}_n = \sum_{z=1}^{Z}\sum_{k=1}^{K}\frac{C_{zk}^t\alpha_{zk}^n}{d_{zn}}\mathbf{h}_z \,/\, \sum_{z=1}^{Z}\sum_{k=1}^{K}\frac{C_{zk}^t\alpha_{zk}^n}{d_{zn}}. \tag{5.2}$$

The solution of equation (5.2) is the optimal location for the decoupled problem with known allocation $\alpha$. However, obtaining an explicit analytical solution of the nonlinear equation (5.2) is difficult due to its complexity. Therefore, a numerical algorithm is developed below based on the "successive substitution" proposed by Hildebrand (1987).

**Algorithm 5.A: Optimal Location of Reactors**

Step 5.A-1: Generate random initial conditions $\mathrm{r}_n$ and denote them as $\mathrm{r}_n^{curr}$.

Step 5.A-2: Update the next coordinate for the reactors by

$$\mathrm{r}_n^{next} = \sum_{z=1}^{Z}\sum_{k=1}^{K}\frac{C_{zk}^t\alpha_{zk}^n}{d_{zn}(\mathrm{r}_n^{curr},\mathbf{h}_z)}\mathbf{h}_z \,/\, \sum_{z=1}^{Z}\sum_{k=1}^{K}\frac{C_{zk}^t\alpha_{zk}^n}{d_{zn}(\mathrm{r}_n^{curr},\mathbf{h}_z)}.$$

Obtain the step size $\Delta = \|\mathrm{r}_n^{next} - \mathrm{r}_n^{curr}\|$, where $\|\cdot\|$ indicates the 2-norm of a vector. Let $\mathrm{r}^{next} := \mathrm{r}_n^{curr}$.

Step 5.A-3: If $\Delta >$ set precision, go to Step 5.A-2; otherwise, stop. The optimal location is stored in $\mathrm{r}_n^{curr}$ and the optimal total cost is $TC(\mathrm{r}_n^{curr}, \alpha^1, \ldots, \alpha^N)$. □

Algorithm 5.A numerically solves the equation (5.2) and finds the optimal solution for the first set of decoupled problem which is considered with a known allocation $\boldsymbol{\alpha}^n$. The second set of decoupled problem, which is defined as the reactors' locations $\mathbf{r}_n$ are known and an optimal allocation $\boldsymbol{\alpha}^n$ is required to solve, will be addressed next.

### 5.4.2 Decoupling the Mixed Integer Non-Linear Programming in Terms of α

Before addressing the heuristic, the second decoupled problem is transferred to a linear programming with a more concise format. The following new problem is provided first, which can be verified by algebraic computation from (5.1). The purpose of applying matrix transformation is to simplify the original model (5.1) with a standard linearized programming such that conventional optimization methods, such as B&B can be applied directly to the problem.

Let $T$: $\mathbb{R}^{Z\times K} \rightarrow \mathbb{R}^{ZK}$ be a function that transforms a $Z \times K$ matrix to a vector with length $ZK$ by rearranging all columns of the matrix into one column. Denote $\mathbf{1}_s$ a length $s$ vector of all ones and $\mathbf{I}_s$ an $s \times s$ identity matrix. Also denote the symbol $\otimes$ to indicate the Kronecker's matrix-product and the symbol $\circ$ to indicate product of the corresponding elements (Refer to Appendix D for definition details and examples of all notations in this section).

**Problem 5.1:**

If the location of the reactor $\mathbf{r}$ is known, the system model (5.1) can be written in the form of a linear integer programming (LIP):

$$\text{Min } TC(\mathbf{V}) = \boldsymbol{B}^T\mathbf{V} + \Theta \tag{5.3}$$

Subject to: $\mathbf{PV} \leq \mathbf{Q}$ (5.3a)

$$\mathbf{V} = (v_i) \in \mathbb{Z}^{ZKN},\ v_i \geq 0 \text{ for } i = 1,\ldots, ZK \quad (5.3b)$$

where $\mathbf{V} = \begin{pmatrix} T(\boldsymbol{\alpha}^1) \\ \vdots \\ T(\boldsymbol{\alpha}^n) \end{pmatrix} \in \mathbb{Z}^{ZKN}$, $\mathbf{B} = \mathbf{1}_n \otimes T(\mathbf{C^r}) + T(\mathbf{1}_k \otimes \mathbf{d}) \circ [\mathbf{1}_n \otimes T(\mathbf{C}^t)] + C^w \mathbf{1}_n \otimes (\mathbf{w} \otimes \mathbf{1}_z)$, $\mathbf{C^r} = (\mathrm{C}^r_{zk}) \in \mathbb{R}^{ZK}$, $\mathbf{C^t} = (\mathrm{C}^t_{zk}) \in \mathbb{R}^{Z \times K}$, $\mathbf{w} = (w_k) \in \mathbb{R}^K$, $\mathbf{d} = (d_{zn}) \in \mathbb{R}^Z$, $\Theta = C^f + \sum_{n=1}^{N} nC^v$, $\mathbf{P} = \begin{bmatrix} \mathbf{I}_n \otimes (\mathbf{w} \otimes \mathbf{1}_z)^T \\ -\mathbf{I}_{kn} \otimes (\mathbf{1}_z^T) \\ \mathbf{I}_{kn} \otimes (\mathbf{1}_z^T) \end{bmatrix}$, and $\mathbf{Q} = \begin{bmatrix} \mathbf{W}_n \\ -T(\mathbf{D}) \\ (1-\beta)\mathbf{1}_n \otimes \big(\mathbf{I}_k \otimes (\mathbf{1}_z^T) T(\mathbf{A})\big) \end{bmatrix}$.

Theorem 5.1 along with Algorithm 5.A provides a numerical solution of the optimal reactor's location $\mathbf{r}$ under a given $\boldsymbol{\alpha}$. On the other hand, Problem BMR-R in (5.3) transforms the problem BMR in (5.1) to a standardized form. The transformation allows B&B method being successfully applied for seeking an optimal allocation $\boldsymbol{\alpha}$ when the reactor's location $\mathbf{r}$ is known. By using the depth-first B&B (DFB) method, the optimal solution of each node is obtained from solving a relaxed problem of (5.3) by using the simplex method. The relaxed problem has the same objective function and constraints except that it has no integer constraint. Algorithm 5.B generalizes the process of applying the B&B method to solve the second set of decoupled problem (5.3).

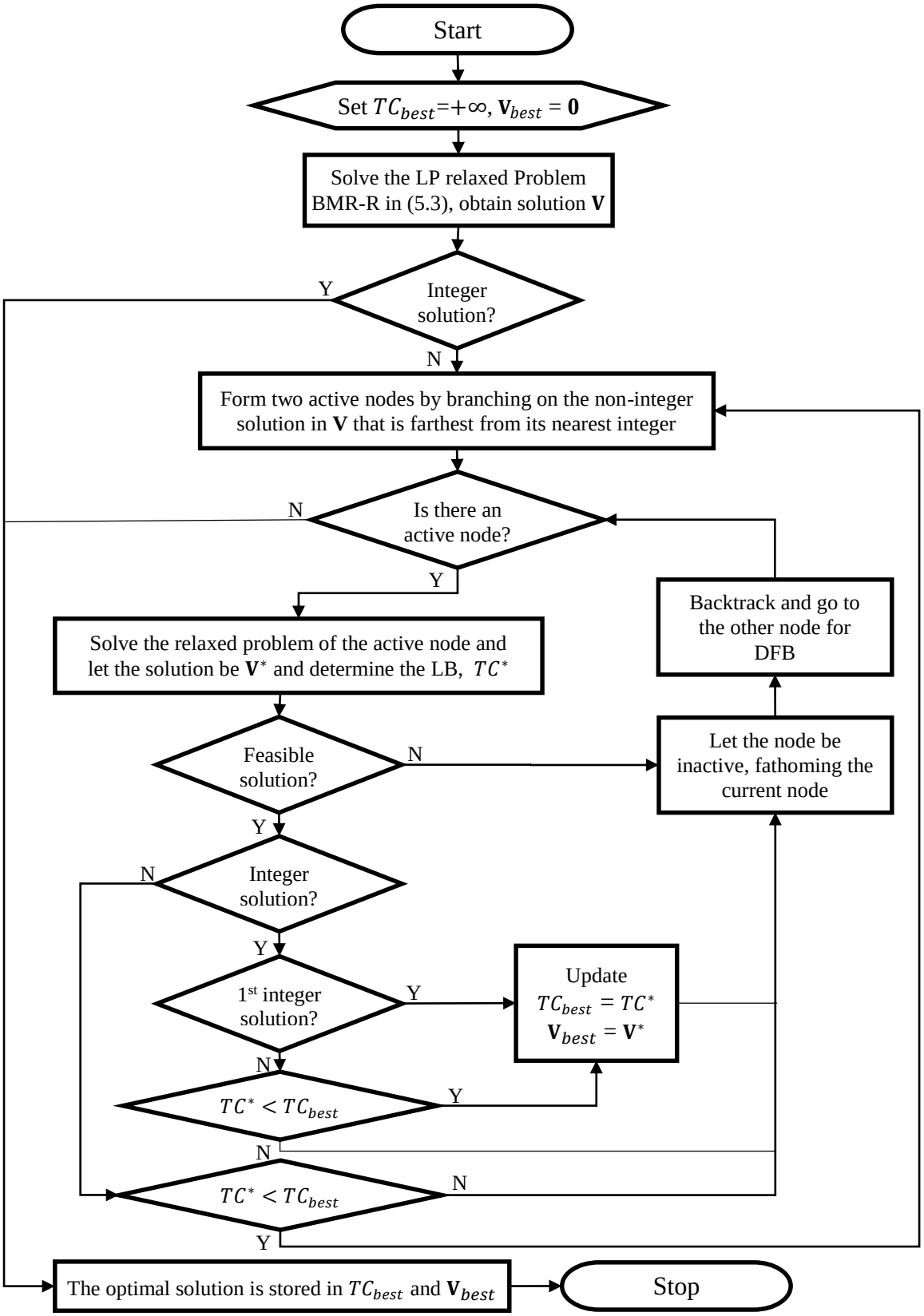


Figure 5.2: The flow chart of the Algorithm 5.B.

**Algorithm 5.B: Depth-first Branch and bound method**

Step 5.B-1: Let the best objective value (upper bound) of the linear integer problem (5.3) be $TC_{best}$ and set $TC_{best} = +\infty$.

Step 5.B-2: Solve the LP relaxed problem based on (5.3). If integer solution of $\mathbf{V}$ is obtained, stop the process. Otherwise, branch on the most-fractional number in $\mathbf{V}$ and form two new active nodes (sub-problems).

Step 5.B-3: Select an active node based on depth-first criterion and let it be inactive. Solve the current relaxed sub-problem. Obtain $\mathbf{V}^*$ and $TC^*$ as the optimal solution and objective value.

Step 5.B-4: If there is no feasible solution of the current node, fathom the current node and make it inactive.

Step 5.B-5: If $\mathbf{V}^*$ is an integer vector that is the first integer obtained, $TC_{best} = TC^*$, fathom the current node and make it inactive. Otherwise, proceed to the next step.

Step 5.B-6: If $\mathbf{V}^*$is an integer vector but is not the first integer obtained, then if $TC^* < TC_{best}$, let $TC_{best} = TC^*$, fathom the current node and make it inactive. Otherwise fathom the current node and make it inactive.

Step 5.B-7: If $\mathbf{V}^*$ is not an integer vector, then if $TC^* \geq TC_{best}$, fathom the current node and make it inactive. Otherwise, branch on the most-fractional number in $\mathbf{V}^*$ and form two new active nodes.

Step 5.B-8: If there exists active node, then go to Step 5.B-3; otherwise, stop. □

The flow chart of the Algorithm 5.B is given in Figure 5.2. Note that an inactive node refers to a node that is currently being computed or has no feasible solution or whose solution is integer but exceeds the lower bound $TC^*$.

### 5.4.3 Heuristic Design

The nature of the original model (5.1) can be considered as two sub-problems being coupled. One of the sub-problem is proved convex in Theorem 5.1 and the global minimum can be obtained using Algorithm 5.A. The other one is a constrained linear integer programming problem which can be written in the form of (5.3) and its optimal/sub-optimal solution can be obtained by B&B method for a reasonable size of instance (say, 50×10×10). A heuristic that solves the original model (5.1) consists of alternatively searching within both sub-problems. The heuristic runs both Algorithm 5.A and 5.B alternatively until the optimal result of both sub-problems becomes consistent. The detailed procedure is proposed as follows.

**Algorithm 5.C (Main Program): Alternative Search to Convergence Heuristic**

Step 5.C-1: Taking $\bar{\mathbf{r}} \in \mathbb{R}^{2N}$ as a random vector for the reactors' location. Set $TC_{opt} = +\infty$.

Step 5.C-2: Running the B&B process in Algorithm 5.B to find the optimal allocation $\overline{\boldsymbol{\alpha}^n}$, $n = 1, \ldots, N$ based on $\bar{\mathbf{r}}$. Let the objective value be $\overline{TC}$.

Step 5.C-3: Running Algorithm 5.B to find the optimal location $\tilde{\mathbf{r}}$ based on $\overline{\boldsymbol{\alpha}^n}$. Let the objective value be $\widetilde{TC}$.

Step 5.C-4: If $\widetilde{TC} < TC_{opt}$, then $TC_{opt} = \widetilde{TC}$, $\boldsymbol{\alpha}_{opt}^n = \overline{\boldsymbol{\alpha}^n}$ for $n = 1, \ldots, N$, $\mathbf{r}_{opt} = \tilde{\mathbf{r}}$.

Step 5.C-5: If $\left|\overline{TC} - \widetilde{TC}\right| >$ infinitesimal number, then $\bar{\mathbf{r}} = \tilde{\mathbf{r}}$ and go to Step 5.C-2. Else stop and the optimal solution are stored in $TC_{opt}$, $\boldsymbol{\alpha}_{opt}^n$ and $\mathbf{r}_{opt}$. □

## 5.5 ILLUSTRATIVE EXAMPLE

A numerical example is provided with 3 hubs ($Z$ = 3), 2 types of residues ($K$ = 2) and 2 reactors (N = 2). Other system parameters are as follows: total workforce availability for the reactor, $W$ = 48 persons, work-force requirement ($w_1$ , $w_2$) = (3, 5) persons/truck-load, percent of deterioration residue $\beta$ = 0.05, demand of residues $\mathbf{D} = [\mathrm{D_{kn}}] = \begin{bmatrix} 6 & 5 \\ 6 & 5 \end{bmatrix}$ truck-loads,

location of the hubs [$(x_1^h, y_1^h)$ , $(x_2^h, y_2^h)$ , $(x_3^h, y_3^h)$] = [(24.97, 28.07), (48.09, 59.91), (88.08, 2.62)], for simplicity, the constants fixed building cost $C^f$ and variable building cost $C_n^v$ are set to 0, and the work-force cost, $C^w$ = \$10/*person*/truck-load. The unit transportation cost $\boldsymbol{C}^t$ = $[C_{zk}^t] = \begin{bmatrix} 3.23 & 3.17 \\ 4.93 & 4.43 \\ 3.87 & 4.01 \end{bmatrix}$ dollar/truck-load/mile, feedstock cost $\boldsymbol{C}^r = [C_{zk}^r] = \begin{bmatrix} 102 & 148 \\ 137 & 114 \\ 125 & 119 \end{bmatrix}$ dollar/truck-load, and *a*vailability of the residue $\boldsymbol{A} = [A_{zk}] = \begin{bmatrix} 2.5 & 4.5 \\ 4.5 & 3.0 \\ 2.6 & 4.0 \end{bmatrix}$ truck-loads.

From Problem 5.1, the original model (5.1) can be transferred to a linear integer problem (5.3) given the reactor's location **r** is known. Therefore, with the parameters provided above,

$$\mathbf{V} = \begin{pmatrix} T(\boldsymbol{\alpha}^1) \\ \vdots \\ T(\boldsymbol{\alpha}^n) \end{pmatrix}$$

$$= [\alpha_{11}^1\ \alpha_{21}^1\ \alpha_{31}^1\ \alpha_{12}^1\ \alpha_{22}^1\ \alpha_{32}^1\ \alpha_{11}^2\ \alpha_{21}^2\ \alpha_{31}^2\ \alpha_{12}^2\ \alpha_{22}^2\ \alpha_{32}^2\ \alpha_{11}^3\ \alpha_{21}^3\ \alpha_{31}^3\ \alpha_{12}^3\ \alpha_{22}^3\ \alpha_{32}^3]^{\boldsymbol{T}}$$

$$B = \mathbf{1}_n \otimes T(\mathbf{C}^r) + T(\mathbf{1}_k \otimes \mathbf{d}) \circ [\mathbf{1}_n \otimes T(\mathbf{C}^t)] + C^w \mathbf{1}_n \otimes (\mathbf{w} \otimes \mathbf{1}_z)$$

$$= [102\ \ 137\ \ 125\ \ 148\ \ 114\ \ 119\ \ 102\ \ 137\ \ 125\ \ 148\ \ 114\ \ 119]^T$$

$$+[3.2d_{11}\ \ 4.9d_{21}\ \ 3.9\ d_{31}\ 3.2d_{11}\ \ 4.4d_{21}\ \ 4.0d_{31}\ \ 3.2d_{12}\ \ 4.9d_{22}\ \ 3.9d_{32}\ \ 3.2d_{12}\ \ 4.4d_{22}\ 4.0d_{32}]^T$$

$$+[\,30\ \ 30\ \ 30\ \ 50\ \ 50\ \ 50\ \ 30\ \ 30\ \ 30\ \ 50\ \ 50\ \ 50]^{\boldsymbol{T}}$$

$$=[132 + 3.2d_{11}\ \ 167 + 4.9d_{21}\ \ \ldots\ \ 164 + 4.4d_{22}\ \ 169 + 4.0d_{32}]^T$$

$$\Theta = C^f + \sum_{n=1}^{N} nC^v = 0$$

$$\mathbf{P} = \begin{bmatrix} \mathbf{I}_n \otimes (\mathbf{w} \otimes \mathbf{1}_z)^T \\ -\mathbf{I}_{kn} \otimes (\mathbf{1}_z^T) \\ \mathbf{I}_{kn} \otimes (\mathbf{1}_z^T) \end{bmatrix}$$

$$= \begin{bmatrix} 3 & 3 & 3 & 5 & 5 & 5 & 0 & 0 & 0 & 0 & 0 & 0 \\ 0 & 0 & 0 & 0 & 0 & 0 & 3 & 3 & 3 & 5 & 5 & 5 \\ -1 & -1 & -1 & 0 & 0 & 0 & 0 & 0 & 0 & 0 & 0 & 0 \\ 0 & 0 & 0 & -1 & -1 & -1 & 0 & 0 & 0 & 0 & 0 & 0 \\ 0 & 0 & 0 & 0 & 0 & 0 & -1 & -1 & -1 & 0 & 0 & 0 \\ 0 & 0 & 0 & 0 & 0 & 0 & 0 & 0 & 0 & -1 & -1 & -1 \\ 1 & 1 & 1 & 0 & 0 & 0 & 0 & 0 & 0 & 0 & 0 & 0 \\ 0 & 0 & 0 & 1 & 1 & 1 & 0 & 0 & 0 & 0 & 0 & 0 \\ 0 & 0 & 0 & 0 & 0 & 0 & 1 & 1 & 1 & 0 & 0 & 0 \\ 0 & 0 & 0 & 0 & 0 & 0 & 0 & 0 & 0 & 1 & 1 & 1 \end{bmatrix}$$

$$\mathbf{Q} = \begin{bmatrix} \boldsymbol{W} \\ -\mathbf{D} \\ (1-\beta)\mathbf{I}_k \otimes (\mathbf{1}_z^T) T(\mathbf{A}) \end{bmatrix}$$

$$= [48.0 \quad 48.0 \quad -6.0 \quad -6.0 \quad -5.0 \quad -5.0 \quad 9.1 \quad 10.9 \quad 9.1 \quad 10.9]^T$$

Running the Algorithm 5.C (Main Program), yields:

Step 5.C-1: Taking $\bar{\mathbf{r}} = [53.71 \;\; 53.71 \; 30.2 \; 30.2]^T$, Set $TC_{opt} = +\infty$.

Iteration *5*.C-1:

Step 5.C-2: Run the B&B method with $\bar{\mathbf{r}} = [53.71 \;\; 53.71 \; 30.2 \; 30.2]^T$. Since the location of the reactor is known, the distance matrix **d** can be obtained $\mathbf{d} = \begin{bmatrix} 28.82 & 28.82 \\ 30.24 & 30.24 \\ 44.06 & 44.06 \end{bmatrix}$.

Therefore, the linear integer programming (5.3) can be solved by B&B method.

Step 5.B: The step of the B&B method is shown in Figure 5.2. Each rectangular box denotes a node in a tree. The depth-first convention renders the visiting order of the nodes as follows: sub-problem 1 → 2→3→4→5→6→8→9→7. The new constraints adding to the sub-problems are shown adjacent to the arrows. The optimal solution is

found in sub-problem 9. Therefore, set $\overline{TC}$= 6321.7, $\overline{\boldsymbol{\alpha}^1}$ = $\begin{bmatrix}2 & 4\\4 & 2\\0 & 0\end{bmatrix}$, $\overline{\boldsymbol{\alpha}^2}$ = $\begin{bmatrix}2 & 4\\3 & 1\\0 & 0\end{bmatrix}$.

Step 5.C-3: Based on $\overline{\boldsymbol{\alpha}^1}$, run Algorithm 5.A and find the optimal location $\tilde{\mathbf{r}}$ = $[48.09\ \ 59.91\ 47.94\ 59.71]^T$, $\widetilde{TC}$= 5279.3.

Step 5.C-4: $\widetilde{TC} < TC_{opt}$, then $TC_{opt} \coloneqq \widetilde{TC}$ = 5279.3, $\boldsymbol{\alpha}^1_{opt}$ = $\begin{bmatrix}2 & 4\\4 & 2\\0 & 0\end{bmatrix}$ $\boldsymbol{\alpha}^2_{opt}$ = $\begin{bmatrix}2 & 4\\3 & 1\\0 & 0\end{bmatrix}$ $\mathbf{r}_{opt}$ = $\tilde{\mathbf{r}}$ = $[48.09\ \ 59.91\ 47.94\ 59.71]^T$.

Step 5.C-5: Setting the infinitesimal number to be 0.1. $\left|\widetilde{TC} - \overline{TC}\right| >$ infinitesimal number, then $\bar{\mathbf{r}}$ = $\tilde{\mathbf{r}}$ and go to Step 5.C-2.

Iteration *5*.C-2:

Step 5.C-2: Running Algorithm 5.B with $\bar{\mathbf{r}}$ = $[48.09\ \ 59.91\ 47.94\ 59.71]^T$. Obtain $\overline{\boldsymbol{\alpha}^1}$ = $\begin{bmatrix}2 & 3\\4 & 3\\0 & 0\end{bmatrix}$, $\overline{\boldsymbol{\alpha}^2}$ = $\begin{bmatrix}1 & 2\\4 & 3\\0 & 0\end{bmatrix}$ and $\overline{TC}$= 4716.6.

Step 5.C-3: Run Algorithm 5.A and find the optimal location $\tilde{\mathbf{r}}$ = $[48.09\ \ 59.91\ \ 48.09\ \ 59.9]^T$ based on $\overline{\boldsymbol{\alpha}^n}$. $\widetilde{TC}$= 4711.0.

Step 5.C-4: $\widetilde{TC} < TC_{opt}$, then $TC_{opt} \coloneqq \widetilde{TC}$= 4711.0, $\boldsymbol{\alpha}^1_{opt}$ =$\begin{bmatrix}2 & 3\\4 & 3\\0 & 0\end{bmatrix}$, $\boldsymbol{\alpha}^2_{opt}$ = $\begin{bmatrix}1 & 2\\4 & 3\\0 & 0\end{bmatrix}$, $\mathbf{r}_{opt}$ = $\tilde{\mathbf{r}}$ = $[48.09\ \ 59.91\ \ 48.09\ \ 59.9]^T$.

Step 5.C-5: $\left|\widetilde{TC} - \overline{TC}\right| >$ infinitesimal number, then $\bar{\mathbf{r}}$ = $\tilde{\mathbf{r}}$ and go to Step 5.C-2.

Step 5.C-2: Running Algorithm 5.B with $\bar{\mathbf{r}}$ = $[48.09\ \ 59.91\ \ 48.09\ \ 59.9]^T$. Obtain $\overline{\boldsymbol{\alpha}^1}$ = $\begin{bmatrix}2 & 3\\4 & 3\\0 & 0\end{bmatrix}$, $\overline{\boldsymbol{\alpha}^2}$ = $\begin{bmatrix}1 & 2\\4 & 3\\0 & 0\end{bmatrix}$ and $\overline{TC}$= 4711.0.

Step 5.C-3: Running Algorithm 5.A and find the optimal location $\tilde{\mathbf{r}}$ = $[48.09\ \ 59.91\ \ 48.09\ \ 59.9]^T$ based on $\overline{\boldsymbol{\alpha}^n}$. $\widetilde{TC}$= 4711.0.

Step 5.C-4: $\widetilde{TC} = TC_{opt}$, then $TC_{opt} \coloneqq \widetilde{TC}$= 4711.0, $\boldsymbol{\alpha}_{opt}^1 = \begin{bmatrix} 2 & 3 \\ 4 & 3 \\ 0 & 0 \end{bmatrix}$, $\boldsymbol{\alpha}_{opt}^2 = \begin{bmatrix} 1 & 2 \\ 4 & 3 \\ 0 & 0 \end{bmatrix}$, $\mathbf{r}_{opt} = \tilde{\mathbf{r}}$ = $[48.09\ \ 59.91\ \ 48.09\ \ 59.9]^T$.

Step 5.C-5: $\widetilde{TC} = \overline{TC}$. Stop and optimal solutions are stored in $TC_{opt}$, $\boldsymbol{\alpha}_{opt}^n$ and $\mathbf{r}_{opt}$. □

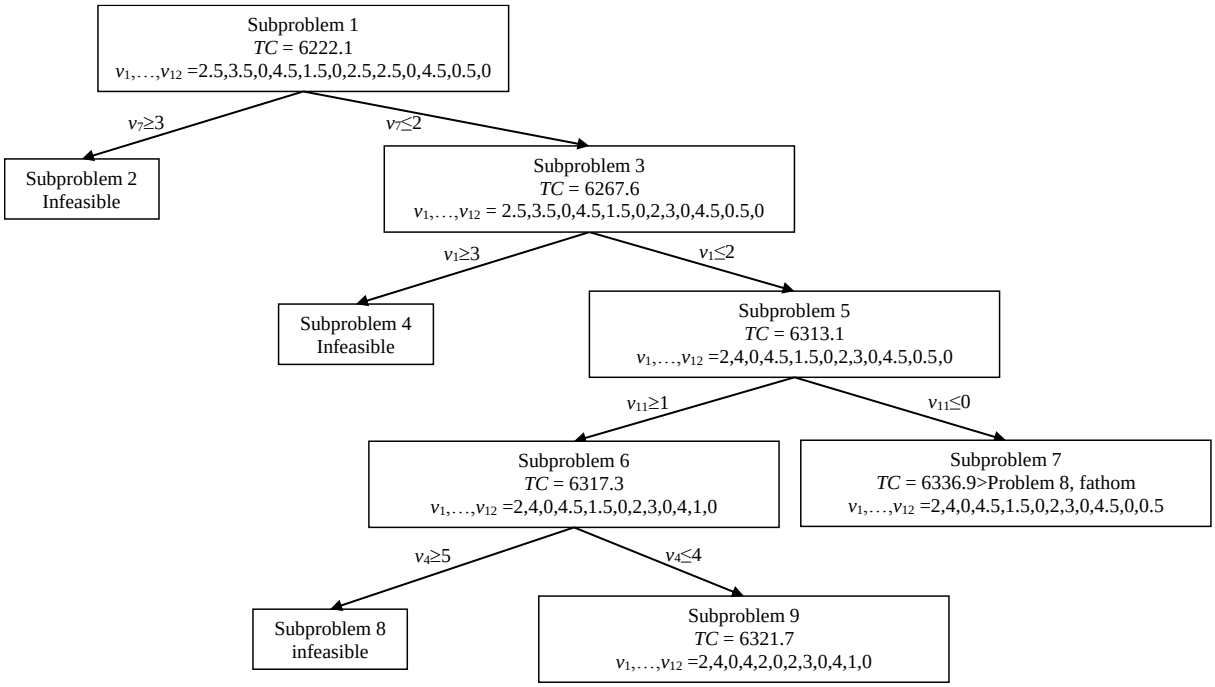


Figure 5.3: Branch and Bound method flow chart for Example 5.2.

A heuristic for the mixed integer programming (5.1) is proposed by alternatively searching minimal for two sets of decoupled sub-problems. An example is provided to go through the heuristic, step by step. To test the efficiency of the heuristic, more numerical examples are tested in the next chapter.

## 5.6 NUMERICAL EXAMPLES

The validity of the proposed heuristic ASTCH is tested in this section using various numerical instances. The parameters of these numerical examples are selected based on real-world applications and most of them are chosen randomly to avoid the effect of artificially created numbers. All the numerical experiment are conducted in the Matlab using computer with Intel® Core ™ i7-4750HQ CPU@2.00GHz. Without loss of generality, common parameters for all numerical examples are chosen as $C^f$ = 2,000,000, $C_n^v$ = 200,000 for $n = 1, \dots, N$, $C^w$ = 10, $\beta$ = 0.05. The rest parameters are selected in a random manner such that the values conform to a uniform distribution within a certain range. The parameter selection process relies on two random-number-generating functions: $\mathrm{rand}(m, n)$ and $\mathrm{randi}([\mathrm{LB}, \mathrm{UB}], m, n)$ where $m$ and $n$ are positive integer, lower bound (LB) and upper bound (UB) are non-negative real numbers. $\mathrm{rand}(m, n)$ generates an $m \times n$ matrix with each element ranging from 0 to 1 and accommodating uniform distribution. $\mathrm{randi}([\mathrm{LB}, \mathrm{UB}], m, n)$ creates an $m \times n$ matrix whose elements are uniformly distributed with LB and UB. The parameters for the hubs locations $\mathbf{x}^h = [x_z^h] \in \mathbb{R}^{\boldsymbol{Z}}$ and $\mathbf{y}^h = [y_z^h] \in \mathbb{R}^Z$, the residue availability $\mathbf{A} = [A_{zk}] \in \mathbb{R}^{Z \times K}$ and the transportation cost $\mathbf{C}^t = [C_{zk}^t] \in \mathbb{R}^{Z \times K}$ are selected as

$\mathbf{x}^h = 100\mathrm{rand}(Z, 1)$, $\mathbf{y}^h = 100\mathrm{rand}(Z, 1)$,

$\boldsymbol{A} = 2 + 3rand(Z, K)$,

$\boldsymbol{C}^t = 3 + 2rand(Z, K)$.

With definition of the function $\mathrm{rand}(m, n)$, the coordinates of hubs' locations are selected and uniformly distributed within the bound $[0,100] \times [0,100]$; the residue availability is bounded by 2 to 5 truck-loads for each hub and the transportation cost for each residue in a hub is between 3 and 5 dollar/truck-load/mile.

The demand for the residues in the reactor $\mathbf{D} = [D_{nk}] \in \mathbb{R}^{N\times K}$, feedstock cost $\mathbf{C}^r = [C^r_{zk}] \in \mathbb{R}^{Z\times K}$ and unit workforce $\mathbf{w} = [w_k] \in \mathbb{R}^K$ are set to

$\mathbf{D} = \text{randi}([1.5Z, 2Z], N, K)$,

$\mathbf{C}^r = \text{randi}([100,150], Z, K)$,

$\mathbf{w} = \text{randi}([3,5], K, 1)$.

The random integers consists of, the demand of each residue at $n$th reactor, the feedstocks costs and the unit workforce. As indicating by the definition of $\text{randi}([\text{LB}, \text{UB}], m, n)$, these three parameters $\mathbf{D}$, $\mathbf{C}^r$ and $\mathbf{w}$ are bounded by $1.5Z$ to $2Z$ truck-loads, 100 to 150 dollars/truck-load and 3 to 5 persons/truck-load, respectively. At last, the total available workforce $W$ is set empirically to $8ZK$.

Numerical examples varies on the number of hubs ($Z$), types of residues ($K$) and reactors ($N$). Ten combinations of $Z$, $K$and $N$ are tested to show a generalized tendency of increasing problem size affecting the computation complexity. Since most parameters are selected randomly without considering the feasibility, the parameter combinations that lead to infeasible solution of the original model are discarded. Only the sets of parameters that results in feasible solutions are tested in the experiment. Table 5.1 shows 10 sets of numerical results. The number of hubs $Z$ are selected from 3 to 50, the types of residues $K$ increases from 2 to 10 and the number of reactors $N$ is from 2 to 10. Detailed results for each set of problem are listed and their corresponding parameters are shown in Wu and Sarker (2014). The experiment uses second for the unit of CPU time. The last two columns are denoted by the number of iterations "$nIter$" and the number of nodes in the ith iteration ($i$ = 1,…,$nIter$) "$nNod_i$." The number of average nodes is computed as $(\sum_{i=1}^{nIter} nNod_i)/nIter$.

Table 5.1: Comparison of numerical results between Lingo and ASTCH.

| | *Prob. Size* | **Lingo** | | **ASTCH** | | | | | |
|---|---|---|---|---|---|---|---|---|---|
| ***Prob.*** | ***Z×K×N*** | $TC^{min}$ | ***CPU Time (s)*** | $TC^{min}$ | ***CPU Time (s)*** | ***No. of Iter.*** | ***Avg. No. of Iter.*** | ***No. of Nodes per Iter. (Avg.)*** | ***Avg. No. of Nodes per Iter.*** |
| *MR1-1* | 3×2×2 | 2404653 | <1 | 2404653 | 0.54 | 3 | 3 | 7.6 | 9.3 |
| *MR1-2* | | 2405639 | <1 | 2405639 | 0.54 | 3 | | 8.4 | |
| *MR1-3* | | 2403467 | <1 | 2403467 | 1.24 | 3 | | 11.5 | |
| *MR1-4* | | 2405858 | <1 | 2405858 | 0.60 | 3 | | 9.6 | |
| *MR2-1* | 3×3×2 | 2406774 | <1 | 2406774 | 0.64 | 3 | 2.5 | 10.8 | 19.4 |
| *MR2-2* | | 2406513 | <1 | 2406513 | 1.36 | 2 | | 19.2 | |
| *MR2-3* | | 2407185 | <1 | 2407185 | 2.89 | 3 | | 28.3 | |
| *MR2-4* | | 2406011 | <1 | 2406011 | 1.09 | 2 | | 19.2 | |
| *MR3-1* | 5×3×3 | 2672248 | <1 | 2672248 | 11.80 | 5 | 4.25 | 116.4 | 105.2 |
| *MR3-2* | | 2683284 | <1 | 2683284 | 11.70 | 4 | | 114.0 | |
| *MR3-3* | | 2675883 | <1 | 2675883 | 15.30 | 5 | | 101.0 | |
| *MR3-4* | | 2669277 | <1 | 2669277 | 8.85 | 3 | | 89.5 | |
| *MR4-1* | 10×3×3 | 2687107 | <1 | 2687107 | 8.83 | 5 | 4.5 | 117.6 | 125.7 |
| *MR4-2* | | 2688171 | <1 | 2686241 | 13.38 | 3 | | 122.4 | |
| *MR4-3* | | 2687125 | <1 | 2685121 | 13.21 | 3 | | 134.4 | |
| *MR4-4* | | 2688786 | <1 | 2687414 | 16.33 | 7 | | 128.4 | |
| *MR5-1* | 10×5×3 | 2709168 | <1 | 2708145 | 16.24 | 3 | 4.75 | 130.8 | 130.6 |
| *MR5-2* | | 2703616 | <1 | 2702951 | 23.64 | 5 | | 149.0 | |
| *MR5-3* | | 2709246 | <1 | 2709106 | 24.64 | 5 | | 122.4 | |
| *MR5-4* | | 2716918 | <1 | 2715741 | 19.72 | 6 | | 120.0 | |
| *MR6-1* | 15×5×5 | 2770456 | 1 | 2768547 | 16.02 | 4 | 4.5 | 174.6 | 193.3 |
| *MR6-2* | | 2773190 | 1 | 2772148 | 45.96 | 5 | | 206.6 | |
| *MR6-3* | | 2770864 | 1 | 2767487 | 66.76 | 6 | | 218.6 | |
| *MR6-4* | | 2758297 | 1 | 2755214 | 24.58 | 3 | | 173.5 | |
| *MR7-1* | 20×5×5 | 2817602 | 1 | 2815365 | 155.10 | 6 | 6 | 391.4 | 375.7 |
| *MR7-2* | | 2849265 | 1 | 2846548 | 133.35 | 5 | | 393.4 | |
| *MR7-3* | | 2829266 | 1 | 2827417 | 100.80 | 7 | | 353.0 | |
| *MR7-4* | | 2825484 | 1 | 2823649 | 90.93 | 6 | | 364.8 | |
| *MR8-1* | 20×10×8 | 2990712 | 1 | 2982011 | 233.70 | 3 | 3.5 | 718.0 | 646.6 |
| *MR8-2* | | 2988124 | 1 | 2985475 | 220.50 | 3 | | 644.8 | |
| *MR8-3* | | 3008394 | 1 | 3006547 | 142.95 | 5 | | 676.8 | |
| *MR8-4* | | 3012105 | 1 | 3001541 | 196.05 | 3 | | 546.7 | |
| *MR9-1* | 30×10×8 | 3245985 | 1 | 3243514 | 684.45 | 5 | 5 | 960.5 | 980.7 |
| *MR9-2* | | 3154785 | 1 | 3152487 | 298.80 | 3 | | 1032.6 | |
| *MR9-3* | | 3321451 | 1 | 3320091 | 591.30 | 7 | | 1023.8 | |
| *MR9-4* | | 3125478 | 1 | 3121462 | 623.70 | 5 | | 906.0 | |
| *MR10-1* | 50×10×10 | 3514264 | 2 | 3510021 | 1092.60 | 4 | 4 | 2871.6 | 2856.8 |
| *MR10-2* | | 3547821 | 2 | 3543145 | 1054.35 | 5 | | 2700.4 | |
| *MR10-3* | | 3415474 | 2 | 3412034 | 1180.80 | 3 | | 3352.0 | |
| *MR10-4* | | 3621101 | 2 | 3610851 | 1243.95 | 4 | | 2503.2 | |

* Computer: *Intel Core i7-4750HQ@ 2.00GHz*

Table 5.2: CPU time of numerical results of ASTCH.

| *Problem Sets* | *Problem Size* | *MAX CPU Time(s)* | *MIN CPU Time(s)* | *Avg CPU Time(s)* |
|---|---|---|---|---|
| *MR1* | 3×2×2 | 1.34 | 0.36 | 0.67 |
| *MR2* | 3×3×2 | 3.01 | 0.38 | 1.54 |
| *MR3* | 5×3×3 | 17.64 | 6.63 | 14.72 |
| *MR4* | 10×3×3 | 20.81 | 8.53 | 16.97 |
| *MR5* | 10×5×3 | 27.65 | 12.96 | 23.38 |
| *MR6* | 15×5×5 | 66.76 | 16.02 | 38.23 |
| *MR7* | 20×5×5 | 169.12 | 89.56 | 146.73 |
| *MR8* | 20×10×8 | 233.70 | 135.98 | 172.95 |
| *MR9* | 30×10×8 | 769.86 | 298.80 | 589.32 |
| *MR10* | 50×10×10 | 1432.80 | 860.01 | 1218.76 |

* Problem size, $Z \times K \times N$. Computer: *Intel Core i7-4750HQ@ 2.00GHz*

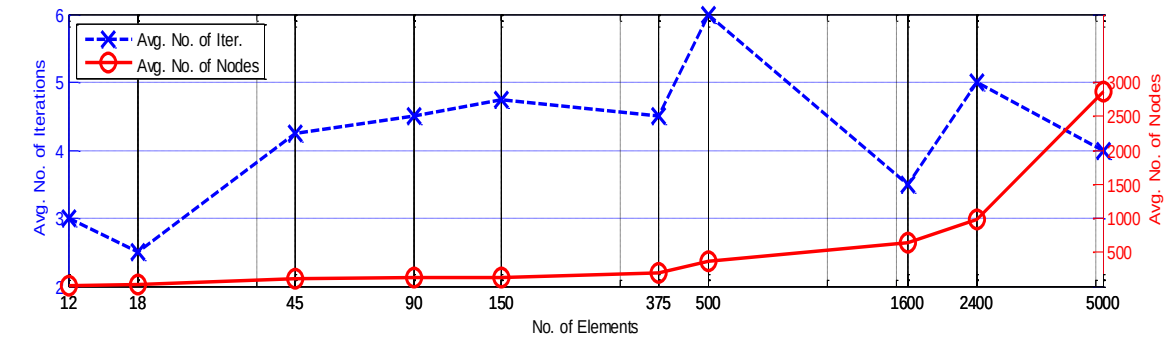


(a)

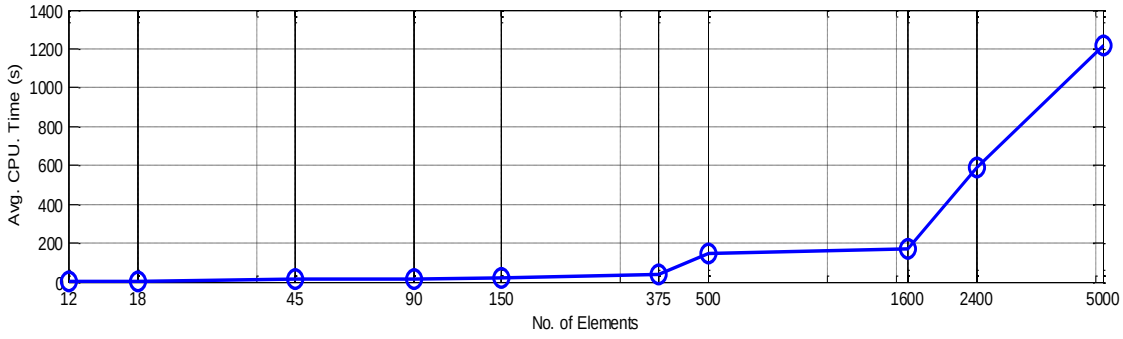


(b)

Figure 5.4: Average iteration/nodes evaluated No. and CPU times versus problem sizes.

It's shown in Table 5.1 that it requires 2 to 6 times the number of iterations for all sets of problem converging to optimal. Since the initial guess of the reactors' locations are selected randomly, the efficient convergence to the optimal solution suggests the effectiveness of the proposed ASTCH. The heuristic guarantees a convergence, a consistency of $\overline{TC}$ and $\widetilde{TC}$, regardless of the initial condition.

The average number of nodes varied from 7.7 to 3352 depending on the size of the problems. The average number of nodes stays close within each set of problem, which is caused by the parameters being bounded in a relatively small range. A clear tendency shows an increasing size of problem leads to an increasing visiting of the nodes when the B&B method is applied. Since the number of nodes increases, the CPU time increases accordingly. These related observations are consistent with the expectance of the numerical examples.

A conventional way of evaluating the performance of a heuristic is to estimate a lower bound. However, due to the existence of nonlinearity in the fourth term in model (5.1) and its non-convex nature, it is trivial to obtain the lower bound for a mixed integer programming. Therefore, a comparison with the results computed by Lingo is conducted to show the validity of the proposed heuristic. The Lingo results and CPU time are shown in the 3$^{rd}$ and 4$^{th}$ column in Table 5.1. By comparing the optimal results from Lingo and ASTCH, it shows that the optimal solutions from Lingo is no better than ASTCH although Lingo takes less computation time. ASTCH compromises a longer CPU time for a better optimal results. Further optimization of the ASTCH code such as parallel programming or coding in C may help to shorten the CPU time of the heuristic. Although ASTCH requires longer time to converge, it is within a reasonable amount of time and is practical for real-world applications. The

comparison results show a satisfactory performance of the proposed ASTCH applying in the location allocation problem of the BMG production system.

In the first experiment, each set of problems contains 4 particular numerical examples. Another experiment is conducted by running 30 numerical examples in each problem set of Table 5.1. The maximum, minimum and average CPU time for solving these problems is provided in Table 5.2. It shows in Table 5.2 that even for a large size problem in real-world scenario ($50 \times 10 \times 10$), a reasonable CPU time can be expected, which further shows the efficiency of the ASTCH.

Two additional columns, the average number of iterations and the average number of nodes per iteration, are added to Table 5.1. Let the problem size be defined as the value of $Z \times K \times N$. Figure 5.4(a) and 5.4(b) uses the problem size as the $x$ axis. Figure 5.4(a) uses the average number of iterations and average number of nodes per iteration as the $y$ axes while Figure 5.4(b) take the average CPU time in Table 5.2 as the $y$ axis. Figure 5.4(a) show the average number of nodes per iteration increases appreciably as the problem size grows. However, since the average number of iteration decrease when the initial guess of the reactors' locations is close to the optimal solution, a random initial guess renders an irregular pattern (neither increase nor decrease) of the number of iterations with respect to the problem size. Figure 5.4(b) shows the CPU time increases while the problem size increases, which is consistent with the expected result.

## 5.7 CONCLUDING REMARKS

With the increasing needs of renewable energy, planning and efficient management are important in BMG manufacturing which can specifically reduce the total cost and increase revenues. The major concern in this model is in multiple BMG reactors building and logistic

optimization. A mathematical model, which can be generalized as a nonlinear mixed integer programming, is established to optimize locations of reactors, determine the supply plan between hubs and reactors, and minimize the total cost. An alternative based heuristic is proposed to solve the programming. Numerical examples are provided to prove effectiveness of the heuristic.

This research is the first in the literature that was reviewed to mathematically modeling a complicated BMG production location-allocation problem. The major contributions lie in two aspects: first, an optimal strategic plan for real-world applications is provided by solving the SS-MRS model for the BMG production system. And, second, the heuristic proposed in this chapter uses the Successive Substitution algorithm which helped to reduce the computation time for solving the MINLP.

# CHAPTER VI
# MODEL III: A THREE-STAGE MULTI-FACILITY SYSTEM PROBLEM

The goal of this chapter is to model a multi-feedstock, multi-facility, and multi-stage BMG production system. A location and distribution plan for facilities will be devised by solving a MINLP model by proposing an alternative search-based algorithm.

## 6.1 PROBLEM DESCRIPTION AND NOTATION

Assume a BMG manufacturing system is built in a given area. The scope of the system involves transporting the residues from the farms, production of the liquefied Carbon Product (LCP), and delivery to its final destinations. The production process involves conversion of residues into the BMG through an anaerobic process and then conversion of BMG into LCP through a condensation process.

A local area is divided into small zones by zip codes. Each zip code area contains several farms that generate various residues, such as livestock feces and plant residues. In each zip code, there is a hub that stores all available residues from farms in that area. A BMG plant is built in the area, and reactors and condensers are constructed for production. Reactors will collect residues by truck from hubs, and each hub is allowed to supply one or more reactors. After BMG is generated, condensers are needed to produce the liquefied final product, which is easy to store and to transport. Pipelines will be laid between reactors and condensers for transport of BMG. Lastly, final products will be delivered by truck to the delivery points for sale (Figure 6.1).

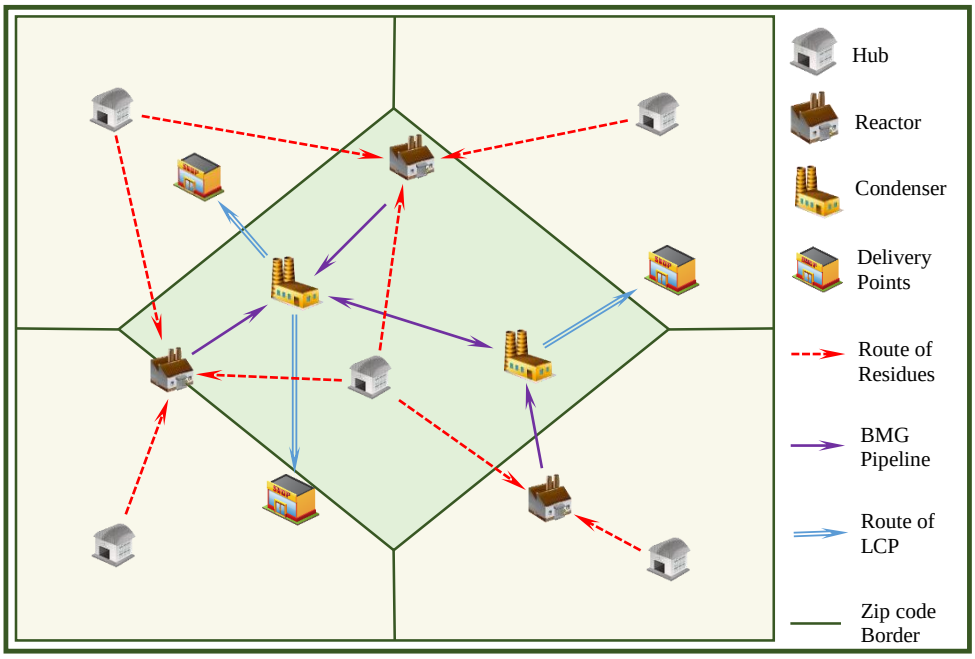


Figure 6.1: Illustration of location-allocation problem in TS-MFS BMG production system.

The total cost of the BMG production model consists of the cost for each stage. In the first stage, the locations of reactors and the amount of residue transported from hubs to reactors, the fixed and variable building costs, the costs of transporting residue, the costs of purchasing residues, and labor costs are included in the objective function. Various constraints, such as workforce availability to handle the residue, the demand for residue at each reactor, and residue availability at each hub are included in this stage and are modeled by inequalities. In the second stage, pipelines are laid from reactors to condensers and among condensers for BMG delivery, and the transportation network is built so that the carbon product can be moved from condensers to delivery points; all costs for this construction and transportation are considered in this stage. Two equalities are modeled as constraints in the second stage, which ensure that each reactor connects to one condenser and that each delivery point is served by one condenser.

The notations are defined under several classifications:

**Parameters**

| | |
|---|---|
| $K$ | Total number of types of residues. |
| $Z$ | Total number of zip codes in the region. |
| $N$ | Total number of reactors to be built. |
| $M$ | Total number of condensers to be built. |
| $L$ | Total number of delivery points. |
| $k$ | Index for residue types, $k = 1, \dots, K$. |
| $z$ | Index of zip codes of a hub, $z = 1, \dots, Z$. |
| $n$ | Index for reactors, $n = 1, \dots, N$. |
| $m$ | Index for condensers, $m = 1, \dots, M$. |
| $l$ | Index for delivery of point, $l = 1, \dots, L$. |
| $A_{zk}$ | Availability of the residue $k$ in the hub in zip code $z$ (truck-load). |
| $C^f$ | Fixed costs to build all reactors and condensers, shared equally among unit time periods (dollar). |
| $C_n^v$ | Variable cost to build the $n$th reactor, shared equally among unit time periods (dollar). |
| $C_m^{vc}$ | Variable cost to build the $m$th condenser, shared equally across each year (dollar). |
| $C^w$ | Unit cost for hiring a worker (dollar /person/truck load). |
| $C_{zk}^t$ | Unit transportation cost of moving residue $k$ from the hub in zip code $z$ to a reactor (dollar/truck-load/mile). |

$C_{zk}^{r}$ Feedstock cost of residue $k$ supplied from the hub in zip code $z$ to a reactor (dollar/truck-load).

$C_{mn}^{p}$ Unit building cost of pipeline laid from reactor $n$ to condenser $m$ (dollar/mile).

$C_{ml}^{d}$ Unit transportation cost for liquefied carbon product from condenser $m$ to delivery point $l$ (dollar/truck-load/mile).

$C_{m-1,m}^{b}$ Pipeline layout costs between condensers $m$ = 2,3, … , $M$ (dollar). Assume pipeline is built to connect condenser $m-1$ and $m$.

$D_{kn}$ Demand for residues $k$ at the $n$th reactor (truck-load).

$w_k$ Unit workforce required for collecting residue $k$ (persons/truck-load).

$W_n$ Total workforce availability at the $n$th reactor (persons).

$\beta$ Percentage of deteriorated residue in hubs.

$\mathbf{h}_z$ $\mathbf{h}_z = (x_z^h, y_z^k)$ represents the coordinate of the hub in zip code $z$.

$\mathbf{p}_l$ $\mathbf{p}_l = \left(x_l^p, y_l^p\right)$ represents the coordinate of the delivery point $l$.

**Variables**

$\mathbf{r}_n$ $\mathbf{r}_n = (x_n^r, y_n^r)$ represents the coordinate of the $n$th reactor.

$\mathbf{r}$ $\mathbf{r} = (\mathbf{r}_n) \in \mathbb{R}^{2N}$ is a vector containing all the coordinates of the reactors.

$\mathbf{s}_m$ $\mathbf{s}_m = (x_m^s, y_m^s)$ represents the coordinate of the $m$th condenser.

$\mathbf{s}$ $\mathbf{s} = (\mathbf{s}_m) \in \mathbb{R}^{2M}$ is a vector containing all the coordinates of the condensers.

$\alpha_{zk}^{n}$ Number of truck-loads for moving residue $k$ from the hub in zip code $z$ to the $n$th reactor.

$\boldsymbol{\alpha}^n$ A series of matrices $\boldsymbol{\alpha}^n = [\alpha_{zk}^n]$, $n$ = 1,…,$N$, representing all truck-loads of residue $k$ ($k$ = 1, … , $k$) to be transported from zip code $z$ ($z$ = 1, … , $Z$) to the $n$th reactor.

$\gamma_{mn}$ $\gamma_{mn}$ = 1 if condenser $m$ connects with reactor $n$ with pipeline; $\gamma_{mn}$ = 0 otherwise.

$\boldsymbol{\gamma}$ $\boldsymbol{\gamma} = [\gamma_{mn}] \in \mathbb{R}^{M \times N}$, a 0-1 matrix denotes that the pipeline is built between the $n$th reactor and $m$th condenser if $\gamma_{mn}$ = 1, otherwise $\gamma_{mn}$ = 0.

$\rho_{ml}$ $\rho_{ml}$= 1 if liquefied carbon product in the $m$th condenser is transported to the $l$th delivery point; $\rho_{ml}$ = 0 otherwise.

$\boldsymbol{\rho}$ $\boldsymbol{\rho} = [\rho_{ml}] \in \mathbb{R}^{M \times L}$, a 0-1 matrix denotes that truck transportation is required between the $m$th condenser and $l$th delivery point if $\rho_{ml}$ = 1, otherwise $\rho_{ml}$ = 0.

**Measure of Performance**

$TC(\mathbf{r}, \mathbf{s}, \boldsymbol{\alpha}^1, \ldots, \boldsymbol{\alpha}^n, \boldsymbol{\gamma}, \boldsymbol{\rho})$ Total supply chain cost of the three-stage system (dollars) as a function of the locations of reactors and condensers, and the amount of residue being transported from the hubs to the reactors.

## 6.2 ASSUMPTIONS FOR MODEL III

The fundamental assumptions that are used for this research are as follows:

1. The reactor has the capability to process all types of residues.
2. The locations of hubs and delivery points are given by GIS.
3. There is no loss of material during transportation between hubs and reactors, as well as condensers.
4. Residue deterioration occurs in hubs.
5. The demand of each reactor for each residue is known.
6. The number of reactors and condensers to be built is given.

## 6.3 MATHEMATICAL MODEL

The BMG production facility location and delivery problem will be modeled in this section. Several practical matters, such as the demands for reactors, labor availability, residue availability, and BMG availability are considered. Transportation costs, feedstocks costs, building costs for facilities and pipelines, and labor costs are considered for the system's total cost.

Before presenting the mathematical model, the Euclidean distance function is defined as $d(\mathbf{a}, \mathbf{b}) = \|\mathbf{a} - \mathbf{b}\|$, where $\mathbf{a} = (x_a, y_a)$and $\mathbf{b} = (x_b, y_b)$are the planar location vectors,$\|\mathbf{a} - \mathbf{b}\| = \sqrt{(x_a - x_b)^2 + (y_a - y_b)^2}$. Then the Problem can be modeled as:

**Problem BMG-RC:**

$$\begin{aligned}\text{Min } TC(\mathbf{r}, \mathbf{s}, \boldsymbol{\alpha}^1, \dots, \boldsymbol{\alpha}^n, \boldsymbol{\gamma}, \boldsymbol{\rho}) = {} & C^f + \sum_{n=1}^{N} C_n^v + \sum_{m=1}^{M} C_m^{vc} + \sum_{z=1}^{Z}\sum_{k=1}^{K}\sum_{n=1}^{N} C_{zk}^r \alpha_{zk}^n \\ & + \sum_{z=1}^{Z}\sum_{k=1}^{K}\sum_{n=1}^{N} d(\mathbf{h}_z, \mathbf{r}_n) C_{zk}^t \alpha_{zk}^n \\ & + C^w \sum_{z=1}^{Z}\sum_{k=1}^{K}\sum_{n=1}^{N} w_k \alpha_{zk}^n \\ & + \sum_{m=1}^{M}\sum_{n=1}^{N} d(\mathbf{s}_m, \mathbf{r}_n) C_{mn}^p \gamma_{mn} \\ & + \sum_{m=1}^{M}\sum_{l=1}^{L} d(\mathbf{s}_m, \mathbf{p}_l) C_{ml}^d \rho_{ml} \\ & + \sum_{m=2}^{M} C_{m-1,m}^b \, d(\mathbf{s}_{m-1}, \mathbf{s}_m) \end{aligned} \tag{6.1}$$

Subject to: $\sum_{z=1}^{Z}\sum_{k=1}^{K} w_k \alpha_{zk}^n \leq W_n$, $n = 1, \dots, n$ (6.1a)

$\sum_{z=1}^{Z} \alpha_{zk}^n \geq D_{kn}$, for $k = 1, \dots, K$, $n = 1, \dots, N$ (6.1b)

$\sum_{z=1}^{Z} \alpha_{zk}^n \leq (1 - \beta) \sum_{z=1}^{Z} A_{zk}$, for $k = 1, \dots, K$, $n = 1, \dots, N$ (6.1c)

$\alpha_{zk}^n \leq (1 - \beta) A_{zk}$ for $n = 1, \dots, N$ (6.1d)

$\sum_{m=1}^{M} \gamma_{mn} = 1$ for $n = 1, \dots, N$ (6.1e)

$\sum_{m=1}^{M} \rho_{ml} = 1$, for $l = 1, \dots, L$ (6.1f)

$\alpha_{zk}^n, \gamma_{nm}, \rho_{ml} \geq 0$ and $\alpha_{zk}^n, \gamma_{nm}, \rho_{ml} \in \mathbb{Z}$, for all $m, n, k, l, z$. (6.1g)

where $\mathbb{Z}$ is the set of all integers. Equation (6.1) is composed of 8 separate costs, which are fixed: reactor building costs, variable building costs for reactors, residues purchasing costs, residues transportation costs from hubs to reactors, labor costs for handling residues, pipeline layout costs between reactors and condensers, liquefied carbon product transportation costs from condensers to delivery points, and pipeline layout costs among condensers. Constraint (6.1a) ensures that the required labor costs for collecting residue from hubs at each reactor is always bounded by workforce availability at that reactor. Constraint (6.1b) indicates that there is a minimum demand for each type of residue from each reactor. Constraint (6.1c) denotes that the total deliverable amount of residue is bounded by its availability, which is subjected to deterioration. Constraint (6.1d) reflects that the amount of $k$th residue that is transported from the hub in zip code $z$ to the $n$th reactor has an upper bound denoted by the availability of residue $k$ at the hub in zip code $z$. Constraint (6.1e) guarantees that each reactor connects to one condenser through a pipeline. Constraint (6.1f) ensures that each delivery point obtains supply from one condenser. Constraint (6.1g) states that $\alpha_{zk}^{n}, \gamma_{mn}$ and $\rho_{ml}$ are all non-negative integers.

The objective function (6.1) can be divided into two sub-problems that are location and allocation problems. Obtaining variables $\mathbf{r}$ and $\mathbf{s}$ corresponds to optimally locating reactors and condensers. Determining variables $\boldsymbol{\alpha}^1, \ldots, \boldsymbol{\alpha}^n, \boldsymbol{\gamma}$ and $\boldsymbol{\rho}$ requires optimal allocation of residue to the reactors, BMG to the condensers, and liquefied carbon product to the delivery points. The characteristics of the two sub-problems are studied in the next section before developing algorithms to solve the MINLP (6.1).

## 6.4 SOLUTION METHODOLOGY

The objective function (6.1) is a function of variables $\mathbf{r}, \mathbf{s}, \boldsymbol{\alpha}^1, \ldots, \boldsymbol{\alpha}^n, \boldsymbol{\gamma}$ and $\boldsymbol{\rho}$, which can be further categorized into two groups. The reactors' locations $\mathbf{r}$ and the condensers' locations $\mathbf{s}$ is the set of location variables (SOLV), and the rest of the variables is the set of allocation variables (SOAV). If the SOAV is known, because there are no constraints for the SOLV, the original MINLP (6.1) becomes an unconstrained nonlinear programming problem (NLP) with the objective function expressed only in terms of the SOLV. On the other hand, if the SOLV is known, the original MINLP (6.1) becomes a mixed-integer linear programming problem (MILP), with an objective function in terms of the SOAV and constraints are from (1a) to (6.1g). The properties of both sub-problems are explored and computational algorithms are proposed to solve the sub-problems separately.

### 6.4.1 Location Sub-Problem

With the assumption that the SOAV is known, the location sub-problem can be written as

$$\begin{aligned}\text{Min } TC(\mathbf{r},\mathbf{s}) = {} & C^f + \sum_{n=1}^{N} C_n^v + \sum_{z=1}^{Z}\sum_{k=1}^{K}\sum_{n=1}^{N} C_{zk}^r \alpha_{zk}^n \\ & + \sum_{z=1}^{Z}\sum_{k=1}^{K}\sum_{n=1}^{N} d(\mathbf{h}_z,\mathbf{r}_n) C_{zk}^t \alpha_{zk}^n \\ & + C^w \sum_{z=1}^{Z}\sum_{k=1}^{K}\sum_{n=1}^{N} w_k \alpha_{zk}^n \\ & + \sum_{m=1}^{M}\sum_{n=1}^{N} d(\mathbf{s}_m,\mathbf{r}_n) C_{mn}^p \gamma_{mn} \\ & + \sum_{m=1}^{M}\sum_{l=1}^{L} d(\mathbf{s}_m,\mathbf{p}_l) C_{ml}^d \rho_{ml} \\ & + \sum_{m=2}^{M} C_{m-1,m}^b \, d(\mathbf{s}_{m-1},\mathbf{s}_m), \end{aligned} \tag{6.2}$$

which is different from the original objective function (6.1) in the sense that only the SOLV is to be determined. The first-order derivation of equation (6.2) with respect to the SOLV renders

$$\frac{\partial TC(\mathbf{r})}{\partial \mathbf{r}_n} = \sum_{z=1}^{Z}\sum_{k=1}^{K} \frac{C_{zk}^t \alpha_{zk}^n}{d(\mathbf{h}_z,\mathbf{r}_n)} (\mathbf{r}_n - \mathbf{h}_z) + \sum_{m=1}^{M} \frac{C_{mn}^p \gamma_{mn}}{d(\mathbf{s}_m,\mathbf{r}_n)} (\mathbf{r}_n - \mathbf{s}_m), \tag{6.3a}$$

$$\frac{\partial TC(\mathbf{r})}{\partial \mathbf{s_m}} = \sum_{n=1}^{N} \frac{C_{mn}^{p}\gamma_{mn}}{d(\mathbf{s}_m,\mathbf{r}_n)}(\mathbf{s}_m - \mathbf{r}_n) + \sum_{l=1}^{L} \frac{C_{ml}^{d}\rho_{ml}}{d(\mathbf{s}_m,\mathbf{p}_l)}(\mathbf{s}_m - \mathbf{p}_l) + T(\mathbf{s}_m), \quad (6.3b)$$

where

$$T(\mathbf{s}_m) = \begin{cases} \frac{C_{1,2}^{b}}{d(\mathbf{s}_1,\mathbf{s}_2)}(\mathbf{s}_1 - \mathbf{s}_2), \text{ for } m = 1 \\ \frac{C_{m-1,m}^{b}}{d(\mathbf{s}_{m-1},\mathbf{s}_m)}(\mathbf{s}_m - \mathbf{s}_{m-1}) + \frac{C_{m,m+1}^{b}}{d(\mathbf{s}_m,\mathbf{s}_{m+1})}(\mathbf{s}_m - \mathbf{s}_{m+1}), \text{for } m = 2, \dots, M-1. \\ \frac{C_{M-1,M}^{b}}{d(\mathbf{s}_{M-1},\mathbf{s}_M)}(\mathbf{s}_M - \mathbf{s}_{M-1}), \text{ for } m = M \end{cases} \quad (6.3c)$$

The optimal solution exists at the points that render the first derivative of the objective function as zero. Therefore, the optimal solution for the NLP (6.2) can be found by setting (6.3a) and (6.3b) to zero. Further inspection of equations (6.3a) and (6.3b) suggests that they are multi-variable, high-order sets of equations. Therefore, there are multiple solutions to equations (6.3a) and (6.3b), which further indicates that the NLP (6.2) is non-convex and has multiple local minima.

Various algorithms that solve a non-convex nonlinear programming problem have been proposed in the literature. The algorithm can be categorized into two classes that are derivative-based and derivative-free. A derivative-based algorithm utilizes the first-order derivative and/or a Hessian Matrix to achieve a local minimum. A popular algorithm that is widely used for solving the nonlinear programming problem is the BFGS Quasi-Newton Method (Broyden, 1970, Fletcher, 1970, Goldfarb, 1970 and Shanno, 1970), which uses the cubic line search method and BFGS formula to compute the Hessian Matrix numerically. This algorithm is effective when the first and second derivative of the objective function are continuous. However, it is apparent from the first-order derivative (6.3) and Hessian Matrix that the distance functions appear in the denominator, which renders a discontinuity in both the first and second order derivatives. Therefore, a derivative-free algorithm is considered to solve the NLP (6.2).

The Nelder-Mead simplex algorithm (NMSA) (Lagarias *et al*., 1998) is a non-derivative based search algorithm that achieves a local optimum by iteratively evaluating the objective function without the information of its first and second-order derivatives. The NMSA for solving the nonlinear programming problem (6.2) is outlined as follows:

**Algorithm 6.A: NMSA**

Step 6.A-0: Let $\mathbf{u} = (u_i) = \begin{bmatrix}\mathbf{r}\\ \mathbf{s}\end{bmatrix} \in \mathbb{R}^{M+N}$. Take an initial guess $\mathbf{u}^0 = (u_i^0) \in \mathbb{R}^{M+N}$ and make a simplex by adding 5% for each $u_i^0$ to $\mathbf{u}^0$. These $M + N$ vectors together with the original $\mathbf{u}^0$ consists of a simplex.

Step 6.A-1: Let $\mathbf{U}_i$ represent the points in the current simplex,$i = 1, \dots, M + N + 1$.

Step 6.A-2: Evaluate the total cost according to the equation (6.2). From the lowest $TC(\mathbf{U}_1)$ to highest $TC(\mathbf{U}_{M+N+1})$, order the points in the simplex. In each iteration, the current worst point $\mathbf{U}_{M+N+1}$ is discarded, and another point is introduced into the simplex. Stop iteration until $\sum_i^{M+N+1}\left(TC(\mathbf{U}_i) - TC(\mathbf{\Omega})\right)^2 \leq \varepsilon$ where $\mathbf{\Omega} = \frac{1}{M+N}\sum_{i=1}^{M+N}\mathbf{U}_i$ and ε is an infinitesimal positive number.

Step 6.A-3: Generate the reflected point $\mathbf{U}^r = 2\mathbf{\Omega} - \mathbf{U}_{M+N+1}$, and compute $TC(\mathbf{U}^r)$.

Step 6.A-4: If $TC(\mathbf{U}_1) \leqslant TC(\mathbf{U}^r) < TC(\mathbf{U}_{M+N+1})$, accept $\mathbf{U}^r$ and go to Step 6.A-2.

Step 6.A-5: If $TC(\mathbf{U}^r) < TC(\mathbf{U}_1)$, compute both the expansion point $\mathbf{U}^s = \mathbf{\Omega} + 2(\mathbf{\Omega} - \mathbf{U}_{M+N+1})$ and its function value $TC(\mathbf{U}^s)$.

a. If $TC(\mathbf{U}^s) < TC(\mathbf{U}^r)$, accept $\mathbf{U}^s$ and go to Step 6.A-2.

b. Otherwise, accept $\mathbf{U}^r$ instead and go to Step 6.A-2.

Step 6.A-6: If $TC(\mathbf{U}^r) \geqslant TC(\mathbf{U}_{M+N})$, a contraction is performed between $\mathbf{\Omega}$ and the better of $\mathbf{U}_{M+N+1}$ and $\mathbf{U}^r$:

a. If $TC(\mathbf{U}^r) < TC(\mathbf{U}_{M+N+1})$, compute both the $\mathbf{\Phi} = \mathbf{\Omega} + (\mathbf{U}^r - \mathbf{\Omega})/2$ and its function value $TC(\mathbf{\Phi})$. If $TC(\mathbf{\Phi}) < TC(\mathbf{U}^r)$, accept $\mathbf{\Phi}$ and go to Step 6.A-2. Otherwise, go to Step 6.A-7.

b. If $TC(\mathbf{U}^r) \geqslant TC(\mathbf{U}_{M+N+1})$, compute both $\mathbf{\Psi} = \mathbf{\Omega} + (\mathbf{U}_{M+N+1} - \mathbf{\Omega})/2$ and its function value $TC(\mathbf{\Psi})$. If $TC(\mathbf{\Psi}) < TC(\mathbf{U}_{M+N+1})$, accept $\mathbf{\Psi}$ and go to Step 6.A-2. Otherwise, go to Step 6.A-7.

Step 6.A-7: Let $\mathbf{T}_i = \mathbf{U}_1 + (\mathbf{U}_i - \mathbf{U}_1)/2$ , $i = 2, \dots, M+N+1$ and compute each function value $TC(\mathbf{T}_i)$. The next iteration period takes the simplex as $\mathbf{U}_1$, $\mathbf{T}_2$,..., $\mathbf{T}_{M+N+1}$. □

### 6.4.2 Allocation Sub-Problem

The original MINLP (6.1) becomes an allocation sub-problem when the SOLV is fixed and the SOAV is to be determined. The procedure for transferring the MINLP (6.1) to an MILP with known SOLV is presented as follows.

Let $T: \mathbb{R}^{Z\times K} \rightarrow \mathbb{R}^{ZK}$ be a function that transforms a $Z \times K$ matrix to a vector with length $ZK$ by rearranging all columns of the matrix into one column. Denote $\mathbf{1}_s$ a length $s$ vector of all ones and $\mathbf{I_s}$ an $s \times s$ identity matrix. Denote the symbol $\otimes$ the Kronecker matrices product and the symbol $\circ$ the element-wise matrices product.

**Problem 6.1:**

If the location of the reactor **r** is known, the system model (6.2) can be written in the form of a MILP:

$$\text{Min } TC(\mathbf{V}) = \boldsymbol{B}^T\mathbf{V} + \Theta \tag{6.4}$$

$$\text{Subject to: } \mathbf{PV} \leq \mathbf{Q} \tag{6.4a}$$

$$\mathbf{P}_{eq}\mathbf{V} = \mathbf{Q}_{eq} \tag{6.4b}$$

$$\mathbf{V} = (v_i) \in \mathbb{Z}^{ZKN+MN+ML},\ v_i \geq 0 \text{ for } i = 1,\ldots, ZK, \tag{6.4c}$$

where $\mathbf{V} = \begin{pmatrix} T(\boldsymbol{\alpha}^1) \\ \vdots \\ T(\boldsymbol{\alpha}^n) \\ T(\boldsymbol{\gamma}) \\ T(\boldsymbol{\rho}) \end{pmatrix} \in \mathbb{Z}^{ZKN+MN+ML}$;

$\mathbf{B} = \mathbf{1}_n \otimes T(\mathbf{C}^r) + T(\mathbf{1}_k \otimes \mathbf{d}_1) \circ [\mathbf{1}_n \otimes T(\mathbf{C}^t)] + C^w \mathbf{1}_n \otimes (\mathbf{w} \otimes \mathbf{1}_z) + T(\mathbf{d}_2 \circ \mathbf{C}^p) + T(\mathbf{d}_3 \circ \mathbf{C}^d)$ given $\mathbf{C^r} = (C^r_{zk}) \in \mathbb{R}^{ZK}$, $\mathbf{C}^t = (C^t_{zk}) \in \mathbb{R}^{Z\times K}$, $\mathbf{C}^p = \left(C^p_{nm}\right) \in \mathbb{R}^{N\times M}$, $\mathbf{C}^d = \left(C^d_{ml}\right) \in \mathbb{R}^{M\times L}$, $\mathbf{w} = (w_k) \in \mathbb{R}^K$, $\mathbf{d}_1 = \left(d(\mathbf{h}_z, \mathbf{r}_n)\right) \in \mathbb{R}^{Z\times N}$, $\mathbf{d}_2 = \left(d(\mathbf{r}_n, \mathbf{s}_m)\right) \in \mathbb{R}^{N\times M}$, $\mathbf{d}_1 = \left(d(\mathbf{s}_m, \mathbf{p}_l)\right) \in \mathbb{R}^{M\times L}$;

$\Theta = C^f + \sum_{n=1}^{N} nC^v + \sum_{m=2}^{M} C^b_{m-1,m}\, d(\mathbf{s}_{m-1}, \mathbf{s}_m)$;

$\mathbf{P} = \begin{bmatrix} \mathbf{I}_n \otimes (\mathbf{w} \otimes \mathbf{1}_z)^T \\ -\mathbf{I}_{kn} \otimes (\mathbf{1}_z^T) \\ \mathbf{I}_{kn} \otimes (\mathbf{1}_z^T) \end{bmatrix}$; $\mathbf{Q} = \begin{bmatrix} \mathbf{W}_n \\ -T(\mathbf{D}) \\ (1-\beta)\mathbf{1}_n \otimes \left(\mathbf{I}_k \otimes (\mathbf{1}_z^T) T(\mathbf{A})\right) \end{bmatrix}$;

$P_{eq} = \begin{bmatrix} \mathbf{0}^T_{ZKN} & \mathbf{1}^T_{MN} & \mathbf{0}^T_{ML} \\ \mathbf{0}^T_{ZKN} & \mathbf{0}^T_{MN} & \mathbf{1}^T_{ML} \end{bmatrix}$; $\mathbf{Q}_{eq} = \begin{bmatrix} 1 \\ 1 \end{bmatrix}$.

The Branch and Bound (B&B) Method is widely applied and adopted to solve the MILP (6.4). Note that when constraint (6.4b) is relaxed, the MINLP becomes a linear integer programming (LIP) relaxed problem.

**Algorithm 6.B: Breath-first Branch and Bound Method**

Step 6.B-1: Let the best objective value (lower bound) of the MILP (6.4) be $TC_{best}$ , set $TC_{best} = +\infty$.

Step 6.B-2: Solve the LP relaxed problem (6.4) by the simplex method. If an integer solution of **V** is obtained, stop. Otherwise, branch the non-integer element that is the furthest from its nearest integer in **V** and form two new active nodes.

Step 6.B-3: Select an active node based on breath-first criterion and let it be inactive. Solve the current relaxed node. Obtain $\mathbf{V}^*$ and $TC^*$ (current optimal solution).

Step 6.B-4: If there is no feasible solution for the current node, fathom it, make it inactive.

Step 6.B-5: If $\mathbf{V}^*$ is an integer vector that is the first integer obtained, $TC_{best} = TC^*$, fathom the current node and make it inactive. Otherwise proceed to the next step.

Step 6.B-6: If $\mathbf{V}^*$is an integer vector but is not the first integer obtained, then if $TC^* < TC_{best}$, let $TC_{best} = TC^*$, fathom the current node and make it inactive. Otherwise directly fathom the current node and make it inactive.

Step 6.B-7: If $\mathbf{V}^*$ is not an integer vector, then if $TC^* \geq TC_{best}$, fathom the current node and make it inactive. Otherwise, branch on the most-fractional number in $\mathbf{V}^*$ and form two new active nodes.

Step 6.B-8: If there exists an active node, then go to Step 6.B-3; otherwise, stop. □

The characteristics and complexity of the problem were discussed in this section. The next section shows the entire algorithm and provides numerical examples to illustrate the algorithm step by step.

### 6.4.3 Heuristic Design

Although the location and allocation sub-problems can be resolved by the NMSA and B&B methods, respectively, the non-convexity of the original MINLP prevents a global optimum from being obtained readily. Therefore, an algorithm for the MINLP (6.1) is developed, by alternatively solving the two sub-problems, to search for a local minimum that is close to the global optimum. Specifically, the algorithm begins with an initial guess for the locations of reactors and condensers. The B&B method is then applied to obtain a solution for the allocation sub-problem. The location sub-problem is then solved by the NMSA using the

known SOAV from the last step. The algorithm runs both the NMSA and B&B method alternatively until the optimal result for both sub-problems becomes consistent. The detailed procedure is proposed as follows.

**Algorithm 6.C (Main Program): Alternative Search Algorithm (ASA)**

Step 6.C-1: Take $\bar{\mathbf{r}}_n = \frac{1}{N}\sum_{z=1}^{Z} \mathbf{h}_z$, for $n = 1, \ldots, N$ and $\bar{\mathbf{s}}_m = \bar{\mathbf{r}}_n + \frac{1}{L}\sum_{l=1}^{L} \mathbf{p}_l$, for $m = 1, \ldots, M$ as the initial location vectors for the reactors and condensers. Set $TC_{opt} = +\infty$.

Step 6.C-2: Run the B&B process in Algorithm 6.B to find the optimal allocation $\overline{\boldsymbol{\alpha}^n}$, $n = 1, \ldots, N$, $\bar{\boldsymbol{\gamma}}$ and $\bar{\boldsymbol{\rho}}$ based on $\bar{\mathbf{r}}$ and $\bar{\mathbf{s}}$. Let the objective value be $\overline{TC}$.

Step 6.C-3: Run Algorithm 6.A to find the optimal locations $\tilde{\mathbf{r}}$ and $\tilde{\mathbf{s}}$ based on allocations $\overline{\boldsymbol{\alpha}^n}$, $\bar{\boldsymbol{\gamma}}$ and $\bar{\boldsymbol{\rho}}$. Let the objective value be $\widetilde{TC}$.

Step 6.C-4: If $\widetilde{TC} < TC_{opt}$, then $TC_{opt} = \widetilde{TC}$, $\boldsymbol{\alpha}_{opt}^n = \overline{\boldsymbol{\alpha}^n}$ for $n = 1, \ldots, N$, $\boldsymbol{\gamma}_{opt} = \bar{\boldsymbol{\gamma}}$ and $\boldsymbol{\rho}_{opt} = \bar{\boldsymbol{\rho}}$ $\mathbf{r}_{opt} = \tilde{\mathbf{r}}$ and $\mathbf{s}_{opt} = \tilde{\mathbf{s}}$.

Step 6.C-5: If $\left|\overline{TC} - \widetilde{TC}\right| >$ infinitesimal number, then $\bar{\mathbf{r}} = \tilde{\mathbf{r}}$, $\bar{\mathbf{s}} = \tilde{\mathbf{s}}$ and go to Step 6.C-2. Otherwise, stop, and the optimal solution is stored in $TC_{opt}$, $\boldsymbol{\alpha}_{opt}^n$, $\boldsymbol{\gamma}_{opt}$, $\boldsymbol{\rho}_{opt}$, $\mathbf{r}_{opt}$ and $\mathbf{s}_{opt}$. □

## 6.5 ILLUSTRATIVE EXAMPLE

A small numerical example is provided to apply the algorithm step by step. For simplicity, the fixed building cost $C^f$ and variable building cost $C_n^v$ are set to 0, because they appear to be constant in the model. The other system's data list is as follows:

Total number of types of residues, $K$ = 3; total number of zip codes in the region, $Z$ = 4; total number of reactors to be built, $N$ = 2; total number of condensers to be built, $M$ = 2; total number of delivery points, $L$ = 3. Availability of residue $k$ in the hub in zip code $z$, $\mathbf{A}$ =

$[A_{zk}] = \begin{bmatrix} 3.4 & 2.5 & 2.2 \\ 2.3 & 4.5 & 3.3 \\ 2.7 & 3.6 & 2.3 \\ 4.7 & 5.0 & 4.9 \end{bmatrix}$ (truck-load). Unit cost for hiring a worker, $C^w$ = 10 (dollar /person/truck load). Unit transportation cost of moving residue $k$ from the hub in zip code $z$ to the reactor, $\mathbf{C}^{\mathrm{t}} = [C_{zk}^t] = \begin{bmatrix} 3.3 & 4.1 & 3.7 \\ 3.3 & 3.3 & 4.0 \\ 4.7 & 4.7 & 3.8 \\ 4.2 & 4.2 & 3.1 \end{bmatrix}$ (dollar/truck-load/mile). Feedstock cost of residue $k$ supplied from the hub in zip code $z$ to the reactor, $\mathbf{C}^r = [C_{zk}^r] = \begin{bmatrix} 100 & 104 & 122 \\ 139 & 120 & 146 \\ 141 & 113 & 109 \\ 144 & 140 & 113 \end{bmatrix}$ (dollar/truck-load). Unit building cost of pipeline laid from the reactor $n$ to condenser $m$,$\mathbf{C}^p$ = $[C_{nm}^p] = \begin{bmatrix} 3.39 & 4.23 \\ 3.50 & 3.95 \end{bmatrix}$ (dollar/mile). Unit transportation cost for liquefied carbon product from condenser $m$ to delivery point $l$, $\mathbf{C}^d = [C_{ml}^d] = \begin{bmatrix} 3.70 & 4.17 & 4.83 \\ 4.66 & 4.10 & 3.57 \end{bmatrix}$ (dollar/truck-load/mile). Pipeline layout cost between reactors, $C_{1,2}^b$ = 3.76 (dollar/mile). Demand of residues $k$ at the $n$th reactor, $\mathbf{D} = [D_{kn}] = \begin{bmatrix} 6 & 8 \\ 6 & 8 \\ 7 & 6 \end{bmatrix}$ (truck-load). Unit workforce required for collecting residue $k$, $\mathbf{w} = [w_k] = \begin{bmatrix} 3 \\ 5 \\ 4 \end{bmatrix}$ (persons/truck-load). Total workforce availability at the $n$th reactor, $\mathbf{W}$ = $[W_n] = \begin{bmatrix} 96 \\ 96 \end{bmatrix}$ (persons). Percent of residue to be unaccounted for due to deterioration, $\beta$ = 0.05. The coordinate of the hub in zip code $z$, $[(x_1^h, y_1^h)$ , $(x_2^h, y_2^h)$ , $(x_3^h, y_3^h)$ , $(x_4^h, y_4^h)]$ = [(56.88, 16.22), (46.94, 79.43), (1.19, 31.12) , (33.71, 52.85)]. The coordinate of the delivery point $l$, $[(x_1^p, y_1^p)$ , $(x_2^p, y_2^p)]$ = [(116.56,165.41), (160.20,168.92),(126.30,174.82)].

From the above data, the allocation sub-problem can be written in the form of (6.4). Applying the Algorithm C (Main Program) yields:

Iteration 6.C-1:

Step 6.C-1: Let $\bar{\mathbf{r}}_1 = \bar{\mathbf{r}}_2 = \frac{1}{2}\sum_{z=1}^{3} \mathbf{h}_z = \begin{bmatrix} 69.36 \\ 89.81 \end{bmatrix}$ and $\bar{\mathbf{s}}_1 = \bar{\mathbf{s}}_2 = \bar{\mathbf{r}}_1 + \frac{1}{3}\sum_{l=1}^{3} \mathbf{p}_l = \begin{bmatrix} 203.71 \\ 259.52 \end{bmatrix}$ be the initial location vectors for the reactors and condensers. $TC_{opt}$ is set to $+\infty$.

Step 6.C-2: Algorithm 6.B is applied to find the optimal allocation $\overline{\boldsymbol{\alpha}^1} = \begin{bmatrix} 3 & 0 & 0 \\ 2 & 4 & 3 \\ 0 & 0 & 0 \\ 1 & 2 & 4 \end{bmatrix}$, $\overline{\boldsymbol{\alpha}^2} = \begin{bmatrix} 3 & 0 & 0 \\ 2 & 4 & 3 \\ 0 & 0 & 0 \\ 3 & 4 & 4 \end{bmatrix}$, $\bar{\boldsymbol{\gamma}} = \begin{bmatrix} 1 & 0 \\ 0 & 1 \end{bmatrix}$ and $\bar{\boldsymbol{\rho}} = \begin{bmatrix} 1 & 0 & 0 \\ 0 & 1 & 1 \end{bmatrix}$ based on $\bar{\mathbf{r}}$ and $\bar{\mathbf{s}}$. Obtain the objective value as $\overline{TC}$ = 16061.53

Step 6.C-3: Algorithm 6.A is applied to find the optimal locations $\tilde{\mathbf{r}}_1 = \begin{pmatrix} 40.49 \\ 63.83 \end{pmatrix}$, $\tilde{\mathbf{r}}_2 = \begin{bmatrix} 33.71 \\ 52.85 \end{bmatrix}$ and $\tilde{\mathbf{s}}_1 = \begin{bmatrix} 115.77 \\ 160.17 \end{bmatrix}$, $\tilde{\mathbf{s}}_2 = \begin{bmatrix} 115.72 \\ 160.13 \end{bmatrix}$ based on allocations $\overline{\boldsymbol{\alpha}^n}$, $\bar{\boldsymbol{\gamma}}$ and $\bar{\boldsymbol{\rho}}$. Obtain the objective value as $\widetilde{TC}$ = 10787.69.

Step 6.C-4: Because $\widetilde{TC} < TC_{opt}$, then $TC_{opt} = \widetilde{TC}$ = 10787.69, $\boldsymbol{\alpha}_{opt}^n = \overline{\boldsymbol{\alpha}^n}$ for $n = 1, \ldots, N$, $\boldsymbol{\gamma}_{opt} = \bar{\boldsymbol{\gamma}}$ and $\boldsymbol{\rho}_{opt} = \bar{\boldsymbol{\rho}}$ $\mathbf{r}_{opt} = \tilde{\mathbf{r}}$ and $\mathbf{s}_{opt} = \tilde{\mathbf{s}}$.

Step 6.C-5: Because $\left|\overline{TC} - \widetilde{TC}\right|$ = 5273.8 > set precision = 0.1, then $\bar{\mathbf{r}}_1 = \tilde{\mathbf{r}}_1 = \begin{pmatrix} 40.49 \\ 63.83 \end{pmatrix}$, $\bar{\mathbf{r}}_2 = \tilde{\mathbf{r}}_2 = \begin{bmatrix} 33.71 \\ 52.85 \end{bmatrix}$, $\bar{\mathbf{s}}_1 = \tilde{\mathbf{s}}_1 = \begin{bmatrix} 115.77 \\ 160.17 \end{bmatrix}$, $\bar{\mathbf{s}}_1 = \tilde{\mathbf{s}}_2 = \begin{bmatrix} 115.72 \\ 160.13 \end{bmatrix}$ and go to Step 6.C-2.

The main program continues until $\left|\overline{TC} - \widetilde{TC}\right|$ < set precision = 0.1 after 6 iterations. The optimal total cost is 8902.49.

An algorithm for the MINLP (6.1) is proposed by alternatively searching minima for two sets of decoupled sub-problems. A small size example is provided to illustrate the

algorithm step by step. To test the efficiency of the algorithm, more numerical examples are conducted in the next section.

## 6.6 NUMERICAL EXAMPLES

A small example is shown in section 6.5 to illustrate each step in the proposed algorithm. In a real-world application, more hubs, residue types, number of reactors, condensers and delivery points would be involved. Therefore, an efficient and effective algorithm is required for large systems. More numerical examples is conducted in this section to study the performance of the proposed algorithm.

Ten sets of numerical examples, varying with the problem size, were conducted in Matlab run on a computer with Intel® Core™ i7-4750HQ CPU@ 2.00GHz. The selection of parameters was based on the real world BMG production systems. The data for the ten sets of examples were divided into common parameters and random parameters. The common parameters were fixed and used in all the numerical examples. The random parameters were chosen randomly based on a uniform distribution within a certain range. Two functions that generated the random parameters are defined as follows:

$\mathrm{rand}(m, n)$, where $m$ and $n$ are positive integers, generated a $m \times n$ matrix with each element ranging from 0 to 1, and with a uniform distribution.

$\mathrm{randi}([\mathrm{LB}, \mathrm{UB}], m, n)$, where $m$ and $n$ are positive integers, LB (lower bound) and UB (upper bound) are non-negative integers, creates an $m \times n$ integer matrix with elements that are uniformly distributed with LB and UB. The parameters were selected as follows:

**Common Parameters**

Fixed cost to build $N$ reactors: $C^f$ = 2,000,000 (dollar). Variable cost to build the $n$th reactor: $C_n^v$ = 200,000 (dollar) for $n = 1, \dots, N$. Unit cost for hiring a worker: $C^w$ = 10 (dollar /person/truck load). Percent of residue to be unaccounted for due to deterioration: $\beta$ = 0.05.

**Random Parameters**

Availability of residue $k$ in the hub in zip code $z$: $\mathbf{A} = 2 + 3rand(Z, K)$ (truck-load), which is a $Z \times K$ matrix with entries that vary from 2 to 5 and conform to a uniform distribution. Unit transportation cost of moving residue $k$ from the hub in zip code $z$ to the reactor: $\mathbf{C}^{\mathrm{t}} = 3 + 2rand(Z, K)$ (dollar/truck-load/mile). Feedstock cost of residue $k$ supplied from the hub in zip code $z$ to the reactor, $\mathbf{C}^r$ = randi$([100,150], Z, K)$ (dollar/truck-load). Unit building cost of pipeline laid from the reactor $n$ to condenser $m$,$\mathbf{C}^p = 3 + 2rand(M, N)$ (dollar/mile). Unit transportation cost for liquefied carbon product from condenser $m$ to delivery point $l$, $\mathbf{C}^d = 3 + 2rand(M, L)$ (dollar/truck-load/mile). Pipeline layout costs between reactors, $C_{m-1,m}^b = 3 + 2rand(M - 1,1)$ (dollar/mile), for $M = 2, \dots, M$. Demand for residue $k$ at the nth reactor, $\mathbf{D}$ = randi$([1.5Z, 2Z], N, K)$ (truck-load). Unit workforce required to collect the residue $k$, $\mathbf{w}$ = randi$([3,5], K, 1)$, (persons/truck-load). Total workforce availability for the $n$th reactor, $\mathbf{W} = 8ZK\mathbf{1}_N$ (persons). The coordinate for the hub in zip code $z$, $\mathbf{x}^h$ = 100rand$(Z, 1)$, $\mathbf{y}^h$ = 100rand$(Z, 1)$. The coordinate for the delivery point $l$, $\mathbf{x}^p$ = $100 + 100$rand$(Z, 1)$, $\mathbf{y}^p$ = 100+100rand$(Z, 1)$.

Table 6.1: Comparison of numerical results between Lingo and ASA.

| | ***Prob. Size*** | **Lingo** | | **ASA** | | | | | |
|---|---|---|---|---|---|---|---|---|---|
| ***Prob.*** | ***Z×K×N ×M × L*** | $TC^{min}$ | ***CPU Time (s)*** | $TC^{min}$ | ***CPU Time (s)*** | ***No. of Iter.*** | ***Avg. No. of Iter.*** | ***No. of Nodes per Iter. (Avg.)*** | ***Avg. No. of Nodes per Iter.*** |
| *TS1-1* | 3×2×2 ×2×3 | 2406090 | <1 | 2406090 | 0.95 | 6 | 6.25 | 34.67 | 32.12 |
| *TS1-2* | | 2406784 | <1 | 2406784 | 0.72 | 5 | | 30.40 | |
| *TS1-3* | | 2409033 | <1 | 2405944 | 0.87 | 7 | | 27.29 | |
| *TS1-4* | | 2406518 | <1 | 2406395 | 1.14 | 7 | | 36.14 | |
| *TS2-1* | 5×3×2 ×2×5 | 2415697 | <1 | 2412941 | 0.67 | 4 | 5.25 | 36.75 | 40.54 |
| *TS2-2* | | 2416806 | <1 | 2413384 | 0.94 | 5 | | 40.60 | |
| *TS2-3* | | 2414219 | <1 | 2413285 | 1.11 | 6 | | 40.67 | |
| *TS2-4* | | 2414952 | <1 | 2413191 | 1.23 | 6 | | 44.17 | |
| *TS3-1* | 5×3×3 ×3×5 | 2623328 | <1 | 2617069 | 2.32 | 7 | 7.5 | 70.29 | 66.79 |
| *TS3-2* | | 2623935 | <1 | 2620494 | 2.34 | 8 | | 64.25 | |
| *TS3-3* | | 2625660 | <1 | 2618819 | 1.92 | 6 | | 68.17 | |
| *TS3-4* | | 2622446 | <1 | 2620594 | 2.70 | 9 | | 64.44 | |
| *TS4-1* | 10×3×3 ×3×10 | 2638668 | <1 | 2638473 | 1.67 | 5 | 6 | 77.00 | 96.14 |
| *TS4-2* | | 2656114 | <1 | 2643604 | 2.85 | 6 | | 104.17 | |
| *TS4-3* | | 2650132 | <1 | 2640686 | 2.84 | 6 | | 106.00 | |
| *TS4-4* | | 2645287 | <1 | 2638955 | 2.96 | 7 | | 97.43 | |
| *TS5-1* | 10×5×3 ×3×10 | 2679632 | 1 | 2659682 | 3.28 | 6 | 8.25 | 125.17 | 125.47 |
| *TS5-2* | | 2681378 | 1 | 2669279 | 5.40 | 10 | | 122.00 | |
| *TS5-3* | | 2680503 | 1 | 2665805 | 5.19 | 9 | | 125.22 | |
| *TS5-4* | | 2693405 | 1 | 2681112 | 4.73 | 8 | | 129.50 | |
| *TS6-1* | 15×5×5 ×5×15 | 3181318 | 1 | 3171257 | 20.98 | 11 | 12.25 | 435.91 | 436.98 |
| *TS6-2* | | 3191360 | 1 | 3188813 | 32.37 | 17 | | 438.18 | |
| *TS6-3* | | 3157154 | 1 | 3155038 | 13.48 | 7 | | 439.29 | |
| *TS6-4* | | 3172206 | 1 | 3171755 | 26.61 | 14 | | 434.57 | |
| *TS7-1* | 20×5×5 ×5×20 | 3237151 | 1 | 3220276 | 14.54 | 6 | 11.25 | 523.67 | 510.49 |
| *TS7-2* | | 3267176 | 1 | 3250464 | 23.84 | 11 | | 492.36 | |
| *TS7-3* | | 3237697 | 1 | 3214330 | 25.90 | 12 | | 491.67 | |
| *TS7-4* | | 3247568 | 1 | 3239354 | 40.89 | 17 | | 534.29 | |
| *TS8-1* | 20×10×8×8×20 | 4368808 | 2 | 4342033 | 159.68 | 16 | 33.75 | 2202.19 | 2262.78 |
| *TS8-2* | | 4380463 | 2 | 4375688 | 871.36 | 85 | | 2302.89 | |
| *TS8-3* | | 4301562 | 2 | 4275787 | 154.61 | 15 | | 2344.93 | |
| *TS8-4* | | 4377763 | 2 | 4365151 | 185.58 | 19 | | 2201.11 | |
| *TS9-1* | 30×10×8×8×30 | 4756616 | 2 | 4728902 | 158.64 | 11 | 25 | 3148.09 | 3234.25 |
| *TS9-2* | | 4853291 | 2 | 4782587 | 240.74 | 16 | | 3355.56 | |
| *TS9-3* | | 4754649 | 2 | 4659432 | 689.79 | 47 | | 3318.89 | |
| *TS9-4* | | 4753286 | 2 | 4743565 | 373.08 | 26 | | 3114.46 | |
| *TS10-1* | 50×10×10×10×50 | 5755697 | 2 | 5541279 | 550.82 | 23 | 22.75 | 5340.30 | 5294.71 |
| *TS10-2* | | 5756261 | 2 | 5453786 | 355.03 | 15 | | 5415.93 | |
| *TS10-3* | | 5758067 | 2 | 5499467 | 797.12 | 34 | | 5171.76 | |
| *TS10-4* | | 5754452 | 2 | 5493075 | 451.86 | 19 | | 5250.84 | |

* Computer: *Intel Core i7-4750HQ@ 2.00GHz*

Table 6.2: CPU time of numerical results of ASA.

| *Problem Sets* | *Problem Size* | *MAX CPU Time(s)* | *MIN CPU Time (s)* | *Avg. CPU Time (s)* |
|---|---|---|---|---|
| *TS1* | 3×2×2×2×3 | 2.21 | 0.64 | 1.08 |
| *TS2* | 3×3×2×2×5 | 2.6 | 0.50 | 1.20 |
| *TS3* | 5×3×3×3×5 | 3.20 | 1.70 | 2.10 |
| *TS4* | 10×3×3×3×10 | 4.53 | 1.50 | 2.91 |
| *TS5* | 10×5×3×3×10 | 5.52 | 3.25 | 4.82 |
| *TS6* | 15×5×5×5×15 | 36.13 | 12.58 | 25.53 |
| *TS7* | 20×5×5×5×20 | 45.62 | 13.72 | 34.49 |
| *TS8* | 20×10×8×8×20 | 871.36 | 135.25 | 302.96 |
| *TS9* | 30×10×8×8×30 | 932.53 | 158.64 | 473.21 |
| *TS10* | 50×10×10×10×50 | 1242.16 | 293.76 | 672.16 |

* Problem size $Z \times K \times N \times M \times L$. Computer: *Intel Core i7-4750HQ@ 2.00GHz*

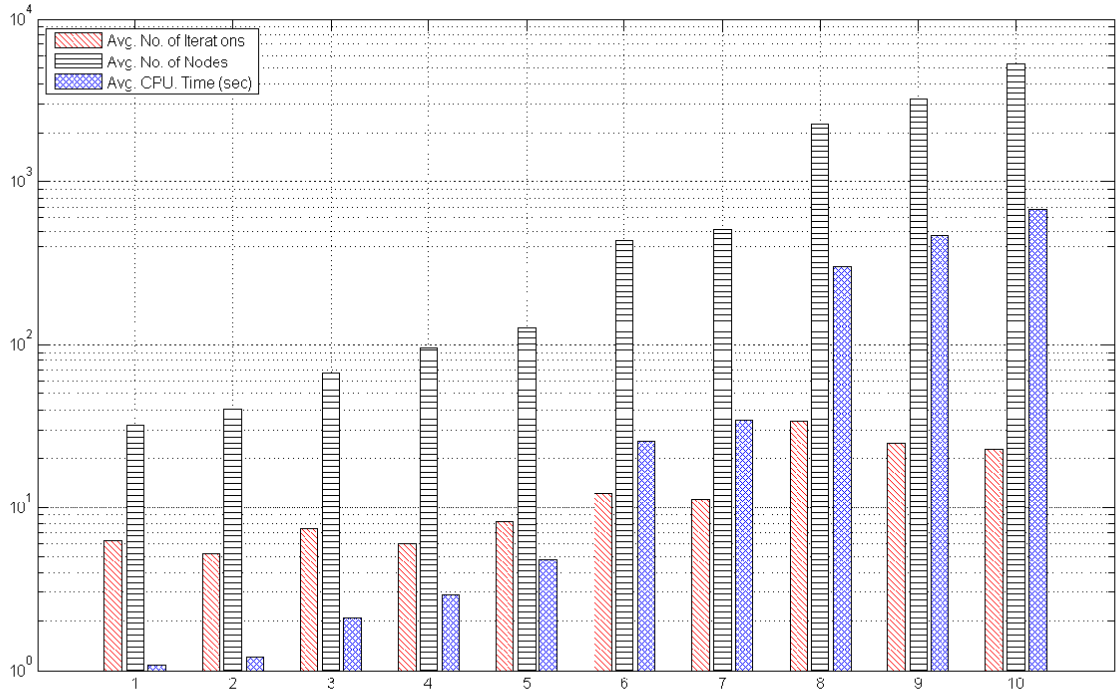


Figure 6.2: Average iteration/nodes evaluated No. and CPU times versus problem sizes.

The result of the first numerical experiment is shown in Table 6.1. Ten sets of examples, each of which contained 4 examples with different parameter sets, were conducted with different problem sizes. The numbers varied for the hubs ($Z$) from 3 to 50, for the types of residues ($K$) from 2 to 10, for the reactors ($N$) from 2 to 8, for the condensers ($M$) from 2 to 8, and for the delivery points from 3 to 50. The ten sets of examples numbered from 1 to 10 are ordered in increasing fashion for the problem size. Due to the existence of random parameters, the generated parameters cannot always ensure the feasibility of the MINLP. Therefore, infeasible combinations of parameters were discarded, leaving only feasible sets of parameters for numerical computation. The parameters that were used for the experiment shown in Table 6.1 are listed in Wu and Sarker (2014). To verify the numerical results from the proposed algorithm, the original MINLP (6.1) with the parameters was also solved by Lingo® for comparison. The optimal objective function value $TC^{min}$ and the required CPU time (in second) were provided for both the Lingo and ASA results. For the $i$th example in one set of examples, denote the number of iterations for the ASA that achieved convergence by $I_i$ and the number of nodes visited per iteration by $E_i$. The average number of iterations was calculated by $\sum_{i=1}^{4} I_i \,/4$ and the average number of nodes per iteration was calculated by $\sum_{i=1}^{4} E_i \,/4$.

The average number of nodes being visited during the B&B algorithm increased with the increase in problem size. Within each set of the numerical examples, the number of nodes per iteration was relatively stable among the four examples. The random selection of parameters caused the number of nodes per iteration to vary in a certain set, but the bound of these random parameters ensured that the variation was kept small. Due to the increasing number of nodes in this computation, a longer CPU time was required for solving the MINLP.

By comparing the results from Lingo and ASA, it is apparent that Lingo and ASA had similar solutions when the problem size was relatively small (before the 5th set of examples, Table 6.1). However, ASA produced a better solution when the problem size increased. The trade-off for obtaining a better solution for ASA is that it takes a longer CPU time than does Lingo to achieve an optimal solution. Because the CPU time needed for ASA to solve the problem was less than 800 sec, which is an acceptable length of time to solve a $50 \times 10 \times 10 \times 10 \times 50$ size problem in this numerical example, it can be concluded that ASA is an effective way of solving the MINLP (6.1).

A second numerical experiment is conducted with the same sets of examples. Each problem size ran with 50 sets of random parameters. The maximum, minimum, and average CPU time was recorded (Table 6.2). Let the number of elements be defined as the value of $Z \times K \times N \times M \times L$. Figure 6.2 plots the number of elements versus the average number of iterations, average number of nodes, and the average CPU time (Table 6.1 and 6.2). The average number of nodes per iteration increased dramatically as the problem size grew (Figure 6.2). However, a random initial guess produced an irregular pattern (neither an increase nor decrease) in the number of iterations with respect to the problem size, because the average number of iterations was reduced when the initial guess of the reactors' locations was close to the optimal solution. CPU time also increased when the problem size increased, which is consistent with the expected result (Figure 6.2).

## 6.7 CONCLUDING REMARKS

The major concern in this chapter was to obtain an optimal supply chain plan for a typical three-stage BMG production system that consisted of building reactors to collect residue and building condensers to liquefy the generated BMG. An optimized supply chain

plan for the BMG production system included optimization of the road transportation network, the building locations of the facilities, and the layout of the pipeline.

An MINLP was developed to describe the supply chain model of the three-stage system. The MINLP was then divided into location and allocation sub-problems. A novel search-based algorithm was proposed to solve the MINLP. Numerical experiments were conducted to verify the performance of the algorithm.

This research is the first to mathematically model a three-stage BMG production location-allocation problem. The major contributions here involve two aspects. First, the modeling process gave us clear guidance for building a BMG plant in a real world situation. Second, an alternative search-based algorithm was proposed in the research, which solved the problem efficiently and effectively compared to other algorithms available at the present.

# CHAPTER VII
# MODEL IV: A FOUR-STAGE MULTI-FACILITY SYSTEM PROBLEM

The objective of this chapter is to model a four-stage BMG production system. The locations of the hubs will be considered as variables and seasoning supplement of the feedstocks is taken into account.

## 7.1 PROBLEM DESCRIPTION AND NOTATION

A typical supply chain of the BMG production system covers four stages, which include the storage and transportation of residues from the farms to the hubs, the transportation of residues from the hubs to the reactors, the supply of generated BMG to the condensers for liquefaction, and the delivering of the liquefied BMG to the delivery points. A supply chain schematic is shown in Figure 7.1 and each stage is described in detail as follows.

### 7.1.1 Farm to Hub and Hub to Reactor Stages: Feedstock Handling

A BMG production system is planned to be built in a certain area that contains several zip codes. Farms with known global location coordinates are scattered in each zip code area and seasonally produce different types of bio-residues. For example, assume a farm produces six types of residues A, B, C, D, E, and F on a yearly basis. Residues A, B, and E are available in spring, residues B, C, and F are available in summer, residues A, B, and E are available in the autumn, and only residue B is available in winter. A hub is needed in each zip code area to centralize and store all the residues from the farms in that zip code area. By assuming that the unit transportation cost for each residue is different, the location of the hub for each zip code area needs to be optimally selected such that the total transportation cost for collecting all the residues is minimized.

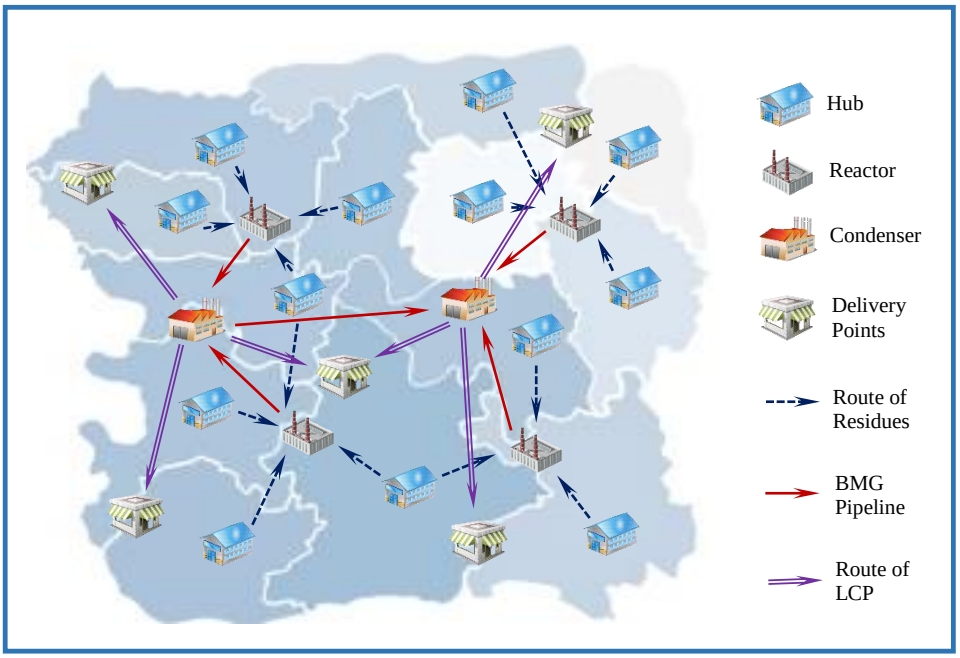


Figure 7.1: Illustration of location-allocation problem in FS-MFS BMG production system.

Once the locations of the hubs are determined, the next objective is to optimize the location of the BMG reactors and the transportation network that efficiently deliver the residues from the hubs to the reactors. The fixed and variable building costs of the reactors, the transportation costs of the residues, and the labor costs are added to represent the supply chain cost. Various constraints, such as the seasonal availability of the residues, the limited workforce, the reactors' demand on the residues, and the deterioration of the residues in the hubs are considered to simulate a pragmatic scenario. When BMG is produced in the reactors, it is ready to enter the next stage.

### 7.1.2 Reactor to Condenser Stage: Supplying of the Generated BMG

The reactor-generated BMG cannot be used directly as an energy source. Instead, a liquefaction process conducted in the condensers is required for ease of storage and transportation. BMG is supplied through the pipelines that connect the reactors to the condensers. The supply chain cost, which can be minimized by optimizing the pipeline network

and the condensers' locations, consists of the pipeline layout costs and the condensers' building costs. The constraints at this stage ensure that each reactor connects to one condenser. After BMG passes from the condensers, liquefied BMG continues to the next stage.

### 7.1.3 Condenser to Delivery Point Stage: Transportation of Liquefied BMG

After BMG is liquefied in the condensers, it becomes the end product that is distributed by tank trucks to the delivery points for the end users. A transportation network needs to be constructed to optimally allocate the liquefied BMG to the delivery points. Assuming that the global location coordinates of the delivery points are known, then the transportation network depends on the locations of the condensers. The constraints guarantee that each delivery point obtains an end product from one condenser.

Note that although the supply chain as a whole can be divided into four stages, it is customary to consider the influence that each stage has on the next. The locations of the hubs can be determined solely by the locations of the farms, but the determination of the locations of the reactor and the condensers, the allocation topology for the residue transportation, the pipeline layout, and the end product distribution affect each other. Therefore, a systematic consideration of the inner relations among these targeting variables is required when the mathematical model is devised.

The notation is divided into three categories: parameters are given beforehand, variable are the values to be determined, and the decision measure is the objective function to be minimized. The notation used in this research is listed below.

**Parameters**

$K$ Total number of types of residues.

$Z$ Total number of zip codes in the region.

$N$ Total number of reactors to be built.

$M$ Total number of condensers to be built.

$L$ Total number of delivery points.

$k$ Index for residue types, $k = 1, \dots, K$.

$z$ Index of zip codes of a hub, $z = 1, \dots, Z$.

$n$ Index for reactors, $n = 1, \dots, N$.

$m$ Index for condensers, $m = 1, \dots, M$.

$l$ Index for delivery of point, $l = 1, \dots, L$.

$Q_z$ Number of farms in zip code $z$.

$q$ Index for farms, $q = 1, \dots, Q_z$, $z = 1, \dots, Z$.

$t$ Season parameter: $t = 1, \dots, 4$ indicate spring, summer, fall, and winter, respectively.

$C_{qkz}^{f \to h}$ Unit transportation cost of moving residue $k$ from the $q$th farm in zip code $z$ (dollar/truck-load/mile). Superscript $f \to h$ stands for farms to hubs.

$S_{zk}^{q}(t)$ Stock amount of the $k$th residue in the $q$th farm of zip code $z$ at different seasons (truck-load).

$C^f$ Fixed cost of building all the hubs, reactors, and condensers shared equally across each year (dollar).

$C_z^{vh}$ Variable cost to build the $z$th hub, shared equally across each year (dollar).

$C_n^{vr}$ Variable cost to build the $n$th reactor, shared equally across each year (dollar).

$C_m^{vc}$ Variable cost to build the $m$th condenser, shared equally across each year (dollar).

$C^w$ Unit cost for hiring a worker (dollar /person/truck load).

$C_{zk}^{h\to r}$ Unit transportation cost of moving residue $k$ from the hub in zip code $z$ to a reactor (dollar/truck-load/mile). Superscript $h \to r$ stands for hubs to reactors.

$C_{zk}^{raw}$ Feedstock cost of residue $k$ supplied from the hub in zip code $z$ to a reactor (dollar/truck-load).

$C_{mn}^{r\to c}$ Normalized unit cost of building pipeline from reactor $n$ to condenser $m$ (dollar/mile), the superscript $r \to c$ stands for reactors to condensers.

$C_{ml}^{c\to d}$ Unit transportation cost for liquefied carbon product from condenser $m$ to delivery point $l$ (dollar/truck-load/mile). Superscript $c \to d$ stands for condensers to delivery points.

$C_{m-1,m}^{c\to c}$ Normalized unit cost of building pipeline between condensers $m = 2,3,\dots,M$ (dollar). Assume pipeline is built to connect the condenser $m-1$ and $m$. Superscript $c \to c$ stands for condensers to condensers.

$D_{kn}(t)$ Demand for residue $k$ for the nth reactor at season $t$ (truck-load).

$w_k$ Unit workforce required for collecting residue $k$ (persons/truck-load).

$W_n$ Total workforce availability at the $n$th reactor (persons).

$\beta$ Percentage of deteriorated residue in hubs.

$\mathbf{f}_{qz}$ $\mathbf{f}_{qz} = \left(x_{qz}^f, y_{qz}^f\right)$ represents the coordinate of the $q$th farm in zip code $z$.

$\mathbf{p}_l$ $\mathbf{p}_l = \left(x_l^p, y_l^p\right)$ represents the coordinate of the delivery point $l$.

**Variables**

$\mathbf{h}_z$ $\mathbf{h}_z = (x_z^h, y_z^k)$ represents the coordinate of the hub in zip code $z$.

$\mathbf{h}$ $\mathbf{h} = (h_z) \in \mathbb{R}^{2Z}$ is a vector containing all the coordinates of the hubs.

$\mathbf{r}_n$ $\mathbf{r}_n = (x_n^r, y_n^r)$ represents the coordinate of the $n$th reactor.

$\mathbf{r}$ $\mathbf{r} = (\mathbf{r}_n) \in \mathbb{R}^{2N}$ is a vector containing all the coordinates of the reactors.

$\mathbf{s}_m$ $\mathbf{s}_m = (x_m^s, y_m^s)$ represents the coordinate of the $m$th condenser.

$\mathbf{s}$ $\mathbf{s} = (\mathbf{s}_m) \in \mathbb{R}^{2M}$ is a vector containing all the coordinates of the condensers.

$\alpha_{zk}^n(t)$ Number of truck-loads for moving residue $k$ from the hub in zip code $z$ to the $n$th reactor at season $t$.

$\boldsymbol{\alpha}^n(t)$ A series of matrices $\boldsymbol{\alpha}^n(t) = [\alpha_{zk}^n(t)]$, n = 1,…,N, representing all truck-loads of residue $k$ ($k = 1, \dots, k$) to be transported from zip code $z$ ($z = 1, \dots, Z$) to the nth reactor at season $t$ ($t = 1, \dots, 4$).

$\gamma_{mn}$ $\gamma_{mn}$ = 1 if condenser $m$ connects with reactor $n$ with pipeline; $\gamma_{mn}$ = 0 otherwise.

$\boldsymbol{\gamma}$ $\boldsymbol{\gamma} = [\gamma_{mn}] \in \mathbb{R}^{M \times N}$, a 0-1 matrix denotes that the pipeline is built between the $n$th reactor and $m$th condenser if $\gamma_{mn} = 1$, otherwise $\gamma_{mn} = 0$.

$\rho_{ml}$ $\rho_{ml}$= 1 if liquefied carbon product in the $m$th condenser is transported to the $l$th delivery point; $\rho_{ml} = 0$ otherwise.

$\boldsymbol{\rho}$ $\boldsymbol{\rho} = [\rho_{ml}] \in \mathbb{R}^{M \times L}$, a 0-1 matrix denotes that truck transportation is required between the $m$th condenser and $l$th delivery point if $\rho_{ml} = 1$, otherwise $\rho_{ml} = 0$.

**Measure of Performance**

$TC(\mathbf{h}, \mathbf{r}, \mathbf{s}, \boldsymbol{\alpha}^1, \dots, \boldsymbol{\alpha}^n, \boldsymbol{\gamma}, \boldsymbol{\rho})$ Total supply chain cost of the four-stage system (dollars) as a function of the locations of hubs, reactors and condensers, and the amount of residue being transported from the hubs to the reactors.

## 7.2 ASSUMPTIONS FOR MODEL IV

The system modeling requires reasonable assumptions for the complicated four-stage supply chain system. To reflect the essence of a practical BMG supply chain system, the

assumptions below are made in a way such that their presence in a real-world application is justifiable.

**Feedstock Handling Stages:**

1. The location coordinates of the farms are given by GIS and the zip code of each farm is known.
2. The stock amount of each residue in each farm at each season is known.
3. Each hub has the capacity to store all the residues in its zip code area.
4. Deterioration occurs on the residues stored in each hub.
5. Each reactor has minimum demand for the residues because there is a minimum demand on BMG in the market.
6. There is no loss of residue during the transportation.
7. The number of reactors to be built is given.

**R2C Stage:**

1. Each reactor connects at least one condenser through a pipeline.
2. Each condenser connects at least one reactor through a pipeline.
3. Some of the condensers are connected with each other through pipelines to increase system redundancy such that when one condenser stops working, BMG that is transferred to that condenser can be rerouted to the remaining condensers.
4. The number of condensers to be built is known.

**C2DP Stage:**

1. Each condenser connects at least one delivery point via roadway.
2. Each delivery point connects at least one condenser via roadway.

3. The unit transportation costs for the condensers is known and varies due to the different geographic locations of the condensers.

4. The location coordinates of the delivery points are given by GIS.

## 7.3 MODEL FORMULATION

The modeling of the first stage total assumes that a seasonal change in the amount of residues is imposed. Therefore, the quantity of residues transported from the farms to the hubs is season-dependent, and the amount of residues delivered from the hubs to the reactors is also a variant of time. The R2C and C2DP stages are modeled such that the total cost of each stage is a function of the distance between each reactor and condenser or between each condenser and delivery point. Before proposing the model, a distance function is defined

$$d(\mathbf{a}, \mathbf{b}) = \sqrt{(x_a - x_b)^2 + (y_a - y_b)^2} \tag{7.1}$$

where $\mathbf{a} = (x_a, y_a)$ and $\mathbf{b} = (x_b, y_b)$ denotes the coordinates of points $a$ and $b$ on a plane. The model is presented as follows.

**Problem BMG-HRC:**

$$\begin{aligned}
&\text{Line 1: Min } TC(\mathbf{h}, \mathbf{r}, \mathbf{s}, \boldsymbol{\alpha}^1, \dots, \boldsymbol{\alpha}^n, \boldsymbol{\gamma}, \boldsymbol{\rho}) = C^f + \sum_{z=1}^{Z} C_z^{vh} + \sum_{n=1}^{N} C_n^{vr} + \sum_{m=1}^{M} C_m^{vc} \\
&\text{Line 2:} \quad + \sum_{t=1}^{4} \sum_{z=1}^{Z} \sum_{q=1}^{Q_z} \sum_{k=1}^{K} d\left(\mathbf{f}_{qz}, \mathbf{h}_z\right) C_{qkz}^{f \to h} S_{zk}^{q}(t) \\
&\text{Line 3:} \quad + \sum_{t=1}^{4} \sum_{z=1}^{Z} \sum_{k=1}^{K} \sum_{n=1}^{N} C_{zk}^{raw} \alpha_{zk}^{n}(t) \\
&\text{Line 4:} \quad + \sum_{t=1}^{4} \sum_{z=1}^{Z} \sum_{k=1}^{K} \sum_{n=1}^{N} d(\mathbf{h}_z, \mathbf{r}_n) C_{zk}^{h \to r} \alpha_{zk}^{n}(t) \\
&\text{Line 5:} \quad + C^w \sum_{t=1}^{4} \sum_{z=1}^{Z} \sum_{k=1}^{K} \sum_{n=1}^{N} w_k \alpha_{zk}^{n}(t) \\
&\text{Line 6:} \quad + \sum_{m=1}^{M} \sum_{n=1}^{N} d(\mathbf{s}_m, \mathbf{r}_n) C_{mn}^{r \to c} \gamma_{mn} \\
&\text{Line 7:} \quad + \sum_{m=2}^{M} C_{m-1,m}^{c \to c} \, d(\mathbf{s}_{m-1}, \mathbf{s}_m) \\
&\text{Line 8:} \quad + \sum_{m=1}^{M} \sum_{l=1}^{L} d(\mathbf{s}_m, \mathbf{p}_l) C_{ml}^{c \to d} \rho_{ml}
\end{aligned} \tag{7.2}$$

$$\text{Subject to:} \quad \sum_{z=1}^{Z} \sum_{k=1}^{K} w_k \alpha_{zk}^{n}(t) \leq W_n, \; n = 1, \dots, N, \; t = 1, \dots, 4 \tag{7.2a}$$

$$\sum_{z=1}^{Z} \alpha_{zk}^{n}(t) \geq D_{kn}(t), \text{ for } k = 1,\ldots, K, n = 1, \ldots, N, t = 1, \ldots, 4 \quad (7.2b)$$

$$\sum_{n=1}^{N} \alpha_{zk}^{n}(t) \leq (1-\beta) \sum_{q=1}^{Q_z} S_{zk}^{q}(t),$$

$$\text{for } z = 1, \ldots, Z, k = 1, \ldots, K \text{ and } t = 1, \ldots, 4. \quad (7.2c)$$

$$\sum_{m=1}^{M} \gamma_{mn} \geq 1 \text{ for } n = 1, \ldots, N \quad (7.2d)$$

$$\sum_{n=1}^{N} \gamma_{mn} \geq 1 \text{ for } m = 1, \ldots, M \quad (7.2e)$$

$$\sum_{m=1}^{M} \rho_{ml} \geq 1, \text{ for } l = 1, \ldots, L \quad (7.2f)$$

$$\sum_{l=1}^{L} \rho_{ml} \geq 1, \text{ for } m = 1, \ldots, M \quad (7.2g)$$

$$\alpha_{zk}^{n}(t), \gamma_{nm}, \rho_{ml} \geq 0 \text{ and } \alpha_{zk}^{n}(t) \in \mathbb{Z}, \gamma_{nm}, \rho_{ml} \in \{0,1\},$$

$$\text{for all } m, n, k, l, t, z. \quad (7.2h)$$

where $\mathbb{Z}$ in equation (7.2h) denotes the set of all integers.

The first line on the right side of the equality in equation (7.2) contains all the fixed and variable building costs of the hubs, reactors, and condensers. The second line is the total cost for transporting all the residues from the farms to the hubs in all seasons. Line 3 stands for the residues procurement costs for all the reactors. Line 4 is the transportation costs for the residues that is transported from the hubs to the reactors. Line 5 represents the labor costs for handling all the residues in the reactors. Line 6 is the pipeline layout costs for transferring BMG between the reactors and condensers. Line 7 is the pipeline layout costs between some of the condensers, which results from assumption 2 in the R2C stage. The pipeline connecting topology is defined as the $m$th condenser connects to the $(m+1)$th condenser while $m = 1,\ldots, m-1$ and the $m$th condenser connects to the first condenser. Line 8 denotes the transportation costs for the liquefied BMG that is transferred from the condensers to the delivery points.

Constraint (7.2a) follows because the workforce availability for collecting the residues from the hubs is upper bounded. Constraint (7.2b) matches assumption 5 in the feedstock

handling stage while each reactor has a demand that serves as the lower bound for the amount of residues that is transported to that reactor. Constraint (7.2c) considers the deterioration of the residues in the hubs and limits the amount of residues that is transported to the reactors to the residue availability in the hubs. Constraints (7.2d) - (7.2g) correspond to the first and second assumptions in the R2C and C2DP stages, respectively. Constraint (7.2f) states that $\alpha_{zk}^{n}(t), \gamma_{nm}, \rho_{ml}$ are all non-negative integers.

The objective function (7.2) is a nonlinear function due to the existence of the distance function (7.1). With the presence of the integer constraint (7.2f), the set of equations (7.2) forms a MINLP whose feasible solutions are discontinuous and contain multiple local minima. Conventional convex optimization techniques cannot be directly applied in solving this problem and a heuristic is required to obtain a nearly optimal solution.

## 7.4 HEURISTICS

Based on the convexity of the nonlinear objective function, the MINLP problem can be divided into two categories, convex MINLP (CMINLP) and non-convex MINLP (NCMINLP). The conventional way of solving a CMINLP usually involves the use of a tree-search method such as the B&B algorithm. When the B&B is applied to a CMINLP, each node of the tree is a convex, nonlinear programming (NLP) that guarantees, if a feasible solution exists, a unique minimum as the lower bound of the original MINLP. Therefore, a traditional B&B algorithm for a linear integer programming (LIP) problem can be modified easily to accommodate a CMINLP problem. In contrast, an NCMINLP induces more challenges if a B&B algorithm is applied, because solving a non-convex NLP for each node cannot always ensure a global minimum, which may further reduce the searching accuracy of the lower bound for the original MINLP.

The objective function (7.2) can be categorized as an NCMINLP problem due to the existence of the nonlinear distance function and integer constraints. Because the tree-search based methods cannot be applied readily to solve the NCMINLP, and the computational techniques that have been developed for solving the NCMINLP are usually confined to certain problems, various heuristics that are effective for the general NCMINLP were developed for searching a feasible solution that is close to the global optimum. This research adopted one the prevailing heuristics that is the Genetic Algorithm (GA) for solving the NCMINLP (7.2).

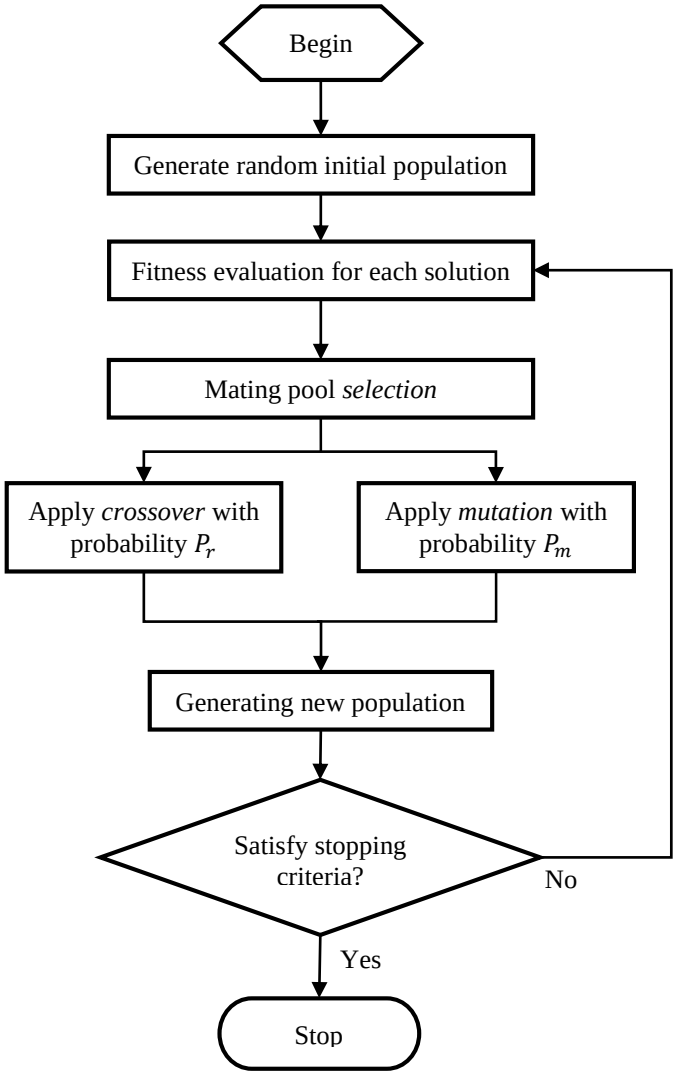


Figure 7.2: Flow chart for GA applied in generalized optimization problem.

The GA tends to achieve a sub-optimal solution by evolving a large group of randomly generated populations and picking the best one as the final solution. The process that the algorithm employs resembles the natural gene selection process, which consists of selection, crossover, and mutation. The general steps that the GA applies to a generalized optimization problem is shown in Figure 7.2, and each step in the flow chart is further expanded in detail to accommodate the NCMINLP (7.2).

### 7.4.1 Random initial population

The initialization process generates a large set of candidate solutions before the algorithm enters the genetic operation loop. The decision variables in the MINLP (7.2) include $\mathbf{h}$, $\mathbf{r}$, $and$ $\mathbf{s}$, which are non-integer variables, $\boldsymbol{\alpha}^n(t)$, which are integer variables, and $\boldsymbol{\gamma}$, $\boldsymbol{\rho}$, which are binary variables. A proper selection of the initial value for these variables results in a faster converging speed and a solution that is closer to the global optimum.

The initial value of the non-integer variables is generated randomly within a certain range and conforming to a uniform distribution. Because each hub is located in a certain zip code area, its initial location, $\mathbf{h}_z = (x_z^h, y_z^k)$, is within the range

$$\min_{q=1,\dots Q_z} x_{qz}^f \le x_z^h \le \max_{q=1,\dots Q_z} x_{qz}^f, \text{ for } z = 1, \dots, Z \tag{7.3}$$

$$\min_{q=1,\dots Q_z} y_{qz}^f \le y_z^h \le \max_{q=1,\dots Q_z} y_{qz}^f, \text{ for } z = 1, \dots, Z \tag{7.4}$$

where $\left(x_{qz}^f, y_{qz}^f\right)$ represents the coordinate of the $q$th farm in zip code $z$. The reactors and condensers are located in the area where the farms and delivery points are located. Therefore, the locations of the reactors, $\mathbf{r}_n$, and the condensers, $\mathbf{s}_m$, are selected within the following range.

$$\min_{\text{all } z,q,l} (x_{qz}^f, x_l^p) \le x_n^r \le \max_{\text{all } z,q,l} (x_{qz}^f, x_l^p), \text{ for } n = 1, \dots, N \tag{7.5}$$

$$\min_{\text{all } z,q,l}(y_{qz}^{f}, y_{l}^{p}) \le y_{n}^{r} \le \max_{\text{all } z,q,l}(y_{qz}^{f}, y_{l}^{p}) \text{ , for } n = 1, \dots, N \tag{7.6}$$

$$\min_{\text{all } z,q,l}(x_{qz}^{f}, x_{l}^{p}) \le x_{m}^{s} \le \max_{\text{all } z,q,l}(x_{qz}^{f}, x_{l}^{p}) \text{ , for } m = 1, \dots, M \tag{7.7}$$

$$\min_{\text{all } z,q,l}(y_{qz}^{f}, y_{l}^{p}) \le y_{m}^{s} \le \max_{\text{all } z,q,l}(y_{qz}^{f}, y_{l}^{p}) \text{ , for } m = 1, \dots, M \tag{7.8}$$

where $\left(x_{l}^{p}, y_{l}^{p}\right)$ represents the coordinate of the delivery point $l$.

From the constraints (7.2a) – (7.2c) and (7.2f), the initial population for the integer variables, $\boldsymbol{\alpha}^{n}(t)$, is selected as integers with a uniform distribution in the following range

$$0 \le \alpha_{zk}^{n}(t) \le \min\left(\frac{W_n}{w_k}, (1-\beta)\sum_{q=1}^{Q_z} S_{zk}^{q}(t)\right) \text{ , for all } z, k, n, t \tag{7.9}$$

Each of the binary variables, $\gamma_{mn}\ \rho_{ml}$, is selected randomly according to the uniform distribution.

### 7.4.2 Fitness evaluation

For an unconstraint programing, the fitness of a solution stands for the value of the objective function. Due to the existence of the constraints, the fitness test consists of both the evaluation of the original objective function and a penalty function whose value indicates the violation of the solution to the constraints.

The fitness evaluation process adopts the penalty function method proposed by Deb (2000). Let $\mathbf{Y}_i$ be the $i$th candidate solution and the number of the candidate solution be $I$, the fitness is defined as

$$f(\mathbf{Y}_i) = \begin{cases} TC(\mathbf{Y}_i), & if\ \varphi_j(Y_i) \ge 0 \quad \forall j = 1,2,\dots J, \\ TC_{\max} + \sum_{j=1}^{J}\left|\varphi_j(Y_i)\right|, & \text{otherwise.} \end{cases} \tag{7.10}$$

where $TC_{\max} = \begin{cases} \max\limits_{\mathbf{Y}_i \text{ is feasible}} TC(\mathbf{Y}_i), & \text{if there is any feasible solution} \\ 0, & \text{if there is no feasible solution for } \mathbf{Y}_i \end{cases}$, $j$ is the index for the inequality constraints and $J$ is the number of the inequality constraints. $\varphi_j$ denotes the left

hand side of the $j$th inequality constraint, when the constraint is rearranged as the right side of the inequality being 0. For example, the constraint (7.2a) can be rewritten as

$$\sum_{z=1}^{Z}\sum_{k=1}^{K} w_k \alpha_{zk}^{n}(t) - W_n \leq 0,\ n = 1, \ldots, N,\ t = 1, \ldots, 4. \tag{7.11}$$

The fitness evaluation sorts the population of solutions in an order that the best feasible solution has the least value of fitness and the infeasible solution that violates the constraints most has the largest value of fitness.

### 7.4.3 Mating pool selection

The GA uses a selection process to find suitable candidate solutions (parents) to breed new offspring. Two healthy parents (solutions that have better fitness) have a higher chance of having healthy children, which leads to a better solution. The binary tournament selection proposed by Goldberg and Deb (1991) was adopted for the selection process. It randomly chooses two candidate solutions from the population and one of the solutions with better fitness is selected as a parent with a fixed probability between 0.5 and 1. Because the probability of choosing a healthier parent is greater than 0.5, the resulting mating pool eventually has overall better health than those not being selected.

### 7.4.4 Laplace Crossover

In biology, the term "crossover' describes the process that two chromosomes exchange segments with each other and generate new chromosomes. To mimic this natural behavior, a Laplace crossover method proposed by Deep and Thakur (2007) was adopted for this research.

Let the number of decision variables of the MINLP (7.2) be $J$. Define $\mathbf{V}^1 = \left[v_j^1\right] \in \mathbb{R}^J$, $\mathbf{V}^2 = \left[v_j^2\right] \in \mathbb{R}^J$, and let them be two vector solutions for the MINLP (7.2) and they are chosen based on the tournament selection criterion. Their two children $\mathbf{U}^1 = \left[u_j^1\right] \in \mathbb{R}^J$ and $\mathbf{U}^2 = \left[u_j^2\right] \in \mathbb{R}^J$ are given by

$$\begin{aligned} u_j^1 &= v_j^1 + \kappa\left|v_j^1 - v_j^2\right| \\ u_j^2 &= v_j^2 + \kappa\left|v_j^1 - v_j^2\right| \end{aligned}, \tag{7.12}$$

where $\kappa$ is selected by inverting the Laplace distribution function,

$$\kappa = \begin{cases} a - b\log(\epsilon), \epsilon \leq \frac{1}{2} \\ a + b\log(\epsilon),\ \epsilon > \frac{1}{2} \end{cases}, \tag{7.13}$$

where $\epsilon$ is a randomly selected number within the range $[0,1]$ and with a uniform distribution; the number $b$ controls the distance between the parents and children, that is, the smaller (resp. larger) $b$ renders a closer (resp. further) distance.

### 7.4.5 Power Mutation

The biological term "mutation" refers to a permanent change in the genomic sequence. This biological process plays a significant role in evolution, but mutations sometimes cause the organism to malfunction. The mutation process often results in children whose characteristics deviate from their parents.

The power mutation was first introduced by Deep and Thakur (2007) and is applied to solve the MINLP (7.2). Let $\mathbf{V} = \left[v_j\right] \in \mathbb{R}^J$ be the parent solution and $\mathbf{U} = \left[u_j\right] \in \mathbb{R}^J$ be the mutated solution. Denote $v^{ub}$ and $v^{lb}$ as the upper and lower bound of the vector $\mathbf{V}$, respectively, which can be obtained from the estimated bound (7.3)-(7.9). The mutation equation is defined as follows:

$$u_j = \begin{cases} v_j - \tau\left(v_j - v^{lb}\right), \text{ if } \delta < \theta \\ v_j - \tau\left(v_j - v^{ub}\right), \text{ if } \delta \geq \theta \end{cases}, \tag{7.14}$$

where

$$\delta = \frac{v_j - v^{lb}}{v^{ub} - v^{lb}}, \tag{7.15}$$

$\theta$ is a uniform random number within $[0,1]$, $\tau$ is randomly generated within $[0,1]$ according to the power distribution with the density function given by

$$F(x) = x^{\mu}, 0 \leq x \leq 1, \tag{7.16}$$

where $\mu$ is the distribution index and controls the strength of mutation in such a way that large $\mu$ produces diversified children, while small $\mu$ preserves a greater degree of similarity between the children and their parents.

### 7.4.6 New population generation

The values obtained from the crossover and mutation processes are usually real numbers. However, for an MINLP problem, some of the decision variables have integer constraints. Therefore, a truncation method is required to transfer the real number solutions to integer solutions to generate a new population for the next genetic cycle.

The truncation method used in Deep, *et al*. (2009) was applied to generate new population. Let $\mathbf{U} = \lfloor u_j \rfloor \in \mathbb{R}^J$ be the solution obtained from the crossover and mutation processes, but two rules apply to ensure that **U** satisfies the integer constraint.

- if $u_j \in \mathbb{Z}$, keep $u_j$ as the candidate solution, otherwise
- $u_j$ is replaced with either $\lfloor u_j \rfloor$ or $\lfloor u_j \rfloor + 1$ under probability 0.5

where $\lfloor u_j \rfloor$ denotes the greatest integer that does not exceed $u_j$.

All the processes shown in Figure 7.2 have now been defined above, so the GA is completed. Computational experiment is conducted to show the effectiveness of the heuristic applied to solving the MINLP (7.2).

## 7.5 NUMERICAL EXAMPLES

A numerical experiment was conducted to test the performance of the GA applied to solving the MINLP (7.2). The GA was programed in Matlab running on the computer with

Intel Core 2 Duo CPU P8700 @ 2.53GHz. To validate the quality of the solutions, the MINLP (7.2) was also programmed in Lingo running on the same computer for comparison. Most of the system parameters were selected based on the real world application. The parameters for the GA were selected based on the performance of the experimental trials.

The first experiment contained 15 sets of problems varying in size and each problem was run 50 times. The system parameters were selected to reflect a real-world supply chain system of a BMG production system, except that the fixed building cost $C^f$ and variable building costs $C_z^{vh}$, $C_n^{vr}$, $C_m^{vc}$ were set to 0, given that these parameters served as a constant in the MINLP (7.2); one can always add the actual value of these parameters to the final solution when the supply chain cost is calculated in practice. The percentage of the residue lost naturally, $\beta$, was set to $0.05$, the unit labor costs, $C^w$, was set to $10$, and the workforce availability, $W_{n,}$ was set to $8ZK$, which is an empirical number to reduce the probability of obtaining an infeasible MINLP.

To avoid bias in the parameter selection, the rest of the parameters were generated randomly following a uniform distribution. Before presenting these parameters, two random functions were first defined. Let $lb$ and $ub$ be the lower bound and upper bound of a random number selection range, respectively, and $a$ and $b$ are the number of rows and columns for a matrix respectively. Denote rand$(lb, ub)$ to generate a uniform random number within the range $[lb, ub]$ and randi $(lb, ub)$ to generate a uniform random integer within the range $[lb, ub]$.

The list of random parameters is shown in Table 7.1. The description for each parameter, which can be referred to Section 7.1.3, is omitted for simplicity.

Table 7.1: Random parameters for numerical experiment.

| *Variable* | *Random function* | *Lower bound lb* | *Upper bound ub* |
|---|---|---|---|
| $Q_z$ | randi | 5 | 10 |
| $C_{qkz}^{f\to h}$ | rand | 3 | 5 |
| $S_{zk}^{q}(t)$ | randi | 40 | 50 |
| $C_{zk}^{h\to r}$ | rand | 3 | 5 |
| $C_{zk}^{raw}$ | randi | 100 | 150 |
| $C_{mn}^{r\to c}$ | rand | 2 | 4 |
| $C_{ml}^{c\to d}$ | rand | 3 | 5 |
| $C_{m-1,m}^{c\to c}$ | rand | 2 | 4 |
| $D_{kn}(t)$ | randi | 40 | 50 |
| $w_k$ | randi | 3 | 5 |
| $x_{qz}^{f}$ | rand | 0 | 200 |
| $y_{qz}^{f}$ | rand | 0 | 200 |
| $x_{l}^{p}$ | rand | 0 | 200 |
| $y_{l}^{p}$ | rand | 0 | 200 |

Note that the random parameters used in Table 7.1 cannot always guarantee the existence of feasible solutions for the MINLP (7.2). The numerical examples only used the parameters that were generated from Table 7.1 and they rendered a feasible MINLP. The parameters for the GA were selected as follows: crossover probability $P_r$ = 0.8, mutation probability $P_m$ = 0.004, $a$ and $b$ in equation (7.13) are set to 0.4 and 6, respectively. The numerical results are shown in Table 7.2 where the problem size was ordered increasingly by the value of $Z \times K \times N \times M \times L$. $TC_{\min}$ was the optimal value obtained by Lingo and the CPU time (sec) required to obtain the optimal value is also shown in the table. Five columns are shown as the results for the GA. $TC_{\text{worst}}$, $TC_{\text{best}}$, and $TC_{\text{avg}}$ represent the worst (largest), best (least), and average total cost obtained in 50 runs for each set of problems. PL denotes the

percentage of the GA solutions that are less than the solution obtained by Lingo. For example, PL = 10% means that there are 5 GA solutions that are less than the Lingo solution. The average CPU time (sec) for 50 runs in each set of problems is shown in the last column.

Table 7.2: Comparison of numerical results between Lingo and GA.

| | ***Prob. Size*** | **Lingo** | | **GA** | | | | |
|---|---|---|---|---|---|---|---|---|
| ***Prob.*** | $Z \times K \times N \times M \times L$ | $TC^{min}$ | ***CPU Time (s)*** | $TC_{\text{worst}}$ | $TC_{\text{best}}$ | $TC_{\text{avg}}$ | **PL (%).** | **Avg Time *(s)*** |
| *FS1* | 3×1×1×1×3 | 998653 | <1 | 1025725 | 985253 | 1005008 | 12 | 16.00 |
| *FS2* | 3×2×1×1×5 | 2399293 | <1 | 2503104 | 2342750 | 2404046 | 16 | 19.27 |
| *FS3* | 5×3×2×2×3 | 7855511 | <1 | 8569933 | 7719233 | 7996566 | 14 | 34.37 |
| *FS4* | 8×3×2×3×5 | 15125698 | <1 | 15781851 | 15049279 | 15337286 | 18 | 45.38 |
| *FS5* | 5×5×3×3×8 | 13381934 | <1 | 14194134 | 13169258 | 13806906 | 16 | 51.54 |
| *FS6* | 10×5×5×3×8 | 53526391 | <1 | 56579094 | 52167270 | 53540331 | 12 | 71.58 |
| *FS7* | 8×5×3×5×15 | 27276474 | <1 | 28268357 | 26874557 | 27350552 | 14 | 56.37 |
| *FS8* | 15×5×3×5×15 | 62924896 | <1 | 64109901 | 62526252 | 63495108 | 10 | 68.18 |
| *FS9* | 10×8×3×5×15 | 63074312 | <1 | 64609389 | 62619954 | 63393264 | 4 | 71.25 |
| *FS10* | 20×5×5×8×15 | 109340562 | <1 | 114460889 | 109146806 | 111205308 | 2 | 142.86 |
| *FS11* | 15×8×5×5×25 | 129406474 | <1 | 133684893 | 128053743 | 130243128 | 6 | 214.32 |
| *FS12* | 25×8×5×8×15 | 233275303 | 2 | 242969075 | 233098671 | 237059880 | 6 | 409.52 |
| *FS13* | 30×8×10×5×30 | 469966196 | 2 | 495528121 | 464735734 | 479232816 | 8 | 2251.09 |
| *FS14* | 20×8×8×10×30 | 254216529 | 2 | 265727480 | 248404370 | 256167101 | 8 | 858.43 |
| *FS15* | 25×10×8×8×30 | 399617572 | 2 | 415199575 | 389678923 | 401337394 | 6 | 1787.70 |

* Computer: *Intel Core i7-4750HQ@ 2.00GHz*

The GA is capable of finding a better solution than the Lingo, although the average CPU time is much longer, but it was still acceptable for a large size problem (Table 7.2, see Wu and Sarker 2014 for all data). Unlike the B&B-based algorithm that resulted in the average CPU time increasing as the problem size increased, average CPU time of the GA exhibited no increasing pattern when the problem size increased. The random characteristic of the GA introduces the unpredictability of the CPU time. The PL value was no less than 10% in the first 8 problems and it was kept below 10% thereafter. This suggested that the GA has a relatively better chance of finding a good solution when the problem size is small. This is reasonable, because the GA tends to search a wide range of points, and a larger problem size

leads to a wider search area. Therefore, the performance of the GA decreased when the problem size increased and more experimental trials would be required to obtain a satisfactory solution.

It can be found that the overall performance of the GA was better than Lingo in finding a better solution when applied to the given problems (Table 7.2). The GA might be applied to solve MINLP (7.2) when the primary concern is finding a better sub-optimal solution rather than the speed of obtaining the solution.

## 7.6 CONCLUDING REMARKS

BMG is a candidate energy source that might remedy the energy crisis in the future. Its sustainability and high heat of combustion has drawn wide attention recently and numerous BMG production systems have been constructed around the world. Controlling supply chain cost of BMG production systems, specifically, by optimizing facility locations and transportation networks, was studied in this research. Strategic plans can be developed following the rigorous mathematical modeling process and global optimization techniques that were used in this research.

An MINLP is built to measure the total cost of a four-stage supply chain which included the feedstock collecting stage, feedstock distribution stage, BMG pipeline transportation stage, and the liquefied BMG delivering stage. Decision variables included the locations of the hubs, reactors, and condensers; road transportation networks between hubs and reactors, condensers, and delivery points; and the pipeline transportation network between the reactors and condensers. Constraints, such as labor availability, reactor demand and the deterioration of residues, were incorporated into the model.

A GA-based heuristic was applied by combining the genetic operation techniques proposed in the literature. Numerical experiments validated the performance of the GA to solve

the proposed MINLP. The GA obtained a better solution than Lingo when computation time is not the primary focus.

# CHAPTER VIII
# EMPIRICAL TESTING

Fundamental analysis on the numerical results for each model is presented in the previous chapters. More analysis is conducted in this chapter to show the performance of the proposed heuristic and to compare it with other existing heuristics.

## 8.1 SENSITIVITY ANALYSIS

The number of facilities is assumed to be known in all four models. This assumption reduces the computational complexity, but this might not be true in practice given that these numbers are not always given before planning BMG production systems. A proper selection of these numbers may further minimize the total cost and render a better supply chain plan. The influence of these values on the final solution is studied in this section. Because the SS-MRS varies from the SS-SRS in the number of reactors, the study starts from the SS-MRS instead of SS-SRS.

### 8.1.1 Sensitivity Analysis on $N$ for Single-Stage Multi-Reactor System

Assume $N \in [1, Z]$, which denotes the number of reactors to be built, is bounded by the number of hubs. The numerical examples are conducted with the same parameters used in problems MR1-1, MR2-1, MR3-1, MR4-1, and MR5-1 in Table 5.1. The number of reactors to be built is varied from 1 to $Z$. The total cost versus the number of reactor for each problem is shown in Table 8.1.

### 8.1.2 Sensitivity Analysis on $N$ and $M$ for Three-Stage Multi-Facility System

The number of reactors $N$ and the number of condensers $M$ can be changed for the TS-MFS model. Assume $N \in [1, Z]$, as suggested in Section 8.1.1, and $M \in [1, L]$, indicating that the number of condensers is bounded by the number of delivery points. The parameters used

in TS1-1, TS2-1, TS3-1, TS4-1, and TS5-1 are applied to the numerical examples. The sensitivity analysis results are shown in Tables 8.2 and 8.3.

Table 8.1: Optimal total cost of SS-MRS with various number of reactors.

| $N$ | $Z \times K$ | | | | |
|---|---|---|---|---|---|
| | $3 \times 2$ | $3 \times 3$ | $5 \times 3$ | $10 \times 3$ | $10 \times 5$ |
| 1 | 2213547 | 2244128 | 2432148 | 2504785 | 2648745 |
| 2 | 2404653 | 2406774 | 2684517 | 2706427 | 2645210 |
| 3 | 2604874 | 2631798 | 2672248 | 2687107 | 2708145 |
| 4 | - | - | 2814785 | 2941752 | 2948491 |
| 5 | - | - | 3014852 | 3157415 | 3202145 |
| 6 | - | - | - | 3315412 | 3358412 |
| 7 | - | - | - | 3514556 | 3498741 |
| 8 | - | - | - | 3741038 | 3800472 |
| 9 | - | - | - | 4001459 | 3971458 |
| 10 | - | - | - | 4214785 | 4315587 |

* Computer: *Intel Core i7-4750HQ@ 2.00GHz*

It can be shown from Table 8.2 and 8.3 that the total cost shows a similar pattern to that in Table 8.1. If the number of reactors or condensers is treated as the variable, there is no convexity for the objective function (6.1) in terms of these variables. Instead, the optimal number of reactors and condensers cannot be readily obtained given the existence of multiple local minima. The analysis also shows that to gain the optimal supply chain plan for the TS-MFS, an enumeration of all combinations of the number of reactors and condensers is required. Therefore, the computational complexity of the TS-MFS is greater than that of the SS-MRS.

Table 8.2: Optimal total cost of TS-MFS with various number of reactors.

| $N$ | $Z \times K \times M \times L$ | | | | |
|---|---|---|---|---|---|
| | $3 \times 2 \times 2 \times 3$ | $5 \times 3 \times 2 \times 5$ | $5 \times 3 \times 3 \times 5$ | $10 \times 3 \times 3 \times 10$ | $10 \times 5 \times 3 \times 10$ |
| 1 | 2215478 | 2421487 | 2357841 | 2414814 | 2348716 |
| 2 | 2406090 | 2412941 | 2487424 | 2400741 | 2674834 |
| 3 | 2648741 | 2648712 | 2617069 | 2638473 | 2659682 |
| 4 | - | 2879824 | 2854871 | 2854710 | 2900187 |
| 5 | - | 3004871 | 3105487 | 3018871 | 3105214 |
| 6 | - | - | - | 3455742 | 3399748 |
| 7 | - | - | - | 3417915 | 3457715 |
| 8 | - | - | - | 3641871 | 3774847 |
| 9 | - | - | - | 3971582 | 4048792 |
| 10 | - | - | - | 4257105 | 4347014 |

* Computer: *Intel Core i7-4750HQ@ 2.00GHz*

Table 8.3: Optimal total cost of TS-MFS with various number of condensers.

| $M$ | $Z \times K \times N \times L$ | | | | |
|---|---|---|---|---|---|
| | $3 \times 2 \times 2 \times 3$ | $5 \times 3 \times 2 \times 5$ | $5 \times 3 \times 3 \times 5$ | $10 \times 3 \times 3 \times 10$ | $10 \times 5 \times 3 \times 10$ |
| 1 | 2287421 | 2241678 | 2424871 | 2489711 | 2368714 |
| 2 | 2406090 | 2412941 | 2419745 | 2414854 | 2415971 |
| 3 | 2648714 | 2694784 | 2617069 | 2638473 | 2659682 |
| 4 | - | 2898746 | 2814871 | 2847569 | 2948304 |
| 5 | - | 3197855 | 3148795 | 3041578 | 3047821 |
| 6 | - | - | - | 3348741 | 3201887 |
| 7 | - | - | - | 3698741 | 3489712 |
| 8 | - | - | - | 3614587 | 3848710 |
| 9 | - | - | - | 3848710 | 3811497 |
| 10 | - | - | - | 4128791 | 4201781 |

* Computer: *Intel Core i7-4750HQ@ 2.00GHz*

### 8.1.3 Sensitivity Analysis on $N$ and $M$ for Four-Stage Multi-Facility System

The same bounds of $N$ and $M$ as in Section 8.1.2 were selected in the numerical examples for the FS-MFS model. The parameters for the problem FS1-1, FS2-1, FS3-1, FS4-1, and FS5-1 in Table 6.2 are used for the sensitivity analysis, with results shown Table 8.4 and 8.5.

Table 8.4: Optimal total cost of FS-MFS with various number of reactors.

| $N$ | $Z \times K \times M \times L$ | | | | |
|---|---|---|---|---|---|
| | $3 \times 1 \times 1 \times 3$ | $3 \times 2 \times 1 \times 5$ | $5 \times 3 \times 2 \times 3$ | $8 \times 3 \times 3 \times 5$ | $5 \times 5 \times 3 \times 8$ |
| 1 | 1025725 | 2503104 | 8425778 | 14897410 | 14069874 |
| 2 | 1154151 | 2401488 | 8569933 | 15781851 | 15871029 |
| 3 | 1257670 | 2569874 | 8500454 | 15658741 | 14194134 |
| 4 | - | - | 8678415 | 16987415 | 15698714 |
| 5 | - | - | 8798712 | 18741547 | 17485795 |
| 6 | - | - | - | 19787546 | - |
| 7 | - | - | - | 19458792 | - |
| 8 | - | - | - | 21445987 | - |

* Computer: *Intel Core i7-4750HQ@ 2.00GHz*

The results shown in Table 8.4 and 8.5 are the best solutions obtained from GA. The non-convexity of the objective function (7.1) with respect to the number of reactors and condensers is still preserved as in Table 8.1 to 8.3. Because the GA generates random candidate solutions for solving a MINLP problem, it is straightforward to use the GA to solve

for the optimal number of reactors and condensers. Although this process is outside the scope of this dissertation, a generalized discussion can be found in Section 9.5 on future work.

Table 8.5: Optimal total cost of TS-MFS with various number of condensers.

| $M$ | $Z \times K \times N \times L$ | | | | |
|---|---|---|---|---|---|
| | $3 \times 1 \times 1 \times 3$ | $3 \times 2 \times 1 \times 5$ | $5 \times 3 \times 2 \times 3$ | $8 \times 3 \times 2 \times 5$ | $5 \times 5 \times 3 \times 8$ |
| 1 | 1025725 | 2503104 | 7985789 | 13587455 | 14025798 |
| 2 | 1236974 | 2415879 | 8569933 | 16987452 | 14892540 |
| 3 | 1369852 | 2657845 | 8547812 | 15781851 | 14194134 |
| 4 | - | 2782495 | - | 18541597 | 17482560 |
| 5 | - | 2977842 | - | 19875678 | 15697894 |
| 6 | - | - | - | - | 18978501 |
| 7 | - | - | - | - | 19874520 |
| 8 | - | - | - | - | 17845987 |

* Computer: *Intel Core i7-4750HQ@ 2.00GHz*

## 8.2 COMPARISON WITH OTHER RESEARCH

The numerical results of the four models are compared with the Lingo result to verify the performance of the proposed heuristics. However, because Lingo is a commercial software product whose algorithm is not revealed to the public, it is necessary to compare the results from this dissertation to other open source heuristics. OPTI toolbox is a popular example of open-source software, which provides an interface with Matlab. Two general deterministic MINLP solvers, BONMIN and NOMAD, in the OPTI toolbox are used to solve the four models proposed in this dissertation. The BONMIN solver was developed by Bonami *et al*. (2008) and the NOMAD solver was designed by Le Digabel (2011).

Table 8.6: Comparison of three heuristics for SS-SRS Model.

| | *Prob. Size* | **BOMIN** | | **NOMAD** | | **ALMH** | |
|---|---|---|---|---|---|---|---|
| ***Prob.*** | ***Z×K*** | $TC^{min}$ | ***CPU Time (s)*** | $TC^{min}$ | ***CPU Time (s)*** | $TC^{min}$ | ***CPU Time (s)*** |
| *SR1-1* | 3×2 | 2210056 | 1.85 | 2206609 | 2.85 | 2202082 | 0.23 |
| *SR1-2* | | 2205257 | 1.62 | 2212026 | 2.46 | 2203529 | 0.22 |
| *SR1-3* | | 2212118 | 1.41 | 2206708 | 0.64 | 2203557 | 0.36 |
| *SR1-4* | | 2205847 | 1.66 | 2205214 | 2.25 | 2202306 | 0.09 |
| *SR2-1* | 3×3 | 2206807 | 1.25 | 2210540 | 3.99 | 2203560 | 0.20 |
| *SR2-2* | | 2207430 | 0.71 | 2210696 | 2.61 | 2203479 | 0.26 |
| *SR2-3* | | 2211955 | 1.08 | 2211635 | 0.56 | 2204936 | 0.70 |
| *SR2-4* | | 2207633 | 1.06 | 2211562 | 1.31 | 2203118 | 0.22 |
| *SR3-1* | 5×3 | 2214981 | 1.45 | 2209476 | 0.93 | 2207903 | 3.62 |
| *SR3-2* | | 2210050 | 1.91 | 2207786 | 1.20 | 2207546 | 3.72 |
| *SR3-3* | | 2210821 | 1.03 | 2213278 | 2.64 | 2208312 | 5.00 |
| *SR3-4* | | 2214566 | 1.05 | 2212670 | 1.51 | 2209890 | 2.85 |
| *SR4-1* | 10×3 | 2226461 | 0.90 | 2222238 | 3.82 | 2217941 | 2.74 |
| *SR4-2* | | 2220664 | 0.41 | 2217817 | 1.46 | 2214427 | 4.04 |
| *SR4-3* | | 2220205 | 2.02 | 2218714 | 3.33 | 2213769 | 4.05 |
| *SR4-4* | | 2214255 | 2.29 | 2218492 | 3.56 | 2213198 | 10.89 |
| *SR5-1* | 10×5 | 2230640 | 0.75 | 2227712 | 1.96 | 2226864 | 5.08 |
| *SR5-2* | | 2241923 | 1.25 | 2245191 | 4.07 | 2236070 | 7.26 |
| *SR5-3* | | 2233436 | 1.84 | 2234263 | 0.56 | 2229903 | 7.80 |
| *SR5-4* | | 2224324 | 1.65 | 2230171 | 2.31 | 2224048 | 6.34 |
| *SR6-1* | 15×5 | 2247277 | 0.84 | 2242868 | 4.21 | 2238325 | 4.99 |
| *SR6-2* | | 2249080 | 1.22 | 2247353 | 3.57 | 2240143 | 15.03 |
| *SR6-3* | | 2243580 | 2.37 | 2248048 | 1.87 | 2239271 | 19.82 |
| *SR6-4* | | 2245532 | 1.09 | 2242741 | 3.34 | 2240655 | 7.07 |
| *SR7-1* | 20×5 | 2263002 | 3.15 | 2265813 | 2.91 | 2257640 | 40.22 |
| *SR7-2* | | 2261776 | 3.02 | 2257072 | 2.60 | 2253014 | 32.29 |
| *SR7-3* | | 2258123 | 3.27 | 2258557 | 2.03 | 2257674 | 23.01 |
| *SR7-4* | | 2272227 | 2.86 | 2270770 | 4.82 | 2264075 | 19.97 |
| *SR8-1* | 20×10 | 2318424 | 8.72 | 2314782 | 7.67 | 2308714 | 87.41 |
| *SR8-2* | | 2318217 | 7.01 | 2314381 | 7.35 | 2310975 | 79.32 |
| *SR8-3* | | 2317068 | 2.70 | 2315332 | 2.90 | 2308609 | 34.57 |
| *SR8-4* | | 2302700 | 8.60 | 2307512 | 8.35 | 2298559 | 91.43 |
| *SR9-1* | 30×10 | 2349116 | 25.31 | 2350983 | 21.94 | 2348002 | 316.09 |
| *SR9-2* | | 2375283 | 4.94 | 2374174 | 7.20 | 2373483 | 60.88 |
| *SR9-3* | | 2362431 | 10.44 | 2359275 | 11.84 | 2357722 | 123.95 |
| *SR9-4* | | 2363458 | 12.80 | 2354697 | 12.25 | 2354564 | 143.57 |
| *SR10-1* | 50×10 | 2494156 | 31.50 | 2497796 | 28.17 | 2492134 | 395.89 |
| *SR10-2* | | 2494875 | 37.42 | 2499859 | 32.05 | 2490054 | 477.36 |
| *SR10-3* | | 2512673 | 36.58 | 2516773 | 33.87 | 2506995 | 468.81 |
| *SR10-4* | | 2515306 | 29.13 | 2516640 | 25.36 | 2510088 | 365.20 |

* Computer: *Intel Core i7-4750HQ@ 2.00GHz*

Table 8.7: Comparison of three heuristics for SS-MRS Model.

| | *Prob. Size* | **BOMIN** | | **NOMAD** | | **ASTCH** | |
|---|---|---|---|---|---|---|---|
| ***Prob.*** | ***Z×K×N*** | $TC^{min}$ | ***CPU Time (s)*** | $TC^{min}$ | ***CPU Time (s)*** | $TC^{min}$ | ***CPU Time (s)*** |
| *MR1-1* | 3×2×2 | 2414587 | 1.41 | 2406614 | 0.29 | 2404653 | 0.54 |
| *MR1-2* | | 2410103 | 1.07 | 2413611 | 1.04 | 2405639 | 0.54 |
| *MR1-3* | | 2406487 | 0.31 | 2404045 | 3.77 | 2403467 | 1.24 |
| *MR1-4* | | 2407694 | 1.66 | 2406468 | 1.74 | 2405858 | 0.60 |
| *MR2-1* | 3×3×2 | 2408077 | 0.36 | 2412846 | 2.60 | 2406774 | 0.64 |
| *MR2-2* | | 2412807 | 0.90 | 2412747 | 2.17 | 2406513 | 1.36 |
| *MR2-3* | | 2411081 | 1.12 | 2412007 | 4.12 | 2407185 | 2.89 |
| *MR2-4* | | 2408622 | 1.04 | 2410409 | 1.84 | 2406011 | 1.09 |
| *MR3-1* | 5×3×3 | 2674396 | 1.08 | 2676077 | 4.09 | 2672248 | 11.80 |
| *MR3-2* | | 2685284 | 2.89 | 2685079 | 4.56 | 2683284 | 11.70 |
| *MR3-3* | | 2676268 | 1.31 | 2685399 | 3.11 | 2675883 | 15.30 |
| *MR3-4* | | 2675394 | 2.06 | 2676508 | 1.57 | 2669277 | 8.85 |
| *MR4-1* | 10×3×3 | 2689653 | 1.92 | 2692495 | 3.78 | 2687107 | 8.83 |
| *MR4-2* | | 2688046 | 1.75 | 2694976 | 4.83 | 2686241 | 13.38 |
| *MR4-3* | | 2688916 | 1.33 | 2686214 | 3.84 | 2685121 | 13.21 |
| *MR4-4* | | 2688918 | 1.96 | 2690709 | 2.77 | 2687414 | 16.33 |
| *MR5-1* | 10×5×3 | 2710116 | 1.89 | 2709854 | 2.37 | 2708145 | 16.24 |
| *MR5-2* | | 2704294 | 2.52 | 2708448 | 2.73 | 2702951 | 23.64 |
| *MR5-3* | | 2717344 | 2.90 | 2717891 | 3.72 | 2709106 | 24.64 |
| *MR5-4* | | 2718758 | 1.55 | 2724377 | 3.15 | 2715741 | 19.72 |
| *MR6-1* | 15×5×5 | 2769018 | 2.43 | 2775071 | 3.51 | 2768547 | 16.02 |
| *MR6-2* | | 2775926 | 5.40 | 2775831 | 5.15 | 2772148 | 45.96 |
| *MR6-3* | | 2768356 | 5.86 | 2769280 | 4.96 | 2767487 | 66.76 |
| *MR6-4* | | 2760575 | 2.45 | 2761764 | 2.55 | 2755214 | 24.58 |
| *MR7-1* | 20×5×5 | 2820261 | 12.33 | 2816563 | 12.61 | 2815365 | 155.10 |
| *MR7-2* | | 2851121 | 12.12 | 2856036 | 10.44 | 2846548 | 133.35 |
| *MR7-3* | | 2836689 | 9.39 | 2835787 | 7.30 | 2827417 | 100.80 |
| *MR7-4* | | 2827656 | 7.23 | 2826788 | 6.23 | 2823649 | 90.93 |
| *MR8-1* | 20×10×8 | 2988902 | 18.73 | 2986716 | 16.70 | 2982011 | 233.70 |
| *MR8-2* | | 2987076 | 17.05 | 2989364 | 16.13 | 2985475 | 220.50 |
| *MR8-3* | | 3015913 | 12.76 | 3013219 | 11.31 | 3006547 | 142.95 |
| *MR8-4* | | 3009871 | 15.21 | 3009186 | 16.65 | 3001541 | 196.05 |
| *MR9-1* | 30×10×8 | 3251944 | 53.11 | 3247716 | 48.49 | 3243514 | 684.45 |
| *MR9-2* | | 3157959 | 23.99 | 3159516 | 22.03 | 3152487 | 298.80 |
| *MR9-3* | | 3321378 | 47.38 | 3327861 | 41.21 | 3320091 | 591.30 |
| *MR9-4* | | 3130401 | 49.45 | 3131056 | 44.41 | 3121462 | 623.70 |
| *MR10-1* | 50×10×10 | 3512665 | 84.95 | 3518420 | 75.41 | 3510021 | 1092.60 |
| *MR10-2* | | 3549479 | 82.90 | 3547823 | 71.08 | 3543145 | 1054.35 |
| *MR10-3* | | 3415742 | 90.95 | 3414572 | 82.47 | 3412034 | 1180.80 |
| *MR10-4* | | 3618717 | 96.95 | 3620850 | 84.02 | 3610851 | 1243.95 |

* Computer: *Intel Core i7-4750HQ@ 2.00GHz*

Table 8.8: Comparison of three heuristics for TS-MFS Model.

| | *Prob. Size* | **BOMIN** | | **NOMAD** | | **ASA** | |
|---|---|---|---|---|---|---|---|
| ***Prob.*** | ***Z×K×N×M × L*** | $TC^{min}$ | ***CPU Time (s)*** | $TC^{min}$ | ***CPU Time (s)*** | $TC^{min}$ | ***CPU Time (s)*** |
| *TS1-1* | 3×2×2×2×3 | 2406331 | 1.67 | 2406683 | 3.96 | 2406090 | 0.95 |
| *TS1-2* | | 2411674 | 1.10 | 2416462 | 1.84 | 2406784 | 0.72 |
| *TS1-3* | | 2410562 | 1.80 | 2409055 | 3.98 | 2405944 | 0.87 |
| *TS1-4* | | 2408571 | 0.17 | 2413922 | 3.48 | 2406395 | 1.14 |
| *TS2-1* | 5×3×2×2×5 | 2416320 | 2.05 | 2419588 | 1.47 | 2412941 | 0.67 |
| *TS2-2* | | 2418485 | 0.90 | 2415069 | 0.29 | 2413384 | 0.94 |
| *TS2-3* | | 2414732 | 0.65 | 2421401 | 0.87 | 2413285 | 1.11 |
| *TS2-4* | | 2422312 | 2.01 | 2415254 | 4.02 | 2413191 | 1.23 |
| *TS3-1* | 5×3×3×3×5 | 2625304 | 0.67 | 2624065 | 0.36 | 2617069 | 2.32 |
| *TS3-2* | | 2628791 | 1.80 | 2621278 | 1.13 | 2620494 | 2.34 |
| *TS3-3* | | 2622135 | 1.38 | 2626175 | 0.26 | 2618819 | 1.92 |
| *TS3-4* | | 2627652 | 1.14 | 2627195 | 2.68 | 2620594 | 2.70 |
| *TS4-1* | 10×3×3×3×10 | 2638732 | 1.99 | 2639292 | 1.25 | 2638473 | 1.67 |
| *TS4-2* | | 2651949 | 1.26 | 2646014 | 3.23 | 2643604 | 2.85 |
| *TS4-3* | | 2645078 | 0.75 | 2643480 | 1.45 | 2640686 | 2.84 |
| *TS4-4* | | 2642146 | 0.31 | 2644221 | 2.38 | 2638955 | 2.96 |
| *TS5-1* | 10×5×3×3×10 | 2661532 | 1.39 | 2666207 | 1.43 | 2659682 | 3.28 |
| *TS5-2* | | 2679151 | 0.78 | 2670642 | 0.46 | 2669279 | 5.40 |
| *TS5-3* | | 2673790 | 0.53 | 2670721 | 2.62 | 2665805 | 5.19 |
| *TS5-4* | | 2681113 | 1.52 | 2681596 | 2.22 | 2681112 | 4.73 |
| *TS6-1* | 15×5×5×5×15 | 3172736 | 2.37 | 3178303 | 3.47 | 3171257 | 20.98 |
| *TS6-2* | | 3197253 | 4.36 | 3191679 | 5.68 | 3188813 | 32.37 |
| *TS6-3* | | 3164339 | 2.77 | 3158111 | 4.74 | 3155038 | 13.48 |
| *TS6-4* | | 3178111 | 2.54 | 3172243 | 3.63 | 3171755 | 26.61 |
| *TS7-1* | 20×5×5×5×20 | 3222114 | 2.09 | 3222325 | 1.93 | 3220276 | 14.54 |
| *TS7-2* | | 3254326 | 2.39 | 3258758 | 2.76 | 3250464 | 23.84 |
| *TS7-3* | | 3215391 | 3.49 | 3217421 | 5.21 | 3214330 | 25.90 |
| *TS7-4* | | 3246028 | 4.08 | 3245180 | 5.98 | 3239354 | 40.89 |
| *TS8-1* | 20×10×8×8×20 | 4344323 | 12.64 | 4350140 | 13.31 | 4342033 | 159.68 |
| *TS8-2* | | 4376221 | 68.90 | 4378521 | 58.69 | 4375688 | 871.36 |
| *TS8-3* | | 4283803 | 13.15 | 4281732 | 13.40 | 4275787 | 154.61 |
| *TS8-4* | | 4374358 | 14.67 | 4373988 | 15.48 | 4365151 | 185.58 |
| *TS9-1* | 30×10×8×8×30 | 4730649 | 12.28 | 4732813 | 12.89 | 4728902 | 158.64 |
| *TS9-2* | | 4785230 | 18.96 | 4788204 | 19.48 | 4782587 | 240.74 |
| *TS9-3* | | 4665340 | 54.60 | 4667274 | 47.59 | 4659432 | 689.79 |
| *TS9-4* | | 4747334 | 29.99 | 4745493 | 27.43 | 4743565 | 373.08 |
| *TS10-1* | 50×10×10×10×50 | 5544046 | 42.78 | 5549746 | 39.49 | 5541279 | 550.82 |
| *TS10-2* | | 5459540 | 28.15 | 5453836 | 26.79 | 5453786 | 355.03 |
| *TS10-3* | | 5508157 | 62.73 | 5505774 | 53.18 | 5499467 | 797.12 |
| *TS10-4* | | 5494748 | 35.76 | 5497365 | 31.95 | 5493075 | 451.86 |

* Computer: *Intel Core i7-4750HQ@ 2.00GHz*

Table 8.9: Comparison of three heuristics for FS-MFS Model.

| | *Prob. Size* | BOMIN | | NOMAD | | GA | |
|---|---|---|---|---|---|---|---|
| ***Prob.*** | ***Z×K×N ×M × L*** | $TC^{min}$ | ***CPU Time (s)*** | $TC^{min}$ | ***CPU Time (s)*** | $TC^{min}$ | ***CPU Time (s)*** |
| *FS1* | 3×1×1×1×3 | 993713 | 1.32 | 993102 | 4.76 | 985253 | 16.00 |
| *FS2* | 3×2×1×1×5 | 2345371 | 1.79 | 2350747 | 3.91 | 2342750 | 19.27 |
| *FS3* | 5×3×2×2×3 | 7721074 | 2.83 | 7727043 | 4.91 | 7719233 | 34.37 |
| *FS4* | 8×3×2×3×5 | 15058057 | 4.68 | 15053081 | 3.79 | 15049279 | 45.38 |
| *FS5* | 5×5×3×3×8 | 13171253 | 4.91 | 13175698 | 6.26 | 13169258 | 51.54 |
| *FS6* | 10×5×5×3×8 | 52175034 | 6.71 | 52170433 | 8.58 | 52167270 | 71.58 |
| *FS7* | 8×5×3×5×15 | 26883584 | 6.10 | 26880312 | 5.01 | 26874557 | 56.37 |
| *FS8* | 15×5×3×5×15 | 62534462 | 5.70 | 62536251 | 6.30 | 62526252 | 68.18 |
| *FS9* | 10×8×3×5×15 | 62620098 | 5.75 | 62627863 | 7.27 | 62619954 | 71.25 |
| *FS10* | 20×5×5×8×15 | 109149738 | 12.91 | 109153855 | 11.66 | 109146806 | 142.86 |
| *FS11* | 15×8×5×5×25 | 128060256 | 17.67 | 128054440 | 18.21 | 128053743 | 214.32 |
| *FS12* | 25×8×5×8×15 | 233106833 | 33.20 | 233103027 | 27.67 | 233098671 | 409.52 |
| *FS13* | 30×8×10×5×30 | 464737104 | 174.43 | 464745239 | 152.83 | 464735734 | 2251.09 |
| *FS14* | 20×8×8×10×30 | 248411121 | 66.94 | 248406023 | 59.22 | 248404370 | 858.43 |
| *FS15* | 25×10×8×8×30 | 389680450 | 138.03 | 389682762 | 122.79 | 389678923 | 1787.70 |

* Computer: *Intel Core i7-4750HQ@ 2.00GHz*

The numerical experiment uses the same set of parameters as in Table 4.1, 5.1, 6.1, and 7.2 and is shown in the following tables. It can be shown from Table 8.6 to 8.9 that the proposed heuristic in this dissertation always obtains a lower total cost than using the BOMIN or NOMAD. However, the proposed heuristic requires a longer CPU time when the problem size is larger. For example, the ALMH requires more CPU time than BOMIN and NOMAD for SR5-1; the ASTCH requires more CPU time for MR3-1; the ASA uses longer CPU time for TS6-1, and the GA requires longer CPU time for FS1 (Tables 8.6-8.9, respectively).

The heuristic proposed in this dissertation is designed specifically for the MINLP models of BMG production systems and the numerical experiment produced a better result when using the heuristic than when using the generalized MINLP solver, such as BOMIN and NOMAD. More CPU time was needed for solving large size problems, but the required CPU time is still within an acceptable range. With a considerable saving on the supply chain cost of

building a BMG production system, it is more desirable to obtain a better sub-optimal solution while compromising on the required CPU time.

# CHAPTER IX
# GENERAL CONCLUSIONS

This dissertation includes analyses and discussion on the supply chain optimization of a BMG production system. Four models with increasing level of complexity were constructed to describe the supply chain cost to include facilities building costs, transportation costs/pipeline layout costs, residues procurement costs and labor costs. This chapter summarizes the work of the previous chapters, presents research results, emphasizes the significance of this research, presents conclusions, and proposes future work.

## 9.1 SUMMARY

This dissertation thoroughly study the supply chain configuration of a BMG production system. It address a systematic way of modeling the systems and propose various heuristics to obtain optimized solutions.

Chapter I discusses the current status and future projections for conventional energy sources, introduces the recent development of the BMG industry, and briefly presents the BMG production process. The significance of studying the supply chain system of a BMG production system is also addressed at the end of the chapter.

Chapter II provides a thorough literature review on the topics that related to this dissertation. Specifically, the literature on supply chain modeling of the bio-energy production systems, the facility location-allocation problems in the bio-energy industry, and the heuristics that were developed for generalized facility location-allocation problems are reviewed. Shortcomings of previous research are presented to show that there is room for improvement, which is discussed in this dissertation.

Chapter III gives the problem description, research objectives, and goals of this dissertation in detail. The generalized methodologies that are adopted in the following chapters are first presented in this chapter.

Chapter IV introduces the first SS-SRS model, which serves as the foundation for the remaining models. A MINLP model is built with the supply chain cost as the objective function. An ALMH heuristic is proposed to solve the MINLP and numerical experiments are conducted to validate its effectiveness.

Chapter V studies the SS-MRS model, which extended the model introduced in Chapter III. An ASTCH is proposed to solve the MINLP model for the SS-MRS. Illustrative examples are provided to apply the ASTCH step by step. At the end of this chapter, numerical examples with random generated parameters are present to verify the performance of the proposed heuristic.

Chapter VI studies the TS-MFS model, which assumes another two stages in the supply chain model of BMG production systems. A more complex MINLP model is given in this chapter and an Alternative Search Algorithm (ASA) is developed to solve the MINLP. Numerical examples are conducted by applying the ASA.

Chapter VII investigates the complete system configuration of a BMG production supply chain. The FS-MFS includes all four stages for BMG production, starting from feedstock production to the distribution of LCP to the end users. The GA is applied to the complicated MINLP and numerical instances are analyzed to show the validity of the GA.

Chapter VIII provides further numerical examples for the four models. Specifically, a sensitivity analysis on the total cost with respect to the number of facilities are conducted and

the heuristic proposed in this dissertation is compared with the performance of two open-source MINLP solvers in solving the proposed MINLP models.

The results of this research is provided in the next section.

## 9.2 RESULTS

Chapter I introduced the idea that there will be increasing demand on sustainable energy resources, given that the depletion of conventional fossil-based fuels is inevitable. BMG, which can be produced from bio-residues such as wood, crops, or animal waste, has received increased attention in recent years. Being popular as an alternative source of energy, the BMG production process can be divided into two steps (Figure 1.1). Cost control for building BMG reactors has become a concern, because more plants are being planned for construction. An optimal design of the supply chain of the BMG production system can reduce costs and increase profits.

Chapter II includes a literature review on both BMG supply chain modeling and existing heuristics for general location-allocation problems. Most studies on supply chain modeling of the bio-energy production systems did not propose a heuristic that can be applied to this specific problem. Although some generalized facility location-allocation problems have proposed corresponding heuristics, the lack of a practical application has made it difficult to apply these heuristics directly to BMG production systems. Therefore, this dissertation tends to fill the gap between a real-world application and theoretical research, and provides an analytical way of modeling and solving a BMG supply chain optimization problem.

Chapters III describes the research problems in detail and introduced the configuration of a typical BMG production system (Figure 3.1). The supply chain of a BMG production system can be divided into four stages that are denoted as F2H, H2R, R2C, and C2DP. The SS-SRS model presents the H2R stage with a single reactor. The SS-MRS models the H2R

stage with multiple reactors. The TS-MFS addresses the H2R, R2C, and C2DP stages and multiple facilities are considered in the modeling process. The FS-MFS considers all four stages, which completes the supply chain design for a BMG production system. The generalized methodology for solving each model starts from building a MINLP with consideration for real-world constraints. It is then followed by proposing a heuristic to solve the MINLP and to obtain an optimal/sub-optimal result. The efficiency and effectiveness of each heuristic is then tested using numerical examples conducted in Matlab using practical but randomly generated parameters.

Chapter IV dealt with the SS-SRS model. A MINLP model was developed to estimate the total supply chain cost of the BMG production system under various constraints. The fixed and variable building costs, transportation costs, feedstocks costs, and labor costs were included in the supply chain cost. The workforce limitation in a region, residue demand of the reactor, and residue availability in the hubs were modeled as inequality constraints. The objective function in the MINLP was constructed as a function of the reactor's location and the amount of residue that is transported from each hub to the reactor. An enumeration algorithm was used to obtain the optimal solutions. However, the inefficiency of the enumeration method for large scale problems leads to a demand for an efficient heuristic. Further investigation shows that the objective function of the MINLP can be decoupled into two sub-functions that can be solved by Newton-Raphson and B&B methods. A heuristic is developed based on this observation. The essence of the heuristic is to alternatively search between two sub-functions using the described methods until convergence takes place. The proposed heuristic is realized by coding in Matlab and ten sets of numerical examples are provided to verify the performance of the heuristic.

Chapter V solves the SS-MRS model, which differs from the SS-SRS model because it assumes that multiple reactors will be built and residue is allowed to be transported from one hub to multiple reactors. Building more reactors not only increases the BMG production capability, but also increases the complexity of modeling and eventual computation. Instead of using the Newton-Raphson iteration to solve one of the sub-functions from the original objective function, the successive substitution algorithm is applied for computing efficiency. A heuristic is proposed by alternatively applying the Successive Substitution algorithm and the B&B method. Again, the new heuristic is produced using Matlab and numerical examples are presented for validation.

Chapter VI addresses the TS-MFS model, which covers the layers shown in Figure 3.1 from the hubs to the delivery points. The hubs in different zip code areas store different types of residue, which will be transported to reactors for producing BMG. Pipelines connect reactors with condensers in which the BMG will be further liquefied to LCP for ease of transportation. An optimal supply chain plan includes determining the location of the reactors and condensers, the amount of residue transported from each hub to the reactors, the plan for the pipeline system between the reactors and condensers, and the amount of LCP transported from the condensers to the delivery points. A MINLP model is built considering the practical constraints and the ASA is proposed based on the NMSA and B&B methods. The numerical examples demonstrate that better solutions can be obtained than when using Lingo, although a longer time is required for the ASA to achieve these better solutions.

Chapter VII proposed the FS-MFS model that includes all the layers from farms to delivery points (Figure 3.1). This model differs from the TS-MFS model in two aspects. First, besides the three stages addressed in TS-MFS model, a fourth stage that represents the residue

transported from farms to hubs is added to this model. Instead of assuming that the locations of the hubs are predefined, the supply chain plan for this model requires an optimization for the hubs' locations. Second, seasonal residue inventory in the farms is considered. Therefore, feedstocks costs becomes a piecewise function with respect to four seasons. The GA is applied to solve the MINLP constructed for the FS-MFS model. Fifteen sets of numerical examples show that the GA can render better solutions than using Lingo but, again, computational time needed is longer to achieve the better results.

Chapter VIII further exploits the numerical results for each model. Sensitivity analysis is conducted for studying the influence of the facility numbers on the optimized total cost. The results show that the objective function for each model does not constituent a convex function with respect to the number of facilities. An optimized total cost can be found by traversing all possible values for the number of facilities. A comparison study between the proposed heuristic in this dissertation to the open source MINLP solvers BOMIN and NOMAD is presented. The results show that the proposed heuristic achieves better solutions than the other two solvers, but it requires longer computational time.

## 9.3 SIGNIFICANCE OF THE RESEARCH

For seeking an environment-friendly and renewable energy source, BMG is one of the ideal candidates. BMG is produced by series of chemical reactions in reactors and condensers. The BMG production systems developed rapidly in recent years. Therefore, cost control of building BMG reactors is critical in the planning process. The supply chain of the BMG production systems, which plays an important role in cost control, is the major concern in this research. A large portion of the reactants in the system is collected from bio-residues that are produced by local farms. These residues are then gathered in local hubs based on the farms'

zip codes. The supply chain system investigated in this research is a specific problem of the BMG facility location-allocation problem.

This research captures the nature of modeling for the supply chain of BMG production system. Fundamental methodology to derive heuristics is studied from Chapter IV to VII. The proposed process of designing a heuristic is proved to be versatile for it being adaptable to sophisticated models. It's the first research in the known literature that addresses a complex optimization problem of the supply chain model for a BMG production system and proposes a systematic way to obtain heuristics that can adaptively solve these models.

## 9.4 CONCLUSIONS

The BMG is a sustainable and renewable energy source that has received wide attention recently. An optimized plan for planning supply chain cost ensures long-term development of a BMG production system. This dissertation concerns with developing analytical methodologies that eventually lead to optimized strategic plans for BMG supply chain systems. The analytical methodologies include the modeling process and development of heuristics. The proposed modeling process captures the characteristics of BMG supply chain systems well and the proposed heuristic perform efficiently on finding optimal/sub-optimal solutions. Detailed conclusions are presented from Chapters IV to VII. Some of the significant conclusions of this dissertation are emphasized in this section.

1. The supply chain of a typical BMG production system consists of five elements and four stages. Five elements include the farms that provide residues, the hubs that collect and store residues from farms, the reactors that utilize residues from hubs to generate BMG, the condensers that obtain BMG from the reactors through pipelines and liquefies BMG to LCP, and the delivery points that act as the end users and accept the LCP transported from condensers. Four stages include the transportation from farms to

hubs (F2H), from hubs to reactors (H2R), pipeline delivery from reactors to condensers (R2C), and transportation from condensers to delivery points (C2DP).

2. The mathematical model of the supply chain system is a MINLP model whose performance measure is the total cost consisting of the facilities building costs, transportation costs/pipeline layout costs, residues procurement costs, and labor costs. The real-world constraints in the MINLP model include the limitation of workforce availability, the deterioration of the residues in the hubs, the reactors' demands for residues, and the topological constraints on the transportation network and pipeline layout.
3. The proposed heuristics for the SS-SRS, SS-MRS, and TS-MFS are interconnected with the idea of alternatively searching between the location and allocation problems. The heuristic used for solving the FS-MFS adopts the GA that mimics gene mutation, crossover, and the mating process.
4. Numerical experiments are conducted in Matlab for four models by applying their corresponding heuristic. Identical numerical experiments are also conducted in Lingo for comparison. The results generally show that the heuristics proposed in this dissertation can obtain a better solution than Lingo, while the latter solver requires less computational time. However, the time it takes for proposed heuristic to find an optimal/sub-optimal solution (about several minutes) is reasonable.
5. Sensitivity analysis shows that the MINLP for each model does not have a convex property with respect to the number of facilities. A comparison with the open source solvers, BOMIN and NOMAD, shows the proposed heuristic can obtain better results although it sacrifices the CPU time required.

## 9.5 FUTURE RESEARCH

Some problems that emerged during this research might be an ideal candidate for future research topics. The direction of some possible future research is listed as follows.

1. **Generalization of number of facilities**:

The sensitivity analysis in Section 8.1 suggests the potential for properly selecting the number of facilities such that the total cost is further minimized. A simplified way of finding such a solution is through a brute force iteration of all possible numbers of facilities. However, when the problem size grows, the time for traversing all possible numbers increases. Therefore, a new heuristic needs to be developed to take into account the number of facilities as a decision variable.

2. **Obtaining the lower bound**:

The results of all the numerical experiments from Chapter IV to VII are compared with the Lingo results. One of the reasons to make this comparison is that all the MINLPs contain non-convex objective functions. Therefore, an analytical lower bound of these MINLPs cannot be readily obtained. However, it might be possible to obtain a numerical lower bound on the MINLPs by applying the branch and bound algorithm. Future work can leverage the B&B method to find the lower bound of the MINLPs for the four models.

3. **Applying other heuristics**:

The last model utilizes the GA to solve the proposed MINLP. There are other types of heuristics in the literature, such as the Ant colony method, the simulated annealing heuristic, the Tabu search method, and the variable neighborhood searching method. Further research can be devoted to applying these heuristics to the FS-MFS model and the results can be compared with those obtained by the GA. Future work should focus on the heuristic that has the best performance for the proposed BMG supply chain model.

4. **Modeling the pipeline systems**:

The BMG is pumped into the pipelines with high pressure. On one hand, the higher pumping pressure results in faster transporting speed of the BMG, which increases the transporting efficiency. On the other hand, the high pumping pressure increases the equipment cost for the pipeline system. An increasing on the thickness of the pipes and upgrading of the pumps are required to tolerant and deliver high pressure BMG. Future work could consider modeling the cost of the pipeline systems using the factors such as the cost of equipment and the transportation speed of the BMG.

5. **Consideration of inventory control**:

Storage cost occurs since the feedstock is stored in the hubs and the liquefied BMG is stored in the condensers. A well-controlled inventory level could substantially reduce the supply chain cost of the BMG production system. Deterministic inventory models can be derived and incorporated into the original MINLP. Future work includes investigating and modeling the inventory systems, developing heuristics for minimizing the total cost of the BMG supply chain system and determining the optimized ordering strategy for the hubs and condensers.

**6. Cost reduction by selling reactors' residue as fertilizer:**

The BMG is produced through a series of bio-chemical reactions in an anaerobic digester. The reaction generates a significant amount of byproducts which are the ideal candidate as fertilizer or chemically further processed feeding materials to the system itself. Therefore, the total cost of supply chain system can be further reduced if the byproducts can be sold to the local farms. The future work include calculating the amount of byproducts in reactors and building a sales network connecting reactors and local farms.

# REFERENCES


1. Akgul, O., Zamboni, A., Bezzo, F., Shah, N., and Papageorgiou, L. G. (2011), "Optimization-based approaches for bioethanol supply chains," *Industrial and Engineering Chemistry Research*, **50**(9): 4927-4938.

2. Aksoy, B., Cullinan, H., Webster, D., Gue, K., Sukumaran, S., Eden, M., and Sammons,N. (2011), "Woody biomass and mill waste utilization opportunities in Alabama: Transportation cost minimization, optimum facility location, economic feasibility and impact," *Environmental Progress and Sustainable Energy*, **30**(4): 720-732.

3. Akyuz, M., Oncan, T. and Altınel, I. (2009), "Efficient lower and upper bounds for the multi-commodity capacitated multi-facility Weber problem with rectilinear distances," *Logistik Management*, 229-245.

4. Akyuz, M. H., Oncan, T. and Altinel, I. K. (2010), "The multi-commodity capacitated multi-facility Weber problem: Heuristics and confidence intervals," *IIE Transaction*, **42**(11): 825-841.

5. Akyuz, M. H., Oncan, T. and Altinel, I. K. (2012), "Solving the multi-commodity capacitated multi-facility Weber problem using Lagrangean relaxation and a subgradient-like algorithm," *Journal of the Operational Research Society*, **63**(6): 771-789.

6. Aras, N., Orbay, M. and Altınel, I. (2007), "New heuristic methods for the capacitated multi-facility Weber problem," *Naval Research Logistics*, **54**(1): 21-32.

7. Aras, N., Orbay, M. and Altınel, I. (2008), "Efficient heuristics for the rectilinear distance capacitated multi-facilityWeber problem," *Journal of the Operational Research Society*, **59**(1): 64-79.

8. Avami, A. (2012), "A model for biodiesel supply chain: A case study in Iran," *Renewableand Sustainable Energy Reviews*, **16**(6): 4196-4203.

9. Bai, Y., Ouyang, Y. F., and Pang, J. S. (2012), "Biofuel supply chain design under competitive agricultural land use and feedstock market equilibrium," *Energy Economics*, **34**(5): 1623-1633.

10. Brimberg, J. and Mladenovic, N. (1996), "A variable neighbourhood algorithm for solving the continuous location-allocation problem," *Studies in Locational Analysis*, 10: 1-12.

11. Broyden, C.G. (1970), "The Convergence of a Class of Double-Rank Minimization Algorithms," *Journal of the Institute of Mathematics*, **6**(1): 76-90.

12. Bonami,P., Biegler, L. T., Conn, A. R., Cornuejols, G., Grossmann, I. E., Laird, C. D., Lee, J., Lodi, A., Margot, F. and A. Waechter (2008), "An Algorithmic Framework for Convex Mixed Integer Nonlinear Programs," *Discrete Optimization*, **5**(2): 186-204.

13. Bowling, I. M., Ponce-Ortega, J. M., and El-Halwagi, M. M. (2011), "Facility location andsupply chain optimization for a biorefinery," *Industrial and Engineering Chemistry Research,* **50**(10): 6276-6286.

14. Chen, X. and Önal, H. (2014), "An Economic Analysis of the Future U.S. Biofuel Industry, Facility Location, and Supply Chain Network," *Transportation Science,* 48(4): 575-591.

15. Cooper, L. (1963), "Location-Allocation Problems," *Operations Research,* **11**(3): 331-343.

16. Cooper, L. (1972), "The transportation-location problem," *Operations Research,* **20**(1): 94-108.

17. Corsano, G., Vecchietti, A. R., and Montagna, J. M. (2011), "Optimal design for sustainable bioethanol supply chain considering detailed plant performance model," *Computers and Chemical Engineering*, **35**(8), 1384-1398.

18. Cucek, L., Lam, H. L., Klemes, J. J., Varbanov, P. S., and Kravanja, Z. (2010), "Synthesis ofregional networks for the supply of energy and bioproducts," *Clean Technologiesand Environmental Policy*, **12**(6), 635-645.

19. Cucek, L., Mart ń, M., Grossmann, I. E. and Kravanja, Z. (2014), "Multi-period synthesis of optimally integrated biomass and bioenergy supply network," *Computers and Chemical Engineering*, **66**(4), 57-70.

20. Cundiff, J., Dias, N. and Sherali, H. (1997), "A linear programming approach for designing a herbaceous biomass delivery system," *Bioresource Technology*, **59**(1): 47-55.

21. Dal-Mas, M., Giarola, S., Zamboni, A., and Bezzo, F. (2011), "Strategic design and invest-ment capacity planning of the ethanol supply chain under price uncertainty," *Biomass and Bioenergy*, **35**(5): 2059-2071.

22. Deb, K, (2000), "An efficient constraint handling method for genetic algorithms," *Computer Methods in Applied Mechanics and Engineering*, **186**(2-4):311-338.

23. Deep, K. and Thakur, M. (2007), "A new crossover operator for real coded genetic algorithms," *Applied Mathematics and Computation*, **188**(1): 895-911.

24. Deep, K., Singh, K. P., Kansal, M. L. and Mohan, C. (2009), "A real coded genetic algorithm for sloving integer and mixed integer optimization problems," *Applied Mathematics and Computation,* **212**(1): 505-518.

25. du Merle, O., Villeneuve, D., Desrosiers, J. and Hansen, P. (1999), "Stabilized column generation," *Discrete Mathematics*, **194**(1-3): 229-237.

26. Dunnett, A., Adjiman, C. and Shah, N. (2007), "Biomass to heat supply chains: applications of process optimization," *Process Safety and Environmental Protection*, **85**(5): 419-429.

27. Elia, J. A., Baliban, R. C., and Floudas, C. A. (2012), "Nationwide energy supply chain analysis for hybrid feedstock processes with significant CO2 emissions reduction," *AIChE Journal*, **58**(7): 2142-2154.

28. Eksioglu, S. D., Li, S., Zhang, S., Sokhansanj, S., and Petrolia, D. (2010), "Analyzing impact of intermodal facilities on design and management of biofuel supply chain," *Transportation Research Record*, **2191**(2191): 144-151.

29. European Biogas Association (EBA) (2013), Available from: <http://european-biogas.eu/index.php?option=com_content&view=article&id=2&Itemid=4>. [17 September 2014].

30. Fletcher, R. (1970), "A New Approach to Variable Metric Algorithms," *Computer Journal*, **13**(3): 317-322.

31. Francis, R. L., McGinnis, L. F. Jr., and White, J. A. Jr. (1992), "Facility layout and location: An Analytical Approach," Upper Saddle River, NJ: *Prentice Hall*.

32. Gan, J. B., and Smith, C. T. (2011), "Optimal plant size and feedstock supply radius: Amodeling approach to minimize bioenergy production costs," *Biomass and Bioenergy*, **35**(8): 3350-3359.

33. Goldfarb, D. (1970), "A Family of Variable Metric Updates Derived by Variational Means," *Mathematics of Computing*, **24**(109): 23-26.

34. Goldberg, G.E. and Deb, K. (1991), "A Comparative Analysis of Selection Schemes Used in Genetic Algorithm," Foundations of Genetic Algorithms 1, FOGA-1(1):69-93.

35. Hajipour, V., Rahmati, S. H. A., Pasandideh, S. H. R. and Niaki, S. T. A. (2014), "A multi-objective harmony search algorithm to optimize multi-server location–allocation problem in congested systems," *Computers and Industrial Engineering*, **72**: 187-197.

36. Hansen, P., Mladenovic, N. and Taillard, E. (1998), "Heuristic solution of the multisource Weber problem as a p-median problem," *Operations Research Letters*, **22**(2-3): 55-62.

37. Hildebrand, F. B. (1987), "Introduction to Numerical Analysis," Mineola, N.Y: Dover Publications, Inc.

38. Huang, Y., Chen, C. and Fan, Y. (2010), "Multistage Optimization of the Supply Chains of Biofuels," *Transportation Research Part E: Logistics and Transportation Review*, **46**(6): 820-830.

39. Illukpitiya, P., Yanagida J. F., Ogoshi, R. and Uehara G. (2013), "Sugar-ethanol-electricity co-generation in Hawai'i: An application of linear programming (LP) for optimizing strategies," *Biomass and Bioenergy*, **48**: 203-212.

40. International Energy Agency (IEA) (2013), *$CO_2$ Emissions from Fuel Combustion Highlights.* Available from: <http://www.iea.org/publications/freepublications/publication/co2emissionsfromfuelcombustionhighlights2013.pdf>. [26 November 2014].

41. Jason, D. J., Subhash, C. S. and John, S. C. (2012), "Design, modeling, and analysis of a feedstock logistics system," *Bioresource Technology*, **103**(1): 209-218.

42. Kim, J., Realff, M. J., Lee, J. H., Whittaker, C., and Furtner, L. (2011), "Design of biomassprocessing network for biofuel production using an MILP model," *Biomass and Bioenergy*, **35**(2): 853-871.

43. Lagarias, J. C., Reeds, J. A., Wright, M. H., and Wright, P. E. (1998), "Convergence Properties of the Nelder-Mead Simplex Method in Low Dimensions," *SIAM Journal of Optimization*, **9**(1): 112-147.

44. Leduc, S., Starfelt, F., Dotzauer, E., Kindermann, G., McCallum, I., Obersteiner, M., and Lundgren, J. (2010), "Optimal location of lignocellulosic ethanol refineries withpolygeneration in Sweden," *Energy*, **35**(6): 2709-2716.

45. Le Digabel, S. (2011), "Algorithm 909: NOMAD: Nonlinear Optimization with the MADS Algorithm," *ACM Transactions on Mathematical Software*, **37**(4): 1-15.

46. Li, Y. and Hu, G. (2013), "A Sequential Fast Pyrolysis Facility Location-Allocation Model," *Advances in Production Management Systems*, **414**: 409-415.

47. Lin, T., Rodríguez, L. F., Shastri, Y. N., Hansen, A. C. and Ting, K. C. (2014), "Integrated strategic and tactical biomass–biofuel supply chain optimization," *Bioresource Technology*, **156**: 256-266.

48. Lim, Y. S., Koh, S. L. and Morris, S. (2014), "Methodology for optimizing geographical distribution and capacities of biomass power plants in Sabah, East Malaysia," *International Journal of Energy Sector Management*, **8**(1): 100-120.

49. Liu, Z., Qiu, T. and Chen, B. (2014), "A LCA Based Biofuel Supply Chain Analysis Framework," *Chinese Journal of Chemical Engineering*, **22**(6): 669-681.

50. Luis, M., Salhi, S. and Nagy, G. (2011), "A guided reactive GRASP for the capacitated multi-source Weber problem," *Computers and Operations Research*, **38**(7): 1014-1024.

51. Marvin, W. A., Schmidt, L. D., Benjaafar, S., Tiffany, D. G., and Daoutidis, P. (2012), "Economic optimization of a lignocellulosic biomass-to-ethanol supply chain," *Chemical Engineering Science*, **67**(1): 68-79.

52. Mele, F. D., Guillen-Gosalbez, G., and Jimenez, L. (2009), "Optimal planning of supply chains for bioethanol and sugar production with economic and environmental concerns," *Computer Aided Chemical Engineering*, **26**:997–1002.

53. Miehle, W. (1958), "Link length Minimization in Networks," *Operations Research*, **6**(2): 232-243.

54. Parker, N., Tittmann, P., Hart, Q., Nelson, R., Skog, K., Schmidt, A., Gray, E., and Jenkins,B. (2010), "Development of a biorefinery optimized biofuel supply curve for theWestern United States," *Biomass and Bioenergy*, **34**(11): 1597-1607.

55. Rosing, K. (1992), "An optimal method for solving the (generalized) multi-Weber problem," *European Journal of Operational Research*, **58**(3): 414-426.

56. Shabani, N. and Sowlati, T. (2013), "A mixed integer non-linear programming model for tactical value chain optimization of a wood biomass power plant," *Applied Energy*, **104**(C): 353-361.

57. Shanno, D.F. (1970), "Conditioning of Quasi-Newton Methods for Function Minimization," *Mathematics of Computing*, **24**(111): 647-656.

58. Smith, R. K. and Hobbs, B. F. (2013), "Biomass combustion for electric power: Allocation and plant siting using non-linear modeling and mixed integer optimization," *Journal of Renewable Sustainable Energy*, **5**:058113.

59. Tatsiopoulos, I. and Tolis, A. (2003), "Economic aspects of the cotton-stalk biomass logistics and comparison of supply chain methods," *Biomass and Bioenergy*, **24**(3): 199-214.

60. Truckers Report (2013), *The Real Cost of Trucking.* Available from: <http://www.thetruckersreport.com/infographics/cost-of-trucking/>. [26 November 2014].

61. U.S. Energy Information Administration (USEIA) (2013), *International Energy Statistics*. Available from: <http://www.eia.gov/cfapps/ipdbproject/IEDIndex3.cfm?tid=3&pid=26&aid=1>. [26 November 2014].

62. U.S. Energy Information Administration (USEIA) (2014), *How much carbon dioxide is produced when different fuels are burned?* Available from: <http://www.eia.gov/tools/faqs/faq.cfm?id=73&t=11>. [26 November 2014].

63. U.S. Department of Agriculture (USDA) (2010), *EPA Administrator and Agriculture Secretary Team Up to Promote Farm Energy Generation.* Available from: <http://www.usda.gov/wps/portal/usda/usdamediafb?contentid=2010/05/0226.xml&printable=true&contentidonly=true>. [3 May 2010].

64. U.S. BioIntiative (2012), *A Rationale for Biologically-based Public Exposure Standards for Electromagnetic Fields (ELF and RF).*. Available from: < http://www.bioinitiative.org/>. [December 2012].

65. Vidyarthi, N. and Jayaswal, S. (2014), "Efficient solution of a class of location–allocation problems with stochastic demand and congestion," *Computers and Operations Research*, **48**(3): 20-30.

66. Walther, G., Schatka, A., and Spengler, T. S. (2012), "Design of regional productionnetworks for second generation synthetic bio-fuel—A case study in NorthernGermany," *European Journal of Operational Research*, **218**(1): 280-292.

67. Weber, A. (1909), "Über den Standort der Industrien", *Ùber den Standort der Industrien*.

68. Weiszfeld, E. (1937), "Sur le point pour lequel la somme des distances de n points donnés est minimum," *Tohoku Mathematical Journal*, **43**: 355-386.

69. Wu, B. and Sarker, B. R. (2014), *Biogas location-allocation parameter matrices,* < https://www.dropbox.com/s/9dwd5kw7b2ypfzy/Biogas%20location-allocation%20parameter%20matrices.docx?dl=0>.

70. Zainuddin, Z. and Salhi, S. (2007), "A perturbation-based heuristic for the capacitated multisource Weber problem," *European Journal of Operational Research*, **179**(3): 1194-1207.

71. Zamboni, A., Bezzo, F., and Shah, N. (2009), "Spatially explicit static modelfor the strategic design of future bioethanol production systems.2. Multi-objective environmental optimization," *Energy Fuels*, **23**(10): 5134-5143.

72. Zhang, L. and Hu, G. (2013), "Supply chain design and operational planning models for biomass to drop-in fuel production," *Biomass and Bioenergy*, **58**: 238-250.

73. Zhu, X., Li, X., Yao, Q. and Chen, Y. (2011), "Challenges and models in supporting logistics system design for dedicated-biomass-based bioenergy industry," *Bioresour Technol*, **102**(2): 1344-51.

74. Zhu, X. and Yao, Q. (2011), "Logistics system design for biomass-to-bioenergy industry with multiple types of feedstocks," *Bioresource Technology*, **102**(23): 10936-10945.

75. Zittel, W. and Schindler, J. (2007), "Coal: Resources and Future Production," Energy Watch Group, available from: <http://www.resilience.org/stories/2007-04-05/peak-coal-2025-say-researchers>. [17 September 2014].

# APPENDIX A
# PROOF OF THEOREM 4.1

**Proof**: If $\boldsymbol{\alpha}$ is a known parameter, the objective function (4.3) can be re-written as a function of $\mathbf{r}$ only:

$$\text{Min } TC(\mathbf{r}) = C^f + \sum_{z=1}^{Z}\sum_{k=1}^{K} C_{zk}^r \alpha_{zk}$$

$$+\sum_{z=1}^{Z}\sum_{k=1}^{K} d(\mathbf{r},\mathbf{h}_z) C_{zk}^t \alpha_{zk} + C^w \sum_{z=1}^{Z}\sum_{k=1}^{K} w_k \alpha_{zk} \tag{A.1}$$

where $d(\mathbf{r},h_z) = \sqrt{(x-x_z^h)^2+(y-y_z^h)^2}$ represents the distance from the hub in zip code $z$ to the reactor at $\mathbf{r} = (x,y)$. Evaluating the first-order derivative of (A.1) with respect to $\mathbf{r}$, then

$$\frac{\partial TC(\mathbf{r})}{\partial \mathbf{r}} = \sum_{z=1}^{Z}\sum_{k=1}^{K} \frac{C_{zk}^t \alpha_{zk}}{d_z}(\mathbf{r}-\mathbf{h}_z). \tag{A.2}$$

From the fact that $\mathbf{r} = (x,y)$ and let $H[\cdot]$ denote the Hessian matrix of a multi-variable function,

$$H[TC(\mathbf{r})] = \begin{bmatrix} \frac{\partial^2 TC(\mathbf{x},\mathbf{y})}{\partial \boldsymbol{x}^2} & \frac{\partial^2 TC(\mathbf{x},\mathbf{y})}{\partial \mathbf{x}\partial \mathbf{y}} \\ \frac{\partial^2 TC(\mathbf{x},\mathbf{y})}{\partial \mathbf{y}\partial \mathbf{x}} & \frac{\partial^2 TC(\mathbf{x},\mathbf{y})}{\partial \boldsymbol{y}^2} \end{bmatrix} \tag{A.3}$$

where

$$\frac{\partial^2 TC(\boldsymbol{x},\boldsymbol{y})}{\partial \boldsymbol{x}^2} = \sum_{z=1}^{Z}\sum_{k=1}^{K} \frac{C_{zk}^t \alpha_{zk}(y-y_z^h)}{d_z^{3/2}} \tag{A.4}$$

$$\frac{\partial^2 TC(\boldsymbol{x},\boldsymbol{y})}{\partial \boldsymbol{y}^2} = \sum_{z=1}^{Z}\sum_{k=1}^{K} \frac{C_{zk}^t \alpha_{zk}(x-x_z^h)}{d_z^{3/2}} \tag{A.5}$$

$$\frac{\partial^2 TC(\boldsymbol{x},\boldsymbol{y})}{\partial \boldsymbol{x}\partial \boldsymbol{y}} = \frac{\partial^2 TC(\boldsymbol{x},\boldsymbol{y})}{\partial \boldsymbol{y}\partial \boldsymbol{x}} = -\sum_{z=1}^{Z}\sum_{k=1}^{K} \frac{C_{zk}^t \alpha_{zk}(x-x_z^h)(y-y_z^h)}{d_z^{3/2}} \tag{A.6}$$

Let $\boldsymbol{\mu} = (\mu_1,\mu_2)^T \in \mathbb{R}^2$ be any non-zero column vector, from (A.3)-(A.6)

$$\boldsymbol{\mu}^T H[TC(\mathbf{r})]\boldsymbol{\mu} = (\mu_1,\mu_2) \begin{bmatrix} \frac{\partial^2 TC(\mathbf{x},\mathbf{y})}{\partial \boldsymbol{x}^2} & \frac{\partial^2 TC(\mathbf{x},\mathbf{y})}{\partial \mathbf{x}\partial \mathbf{y}} \\ \frac{\partial^2 TC(\mathbf{x},\mathbf{y})}{\partial \mathbf{y}\partial \mathbf{x}} & \frac{\partial^2 TC(\mathbf{x},\mathbf{y})}{\partial \boldsymbol{y}^2} \end{bmatrix} \begin{pmatrix} \mu_1 \\ \mu_2 \end{pmatrix}$$

$$= \frac{\partial^2 TC(\mathbf{x},\mathbf{y})}{\partial \boldsymbol{x}^2}\mu_1^2 + 2\frac{\partial^2 TC(\mathbf{x},\mathbf{y})}{\partial \mathbf{x}\partial \mathbf{y}}\mu_1\mu_2 + \frac{\partial^2 TC(\mathbf{x},\mathbf{y})}{\partial \boldsymbol{y}^2}\mu_2^2$$

$$=\mu_1^2 \sum_{z=1}^{Z} \sum_{k=1}^{K} \frac{C_{zk}^t \alpha_{zk}(y-y_z^h)}{d_z^{\frac{3}{2}}}$$

$$-2\mu_1\mu_2 \sum_{z=1}^{Z} \sum_{k=1}^{K} \frac{C_{zk}^t \alpha_{zk}(x-x_z^h)(y-y_z^h)}{d_z^{3/2}}$$

$$+\mu_2^2 \sum_{z=1}^{Z} \sum_{k=1}^{K} \frac{C_{zk}^t \alpha_{zk}(x-x_z^h)}{d_z^{3/2}}$$

$$=\sum_{z=1}^{Z} \sum_{k=1}^{K} \frac{C_{zk}^t \alpha_{zk}}{d_z^{3/2}} [\mu_1(y-y_z^h) - \mu_2(x-x_z^h)]^2$$

$$\geq 0$$

$$\forall \mu_1, \mu_2 \neq 0 \qquad \text{(A.7)}$$

Therefore, the Hessian matrix in (A.3) is positive semi-definite which indicates that (A.1) is convex.

# APPENDIX B
# LOWER AND UPPER BOUNDS OF $\boldsymbol{\alpha_{zk}}$

The necessary condition of $\boldsymbol{\alpha_{zk}}$ is derived from the constraints (4.3a)-(4.3d). First, inspecting of constraint (4.3a) gives

$w_k \alpha_{zk} \leq W$, for $k = 1,\ldots, K, z = 1, \ldots, Z$

Therefore

$$\alpha_{zk} \leq \frac{W}{w_k} \tag{B.1}$$

Similarly, relaxing the constraint (4.3c) gives

$$\alpha_{zk} \leq (1-\beta) \sum_{j=1}^{Z} A_{jk}, \text{ for } k = 1,\ldots, K, z = 1, \ldots, Z \tag{B.2}$$

from the fact of constraint (4.3d) along with (B.1) and (B.2) give the estimated range of $\alpha_{zk}$, which is

$$\alpha_{zk} \in \left[0, min\left(\frac{W}{w_k}, (1-\beta) \sum_{j=1}^{Z} A_{jk}, A_{zk}\right)\right],$$

$$z = 1,\ldots, Z,\ k = 1,\ldots, K,\ \alpha_{zk} \in \mathbb{R} \tag{B.3}$$

# APPENDIX C
# NEWTON-RAPHSON ITERATION FOR SOLVING NONLINEAR EQUATIONS

Newton-Raphson iteration method also be used to solve nonlinear simultaneous equations. Define two nonlinear simultaneous equations

$$\begin{aligned}\phi(\chi,\gamma) &= 0\\ \psi(\chi,\gamma) &= 0\end{aligned} \tag{C.1}$$

As explained by Hildebeand (1974, pp.598--599), the recurrence formulas are

$$\begin{cases}(\chi^{next}-\chi^{curr})\phi_{\chi}(\chi^{next},\gamma^{next})+(\gamma^{next}-\gamma^{curr})\phi_{\gamma}(\chi^{next},\gamma^{next}) = \phi(\chi^{next},\gamma^{next})\\ (\chi^{next}-\chi^{curr})\psi_{\chi}(\chi^{next},\gamma^{next})+(\gamma^{next}-\gamma^{curr})\psi_{\gamma}(\chi^{next},\gamma^{next}) = -\psi(\chi^{next},\gamma^{next})\end{cases} \tag{C.2}$$

Rearrange (C.2), the solution of (C.1) can be obtained by iterative equation

$$\begin{bmatrix}\chi^{next}\\ \gamma^{next}\end{bmatrix} = \begin{bmatrix}\chi^{curr}\\ \gamma^{curr}\end{bmatrix} - \mathbf{J}^{-1}\begin{bmatrix}\phi\\ \psi\end{bmatrix} \tag{C.3}$$

where *J* is the Jacobian matrix given by

$$\mathbf{J} = \begin{bmatrix}\frac{\partial\phi}{\partial\chi} & \frac{\partial\phi}{\partial\gamma}\\ \frac{\partial\psi}{\partial\chi} & \frac{\partial\psi}{\partial\gamma}\end{bmatrix}. \tag{C.4}$$

Given the set of equations (4.4), the objective is to find the reactor's coordinate (*x*,*y*). It can be shown from (C.4) that the Jacobian matrix of equation (4.4) is the Hessian Matrix obtained in (A.3). Therefore, the iterative equation can be obtained from (C.3) by comparing (4.4) and (C.1)

$$\begin{bmatrix}x^{next}\\ y^{next}\end{bmatrix} = \mathbf{r}^{curr} - H[TC(\mathbf{r}^{curr})]^{-1}\sum_{z=1}^{Z}\sum_{k=1}^{K}\frac{C_{zk}^{t}\alpha_{zk}}{\mathrm{d}(\mathbf{r}^{curr},\mathbf{h}_z)}(\mathbf{r}^{curr}-\mathbf{h}_z). \tag{C.5}$$

where $x^{next}$ and $y^{next}$ are the next iteration value updated from the current value $(x^{curr}, y^{curr})$, $\mathbf{r}^{curr} = (x^{curr}, y^{curr}) \in \mathbb{R}^2$. $H[\cdot]$ is the Hessian matrix defined in (A.3), $TC(\cdot)$ is defined in (A.1) and $d(\cdot,\cdot)$ is defined in (4.2). The procedure of obtaining iteration

equation (4.8) is shown in Appendix C. Computer the step size $\Delta = \sqrt{(x^{next} - x^{curr})^2 + (y^{next} - y^{curr})^2}$.

Note the inevitability of the Hessian matrix in (4.4) is almost always guaranteed based on the observation of the numerical experiments conducted in this research. In fact, if singularity of the Hessian Matrix occurs during iterations, it can be avoided by starting over the iteration and changing the initial guess.

# APPENDIX D
# NOTATIONS IN PROBLEM 4.1 and 5.1

Let $T: \mathbb{R}^{Z\times K} \rightarrow \mathbb{R}^{ZK}$ be a function that transforms a $Z \times K$ matrix to a vector with length $ZK$ by rearranging all columns of the matrix into one column. Denote $\mathbf{1}_s$ a length $s$ vector of all ones and $\mathbf{I_s}$ an $s \times s$ identity matrix. Denote the symbol $\otimes$ the Kronecker matrices product and the symbol $\circ$ the element-wise matrices product.

1. Transformation of a matrix to a column vector.

e.g. if $\boldsymbol{\alpha} = \begin{bmatrix} \alpha_{11} & \alpha_{12} \\ \alpha_{21} & \alpha_{22} \\ \alpha_{31} & \alpha_{32} \end{bmatrix} \in \mathbb{R}^{3\times 2}$, then $T(\boldsymbol{\alpha}) = [\alpha_{11}\ \alpha_{21}\ \alpha_{31}\ \alpha_{12}\ \alpha_{22}\ \alpha_{32}]^T \in \mathbb{R}^6$.

2. $\mathbf{1}_s$: a vector of all ones with length s.

e.g. $\mathbf{1}_3 = [1 \quad 1 \quad 1]^T$.

3. $\mathbf{I_s}$: generates an $s \times s$ identity matrix.

e.g. $\mathbf{I_3} = \begin{bmatrix} 1 & 0 & 0 \\ 0 & 1 & 0 \\ 0 & 0 & 1 \end{bmatrix}$.

4. $\otimes$: for $\boldsymbol{A} = [a_{ij}] \in \mathbb{R}^{m\times n}$ and $\boldsymbol{B} = [b_{ij}] \in \mathbb{R}^{p\times q}$, Kronecker product is defined as

$$\boldsymbol{A} \otimes \boldsymbol{B} = \begin{bmatrix} a_{11}\boldsymbol{B} & \cdots & a_{1n}\boldsymbol{B} \\ \vdots & \ddots & \vdots \\ a_{m1}\boldsymbol{B} & \cdots & a_{mn}\boldsymbol{B} \end{bmatrix}.$$

e.g. $\mathbf{1}_2 \otimes [2\ \ 3\ \ 4]^T = [2\ \ 3\ \ 4\ \ 2\ \ 3\ \ 4]^T$.

5. $\circ$: for $\boldsymbol{A} = [a_{ij}] \in \mathbb{R}^{m\times n}$ and $\boldsymbol{B} = [b_{ij}] \in \mathbb{R}^{p\times q}$, element-wise product is defined as

$$(\boldsymbol{A} \circ \boldsymbol{B})_{ij} = a_{ij}b_{ij}$$

e.g. $\begin{bmatrix} 2 & 3 \\ 4 & 6 \end{bmatrix} \circ \begin{bmatrix} 1 & 5 \\ 2 & 3 \end{bmatrix} = \begin{bmatrix} 2 & 15 \\ 8 & 18 \end{bmatrix}$.

# APPENDIX E
# PROOF OF THEOREM 5.1

**Proof**: The objective function (5.1) is first be re-written as a function of **r** only

$$\begin{aligned}\text{Min } TC(\mathbf{r}) = {} & C^f + \sum_{n=1}^{N} C_n^v + \sum_{z=1}^{Z}\sum_{k=1}^{K}\sum_{n=1}^{N} C_{zk}^r \alpha_{zk}^n \\ & + \sum_{z=1}^{Z}\sum_{k=1}^{K}\sum_{n=1}^{N} d_{zn} C_{zk}^t \alpha_{zk}^n \\ & + C^w \sum_{z=1}^{Z}\sum_{k=1}^{K}\sum_{n=1}^{N} w_k \alpha_{zk}^n \end{aligned} \tag{E.1}$$

To show the convexity of the equation (E.1), one needs to show its Hessian matrix is positive semi-definite. To compute its Hessian matrix, the first-order derivative of (E.1) is obtained

$$\frac{\partial TC(\mathbf{r})}{\partial \mathbf{r}_n} = \sum_{z=1}^{Z}\sum_{k=1}^{K} \frac{C_{zk}^t \alpha_{zk}^n}{d_{zn}} (\mathbf{r}_n - \mathbf{h}_z) \tag{E.2}$$

Let $H[\cdot]$ denote the Hessian matrix of (E.1), that is

$$H[TC(\mathbf{r})] = \text{diag}\begin{pmatrix} \frac{\partial^2 TC(\mathbf{r})}{\partial x_n^2} & \frac{\partial^2 TC(\mathbf{r})}{\partial x_n \partial y_n} \\ \frac{\partial^2 TC(\mathbf{r})}{\partial y_n \partial x_n} & \frac{\partial^2 TC(\mathbf{r})}{\partial y_n^2} \end{pmatrix}, n = 1, \dots, N \tag{E.3}$$

where $\text{diag}(\cdot)$ is the block diagonal matrix and

$$\frac{\partial^2 TC(\mathbf{r})}{\partial x_n^2} = \sum_{z=1}^{Z}\sum_{k=1}^{K} \frac{C_{zk}^t \alpha_{zk}^n (y_n - y_z^h)}{d_{zn}^{3/2}} \tag{E.4}$$

$$\frac{\partial^2 TC(\mathbf{r})}{\partial y_n^2} = \sum_{z=1}^{Z}\sum_{k=1}^{K} \frac{C_{zk}^t \alpha_{zk}^n (x_n - x_z^h)}{d_{zn}^{3/2}} \tag{E.5}$$

$$\frac{\partial^2 TC(\mathbf{r})}{\partial x_n \partial y_n} = \frac{\partial^2 TC(\mathbf{r})}{\partial y_n \partial x_n} = -\sum_{z=1}^{Z}\sum_{k=1}^{K} \frac{C_{zk}^t \alpha_{zk}^n (x_n - x_z^h)(y_n - y_z^h)}{d_{zn}^{3/2}} \tag{E.6}$$

The positive semi-definiteness can be shown directly from its definition. Let $\boldsymbol{\mu} = (\mu_1, \mu_2, \dots, \mu_{2N-1}, \mu_{2N})^T \in \mathbb{R}^{2N}$ be any non-zero column vector, from (E.3)-(E.6)

$$\boldsymbol{\mu}^T H[TC(\mathbf{r})]\boldsymbol{\mu} = \begin{pmatrix} \mu_1 \\ \vdots \\ \mu_{2N} \end{pmatrix}^T \text{diag}\begin{pmatrix} \frac{\partial^2 TC(\mathbf{r})}{\partial x_n^2} & \frac{\partial^2 TC(\mathbf{r})}{\partial x_n \partial y_n} \\ \frac{\partial^2 TC(\mathbf{r})}{\partial y_n \partial x_n} & \frac{\partial^2 TC(\mathbf{r})}{\partial y_n^2} \end{pmatrix} \begin{pmatrix} \mu_1 \\ \vdots \\ \mu_{2N} \end{pmatrix}$$

$$=\sum_{n=1}^{N}\left(\frac{\partial^2 TC(\mathbf{r})}{\partial x_n^2}\mu_{2n-1}^2+2\frac{\partial^2 TC(\mathbf{r})}{\partial x_n \partial y_n}\mu_{2n-1}\mu_{2n}+\frac{\partial^2 TC(\mathbf{r})}{\partial y_n^2}\mu_{2n}^2\right)$$

$$=\sum_{n=1}^{N}\Bigg(\mu_{2n-1}^2\sum_{z=1}^{Z}\sum_{k=1}^{K}\frac{C_{zk}^t\alpha_{zk}^n(y_n-y_z^h)}{d_{zn}^{\frac{3}{2}}}-$$

$$2\mu_{2n-1}\mu_{2n}\sum_{z=1}^{Z}\sum_{k=1}^{K}\frac{C_{zk}^t\alpha_{zk}^n(x_n-x_z^h)\,(y_n-y_z^h)}{d_{zn}^{\frac{3}{2}}}+$$

$$+\mu_{2n}^2\sum_{z=1}^{Z}\sum_{k=1}^{K}\frac{C_{zk}^t\alpha_{zk}^n(x_n-x_z^h)}{d_{zn}^{3/2}}\Bigg)$$

$$=\sum_{n=1}^{N}\sum_{z=1}^{Z}\sum_{k=1}^{K}\frac{C_{zk}^t\alpha_{zk}^n}{d_{zn}^{3/2}}\left[\mu_{2n-1}(y_n-y_z^h)-\mu_{2n}(x_n-x_z^h)\right]^2$$

$$\geq 0,\ \ \forall\mu_1,\mu_2,\ldots,\mu_{2N-1},\mu_{2N}\neq 0 \qquad \text{(E.7)}$$

which indicates that the Hessian matrix for (E.1) is positive semi-definite. Therefore, the decoupled sub-problem (E.1) is convex.

# VITA

Bingqing Wu was born to Min Wu and Shudong Wu in Xuzhou, Jiangsu Province, China. She obtained her bachelor's degree in Mechanical Engineering from Nanjing University of Aeronautics and Astronautics in 2007. After graduation, she worked as a product engineer for Armstrong Machinery Ltd in Beijing, China. In 2009, she entered the Industrial Engineering Program at Louisiana State University (LSU) where she obtained her master's degree in Industrial Engineering in 2012 and started her Ph.D. research the same year. She will receive the Ph.D. degree from LSU in May 2015.

Bingqing Wu worked as a Teaching Assistant for Construction Management course at LSU. She has been the recipient of the Economic Development Assistantship (EDA) at LSU since 2012.

Bingqing Wu published two journal papers in *Journal of the Operational Research Society* and *International Journal of Production Research*. She published five papers in Conference proceedings including the *Proceedings of the 20th Industrial & Systems Engineering Research Conference and EXPO*, the *Proceedings of the IEEE International Conference on Industrial Engineering and Engineering Management*, and *the Proceedings of the Institute for Operations Research and Management Science (INFORMS) National Meeting*. She is also a co-author of a book chapter published by Excel Books in New Delhi, India. Her research interests include facility location-allocation problems, inventory control problems, operations research and supply chain optimization.